

**NUMERICAL SOLUTIONS OF DIFFERENTIAL
EQUATIONS USING WAVELET BASED METHODS**

A Thesis

Submitted for the Award of the Degree of

DOCTOR OF PHILOSOPHY

in

MATHEMATICS

By

Jaya Gupta

Registration Number: 12015110

Supervised By

Dr. Ratesh Kumar (11755)

Associate Professor

Department of

Mathematics

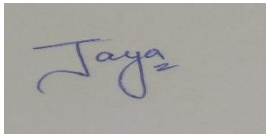


LOVELY PROFESSIONAL UNIVERSITY, PUNJAB

2024

DECLARATION

I hereby declare that the presented work in the thesis entitled “**Numerical Solution of Differential Equation Using Wavelet Based Methods.**” in fulfilment of the degree of **Doctor of Philosophy (Ph. D.)** is the outcome of research work carried out by me under the supervision of **Dr. Ratesh Kumar**, working as an Associate Professor, in the School of Mechanical Engineering of Lovely Professional University, Punjab, India. In keeping with the general practice of reporting scientific observations, due acknowledgement has been made whenever the work described here has been based on the findings of other investigators. This work has not been submitted in part or full to any other university or institute for the award of any degree.



(Signature of Scholar)

Name of the scholar: **Jaya Gupta**

Registration No.: **12015110**

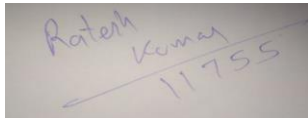
Department/school: **Department of Mathematics**

Lovely Professional University,

Punjab, India

CERTIFICATE

This is to certify that the work reported in the Ph. D. thesis entitled “**Numerical Solution of Differential Equation Using Wavelet Based Methods.**” submitted in fulfillment of the requirement for the reward of the degree of **Doctor of Philosophy (Ph.D.)** in the School of Mechanical Engineering is a research work carried out by **Jaya Gupta, 12015110**, is bona fide record of his/her original work carried out under my supervision, and that no part of the thesis has been submitted for any other degree, diploma, or equivalent course.

A photograph of a handwritten signature in blue ink on a light-colored surface. The signature reads "Ramesh Kumar" and "11755" below it, with a horizontal line under the name.

(Signature of Supervisor)

Name of supervisor: **Dr. Ramesh Kumar**

Designation: Associate Professor

Department/school: School of Mechanical Engineering

University: Lovely Professional University

Dedicated to my almighty God and Parents

ABSTRACT

Differential equations hold a crucial position in the realm of mathematical modeling for a wide range of real-world issues. When tackling physical problems in the form of mathematics, the DEs used for modeling prove to be complex, especially when the mathematical framework incorporates variable coefficients with higher order and nonlinearities present in the model. As a consequence, the need arises for sophisticated numerical techniques that can be viewed as robust solvers capable of obtaining precise numerical solutions for a wide range of such DEs. Researchers are persistently dedicating their efforts to enhancing existing methods and creating innovative hybrid approaches, all aimed at crafting a robust solver for these types of equations. In our review of the literature, we discovered that the Taylor series is a valuable tool for analysing functions on a local scale. However, when the need arises to examine functions globally, the limitations of the Taylor series become apparent, leading to the introduction of Fourier series in the literature. However, Fourier series prove ineffective for analysing functions at a local level. In the recent years, there has been a significant proliferation of numerical methods aimed at addressing the solution of various types of IVPs and BVPs, both on a local and global scale. Among the established approaches are FDM, FEM, and FVM. However, these methods exhibit limitations such as low order accuracy, high computational costs, and constraints related to geometry. While they excel in spatial localization, their overall accuracy is not good. Another category of numerical techniques encompasses spectral methods, where the solution undergoes discretization through approximation via a series of basis functions characterized by infinite differentiability and non-zero values across the entire domain (global support). When the expected solution demonstrates inherent smoothness, spectral methods, combined with the method of weighted residuals, show convergence in exponential form. However, they tend to perform less effectively in terms of spatial localization when dealing with expected solutions

that are discontinuous and lack smoothness. Spectral methods exhibit reduced efficacy when applied to problems featuring intricate geometries, although they are computationally more efficient than FDM, FEM, and FVM. It's noteworthy that spectral methods operate on a global support basis, whereas FDM, FEM, and FVM operate with compact (local) support. Despite their diminished spatial localization for complex problems and irregular geometries, spectral methods offer superior accuracy and minimize errors. Conversely, FDM, FEM, and FVM, while excelling in spatial localization, are comparatively less accurate. Each method possesses advantages as well as limitations in a unique way. Wavelet methods emerge as a promising solution in this context, allowing us to harness the strengths of various approaches, notably superior spatial and temporal localization and enhanced solution accuracy, by employing wavelet bases for approximating the unknown solution. Wavelets offer numerous advantages, including orthonormality, compact support, translation, and dilation via MRA. Their compatibility with computer environments and localization in both spatial and temporal dimensions equip them to effectively address the diverse array of challenges encountered in the realms of science and technology. The literature contains numerous wavelets with diverse characteristics, serving the analysis of various data, signals, images, and solutions. Among the options available, HW stands out as the most mathematically straightforward, computationally efficient, conceptually simple, and memory-friendly wavelet. It holds the distinction of being an orthonormal wavelet with a compact support, as documented in the previous research. The HW is represented most simply with a pair of rectangular pulses, enabling unrestricted integration due to its straightforward, explicit form. The distinctive characteristics of wavelets, particularly the simplicity of their explicit expression, have served as a motivating factor for their integration with spectral methods. In the fields of science and technology, this combination has proven its value in addressing diverse differential equations. Within the domain of the wavelet method, enhancing the solution accuracy can be achieved by modifying the dilation factor within the

family of the wavelet. Existing literature predominantly focuses on HS2W, which are dyadic in nature and characterized by dilation factors that follow the power of 2.

However, in this thesis, innovative approaches are presented. These methods are built upon the HS3W, which is non-dyadic in nature and features a dilation factor following a power of 3. These novel methods are employed to analyze a wide array of linear and nonlinear DEs across various categories. This thesis is dedicated to advancing algorithms based on HS3W in conjunction with established numerical methods such as the Quasilinearization technique, the Gauss elimination method and the collocation method. These algorithms are designed to address a spectrum of linear and nonlinear DEs. For nonlinear challenges, the approach relies on schemes grounded in the Quasilinearization process, leveraging HS3Ws as elaborated in chapters 2 to 4.

The scope encompasses a wide array of numerical problems stemming from diverse fields. These encompass higher-order linear and nonlinear problems. These problems, from a mathematical perspective, represent a spectrum including ODEs with associated BCs and ICs, higher-order linear and nonlinear PDEs, and linear and nonlinear ordinary and partial FDEs.

LIST OF ABBREVIATIONS

DEs	Differential Equations
IVP	Initial Value Problems
BVP	Boundary Value Problems
FDM	Finite Difference Method
FEM	Finite Element Method
FVM	Finite Volume Method
MRA	Multi Resolution Analysis
HW	Haar Wavelet
HS2W	Haar Scale 2 Wavelet
HS3W	Haar Scale 3 Wavelet
ODEs	Ordinary Differential Equations
PDEs	Partial Differential Equations
FDEs	Fractional Differential Equations
HOD	Higher Order Derivatives
KE	Kawahara Equation
DV	Dependent Variable
ES	Exact Solution
AS	Approximate Solution
FDO	Fractional Differential Operator
IPS	Inner Product Space

ACKNOWLEDGEMENT

With deep gratitude, I acknowledge the unwavering support of the Divine Creator and my guru whom blessings have guided me throughout this journey. My sincere appreciation extends to my esteemed research supervisor, Dr. Ratesh Kumar. Dr. Kumar's knowledge, dedication, and insightful guidance have been instrumental in my success. Their leadership, wisdom, and experience have equipped me to navigate every aspect of my Ph.D. studies. I am particularly grateful for Dr. Kumar's patience, invaluable advice, and unwavering support, even during challenging times. Their mentorship has not only enriched my academic journey but also fostered my personal growth. I am thankful for their kind and encouraging nature, as well as for providing access to departmental resources.

I would also like to express my gratitude to Dr. Lovi Raj Gupta, the esteemed Pro Vice-Chancellor at Lovely Professional University, for his gracious support in facilitating this research opportunity. My sincere appreciation extends to the leadership team – Dr. Kailash Juglan, Head of School of Chemical Engineering and Physical Sciences, Dr. Kulwinder Singh, Head of Department of Mathematics, and Dr. Rekha, Head of RDEC – for providing essential resources and facilities at LPU. I would like to thank my Panel members Dr. Pankaj Kumar, Dr. Sanjay Mishra, Dr. Rakesh Yadav and Dr. Anjani Kumar Shukla for their valuable suggestions. Additionally, I am thankful for the timely assistance of the Department of Mathematics staff.

A Special thanks to Dr. Geeta Arora and Dr. Sarabjeet Singh for helping me in my difficult times during my PhD journey.

My deepest gratitude goes to my parents, Mr. Satish Kumar Gupta and Mrs. Rajni Gupta, my brother Gautam Gupta and my entire family. Their unwavering love, support, and encouragement have been the bedrock of my success. They instilled in me the value of hard work and nurtured my aspirations, shaping my perspective on life. Fulfilling my parents' dream of pursuing a doctorate fueled my motivation and perseverance. Their love, patience, sacrifices, and prayers have been a constant source of strength, teaching me the true meaning of resilience and the importance of family. I am incredibly grateful for the unwavering motivation and support of my niece, Ira. Her constant encouragement has been a grounding influence, propelling me forward throughout this journey.

I'm incredibly grateful for the unwavering support of my friends and colleagues Kartik, Amandeep Kaur, Ritika, Sapana, Dr. Sabiha, Dr. Rupali and last but not the least Dr. Shubham Mishra. Their constant encouragement, prompt assistance, and genuine camaraderie have been invaluable throughout my journey. They believed in my potential and actively helped me explore it. Despite their own challenges, their support never wavered. I am truly fortunate to have them in my life.

“Thank-you Everyone for Your Support and Motivation.”

TABLE OF CONTENTS

DECLARATION.....	ii
CERTIFICATE.....	iii
ABSTRACT.....	v
LIST OF ABBREVIATIONS	viii
ACKNOWLEDGEMENT	ix
TABLE OF CONTENTS	xi
LIST OF TABLES	xvi
LIST OF FIGURES	xix
Chapter 1 General Introduction	1
1.1 Introduction	1
1.1.1 Ordinary Differential Equation:	2
1.1.2 Partial Differential Equation:	2
1.1.3 Fractional Differential Equation:	3
1.2 Fractional Calculus:.....	4
1.3 Definition of Fractional calculus:.....	5
1.3.1 Mittag Leffler:.....	5
1.3.2 Reimann-Liouville fractional operator of order μ :	6
1.3.3 Caputo Fractional operator of order μ :	6
1.4 Multi resolution analysis:	6

1.5	Quasi-linearisation:	7
1.6	Collocation Points:	7
1.7	Historical Background of Wavelets:.....	8
1.7.1	Wavelet transform:	10
1.8	Types of Wavelets:	11
1.8.1	Continuous wavelet:.....	11
1.8.2	Discrete wavelet:.....	11
1.8.3	Haar Wavelets:	12
1.8.4	Haar Scale 2 (HS2WM):.....	14
1.8.5	Haar Scale 3 (HS3WM):.....	16
1.9	Literature Review:.....	21
1.10	Research Gap:	28
1.11	Objectives:.....	28
1.12	Layout of the thesis:	29
Chapter 2.....		30
A non-dyadic wavelet-based approximation method for the solution of higher-order ordinary differential equations that appears in Astrophysics with singularity at origin.		30
2.1	Introduction:	30
2.2	Lane Emden equation for a Stellar structure:.....	30
2.3	Quasi-linearisation process	33
2.4	Approximation of Emden Fowler differential equation by Scale-3 Haar wavelet:.....	34
2.5	Methods for the solution of LEE:.....	36

2.6	Error analysis with test problems	37
2.7	Numerical Observations:.....	38
2.7.1	Fourth non-order linear EFE:.....	38
2.7.2	Third order non-linear ODE (EFE).....	40
2.7.3	A Fourth order linear ODE:	42
2.7.4	For $\mu X = 1$ and $\lambda y = Yb$ the fundamental LEE introduced to analyze the thermal behavior of a gas cloud that was spherical.	45
	For $b = 1$, equation becomes:	46
2.7.5	For $b = 5$, equation becomes:.....	48
2.7.6	Basic LEE:	49
2.7.7	Lane Emden equation:	51
2.7.8	Basic LEE:	53
2.7.9	LEE:	55
2.8	Conclusion:.....	56
Chapter 3		57
A numerical analysis for solving various mathematical 2D-partial differential equations via scale 3 Haar wavelets.....		57
3.1	Introduction:	57
3.2	Haar Scale-3 Wavelet:	59
3.3	Discretization Scheme for second and third order partial differential equation:	59
3.4	Numerical Methods:	65
3.4.1	Linear homogeneous equation	65

3.4.2	Linear Non-homogeneous Equation	67
3.4.3	Non-Linear KdV Equation.....	69
3.4.4	“A Non-linear KGE”:.....	71
3.4.5	Numerical Experiment:.....	73
3.5	Discussion:	76
3.6	Conclusion.....	76
Chapter 4.....		77
An effective computational scheme for solving various mathematical fractional differential models via non-dyadic Haar wavelets.		77
4.1	Introduction:	77
4.2	Basic definition of fractional calculus:.....	78
4.3	Quasilinearisation technique:	79
4.4	Applications of Fractional differential equation	80
4.4.1	Numerical Experiment: Fractional Riccati Equation.	80
4.4.2	Numerical Experiment: Fractional Vander-Pol Oscillator Problem	83
4.4.3	Numerical Experiment: Non-linear Oscillator Ordinary Differential Equation ..	85
4.4.4	Numerical Experiment: Composite Fractional Oscillation Equation.	88
4.4.5	Numerical Experiment: Fractional Relaxation-Oscillation Equation.	91
4.4.6	Numerical Experiment: Fractional Kawahara Equation	94
4.4.7	Numerical experiment 4.5.7: Fractional Kawahara Equation.....	103
4.4.8	Conclusion:	106
Chapter 5.....		107

Conclusion and Future Work	107
References.....	111
LIST OF PUBLICATION.....	125
LIST OF CONFERENCES.....	126

LIST OF TABLES

Table 2.1 A comparison study of Absolute errors of proposed method with other methods.	39
Table 2.2 A comparison study of Absolute errors by proposed method at different points for LOR $J=2$	39
Table 2.3 Value of the L_2 and L_∞ error at different LOR:	39
Table 2.4 A comparison study of Absolute errors of proposed method with other methods at resolution level $J=3$	41
Table 2.5 Value of the L_2 and L_∞ error at different LOR	41
Table 2.6 A comparison study of Absolute errors of proposed method with other methods at resolution level $J=3$	43
Table 2.7 A comparison study of Absolute errors by proposed method at different points for LOR $J=2$	43
Table 2.8 Value of the L_2 and L_∞ error at different LOR:	44
Table 2.9 A comparative study of Absolute errors obtained using proposed method with methods available in the literature.	46
Table 2.10 A comparative study of Absolute errors obtained using proposed method with methods available in the literature.	46
Table 2.11 A comparative study of Errors obtained using proposed method at different LOR.	47
Table 2.12 A comparative study of Absolute errors obtained using proposed method with methods available in the literature.	48
Table 2.13 A comparative study of Errors obtained using proposed method at different resolution levels.	48
Table 2.14 A comparative study of Absolute errors obtained using proposed method with methods available in the literature.	50

Table 2.15 A comparative study of Errors obtained using proposed method at different LOR.	50
Table 2.16 A comparative study of Absolute errors obtained using proposed method with methods available in the literature.	52
Table 2.17 A comparative study of Errors obtained using proposed method at different LOR.	52
Table 2.18 A comparative study of Absolute errors obtained using proposed method with methods available in the literature.	53
Table 2.19 A comparative study of Errors obtained using proposed method at different LOR.	54
Table 2.20 A comparative study of Absolute errors obtained using proposed method with methods available in the literature.	55
Table 3.1 Comparison of results achieved for test problem 3.4.1 with ES.	66
Table 3.2 L_2 and L_∞ errors at different values of J for test problem 3.4.1.....	66
Table 3.3 Comparison of results achieved for test problem 3.4.2 with ES.....	68
Table 3.4 L_2 and L_∞ errors at different values of J for test problem 3.4.2.....	68
Table 3.5 Comparison of AS and ES with Absolute error for numerical problem	70
Table 3.6 L_2 and L_∞ errors at different values of J for test problem 3.4.3.....	71
Table 3.7 At different of 'J', value L_2 and L_∞ errors for Test problem 3.4.4	72
Table 3.8 Comparison of ES for Test problem 3.4.4 with results achived.....	72
Table 3.9 At different of 'J', value L_2 and L_∞ errors for Test problem 3.4.5	75
Table 3.10 Comparison of ES for Test problem 3.4.5 with results achived.....	72
Table 4.1 Comparison of ES and AS at different values of x. Discussion of Absolute Error by HS3WM with HSW.	81
Table 4.2 Comparison of value of Error of HS3WM at different levels of resolution.	82
Table 4.3 Comparison of ES and AS at different values of x. Discussion of Absolute Error by HS3WM with HSW.	84
Table 4.4 Comparison of value of Error of HS3WM at different LOR.	84

Table 4.5 Comparison of ES and AS at different values of x . Discussion of Absolute Error by HS3WM with HSW.	87
Table 4.6 Comparison of value of Error HS3WM at different LOR	87
Table 4.7 Comparison of ES and AS at different values of x . Discussion of Absolute Error by HS3WM with HSW at different values of α	89
Table 4.8 Comparison of value of Error of HS2WM and HS3WM at different LOR.....	90
Table 4.9 Comparison of ES and AS at different values of x . Discussion of Absolute Error by HS3WM with HSW at different values of α	92
Table 4.10 Comparison of value of Error of HSW2M and HSW3M at different LOR.....	93
Table 4.11 At different values of z and t , comparison of AS and ES with the value of Absolute error.	101
Table 4.12 At different values of μ , value of L_2 error and L_∞ error.	101
Table 4.13 At different values of z and t , comparison of AS and ES with the value of Absolute error at $\mu=1$	104
Table 4.14 Value L_2 and L_∞ errors for Test problem 4.47 at $\mu=0.2, 0.4$ and 0.6	105

LIST OF FIGURES

Figure 2.1 For NE no. 2.7.1, graphical presentation of ES and AS of $u(z, t)$ at distinct point of z	40
Figure 2.2 For NE no. 2.7.1, Value of Absolute error for different values of z	40
Figure 2.3 For NE no. 2.7.2, graphical presentation of ES and AS of $u(z, t)$ at distinct point of z	42
Figure 2.4 For NE no. 2.7.2, Value of Absolute error for different values of z	42
Figure 2.5: For numerical Experiment no. 2.7.3, graphical presentation of ES and AS of $u(z, t)$ at distinct point of z	44
Figure 2.6 For NE no. 2.7.3: Value of Absolute error for different values of z	45
Figure 2.7 Graphical depiction of AS and ES for NE no. 2.7.4 for case (a).....	47
Figure 2.8 Graphical depiction of AS and ES for NE no. 2.7.4 for case (b).....	47
Figure 2.9 Graphical depiction of ES, AS and Absolute error for NE no. 2.7.5 for case (c).....	49
Figure 2.10 Graphical depiction of ES, AS, Absolute error for NE no. 2.7.6.....	51
Figure 2.11 Graphical depiction of ES, AS, Absolute error for NE no.2.7.7.....	53
Figure 2.12 Graphical depiction of the ES, the AS, and the absolute error for NE no. 2.7.8....	55
Figure 2.13 Graphical depiction of the ES, the AS, and the absolute error for NE no. 2.7.9....	56
Figure 3.1 Graphical Representation of Numerical Problem.....	67
Figure 3.2 Graphical Representation of Numerical Problem.....	69
Figure 3.3 Graphical Representation of Numerical Problem.....	71
Figure 3.4 The solution for numerical Experiment no. 3.4.4 includes four graphical representations: ES, AS, contour view of the ES, and absolute error.	73
Figure 3.5 The solution for numerical Experiment no. 3.4.5 includes four graphical representations: ES, AS, contour view of the ES, and absolute error.	75

Figure 4.1 Graphical representation of ES and AS at $\alpha = 1$	82
Figure 4.2: Graphical representation exact and approximate value for different values of α lies between 0 and 1. At J=2 resolution level.	82
Figure 4.3 Graphical representation of ES and AS	85
Figure 4.4 Graphical representation of ES and AS at LOR J=2.	85
Figure 4.5 Graphical representation of ES and AS	88
Figure 4.6 Graphical representation ES and AS for different values of α lies between 0 and 1. At J=2 resolution level.	88
Figure 4.7 Graphical representation of ES and AS.	90
Figure 4.8 Graphical representation ES and AS for different values of α lies between 0 and 1. At J=2 resolution level.	91
Figure 4.9 Graphical representation of ES and AS	93
Figure 4.10 Graphical representation ES and AS for different values of α lies between 0 and 1. At Resolution-level J=2	94
Figure 4.11 Graphical Representation of AS, ES and absolute error with contour view of ES.	102
Figure 4.12 Graphical representation for $\mu=0.25, 0.50$ and 0.75 with AS at $\mu=1$	103
Figure 4.13 Graphical Representation of AS, ES at $\mu = 1$	105
Figure 4.14 Graphical representation for $\mu=0.20, 0.40$ and 0.60 with graph of collocation points.	106

Chapter 1

General Introduction

1.1 Introduction

The modeled DEs are difficult to solve because they consist of nonlinearities, variable coefficients, and higher-order complexities. The vast majority of real-time events, such as numerous reactions, diffusion processes, dispersive equations, and equilibrium criteria, are governed by these systems of DEs; however, only a few analytical methods are available for studying these equations. Despite significant progress in today's mathematics, there are numerous equations whose solutions are difficult to approach. However, we require some kind of solution in order to obtain satisfactory results. There are many ODEs, PDEs, and FDEs that are not discovered in analytical methods with satisfactory results.

In instances where an analytical solution is unavailable, a diverse range of phenomena necessitate numerical evaluation. The complexity inherent in nonlinear differential equations (DEs) poses challenges to their solution. This underscores the significance and efficacy of numerical approaches. Numerous methods have been devised to ascertain outcomes for DEs of intricate nature, aiming for results closely aligned with exact values. Techniques such as the "finite difference method," "finite element method," "spectral method," and "Haar scale 2 wavelet method" are commonly employed. These methods entail discretizing the domain of the problem and employing iterative algorithms to approximate a solution that accommodates a defined margin of error.

As a result, for solving these types of equations, more numerical methods are necessary. Therefore, to solve these forms of DEs, researchers have been focusing on enhancing existing methods and developing hybrid approaches. Numerical analysis, a mathematical discipline dedicated to devising effective methods for tackling challenging mathematical problems, plays a crucial role. One of the effective methods used for facing these challenges is wavelet methods. Basically, wavelets are mathematical expressions that attain attention in different fields of science like signal process, data analysis and image compression. In comparison to Fourier series, wavelets gained more importance due to its ability to find out the solution of physical problem in respect to both space and time. In this study, we advanced the numerical solutions for nonlinear differential equations (DEs) by incorporating the Haar scale 3 wavelet method

(HS3WM) with the collocation method, the Quasilinearization technique, and the Gauss elimination method.

The objective is to develop a numerical methodology for solving nonlinear differential equations (DEs). Incorporating various equations, such as the Korteweg-de Vries (KdV), Lane-Emden and Emden-Fowler, fractional Kawahara equations, and many more, is crucial for constructing diverse mathematical models, thereby enhancing their relevance in scientific research. By formulating a numerical approach to solving these equations, researchers can gain a deeper understanding of their behavior and potential applications. This, in turn, facilitates the generation of innovative solutions to a wide range of scientific and engineering challenges.

1.1.1 Ordinary Differential Equation:

In mathematics, a DE with one or more functions of a single independent variable and their derivatives is known as an ODE. ODE can be found in a diverse range of disciplines, such as geometry, mechanics, astronomy, and population modeling. Lane-Emden, Leibnitz, the Bernoulli's, Riccati, Vander-Pol, Clairaut, D'Alembert, and Euler are only a few of the notable mathematicians who studied DEs and contributed to the area.

LEE:

$$y'' + \frac{2}{x}y' + y^b = 0$$

EFE:

$$\chi''(l) + k\chi'(l) + \chi(l) = 0.$$

1.1.2 Partial Differential Equation:

PDEs have one dependent variable and more than one independent variable, as well as their partial derivatives with respect to the independent variable.

$$F\left(x_1, x_2, x_3, \dots, x_n, y, \frac{\partial y}{\partial x_1}, \frac{\partial y}{\partial x_2}, \frac{\partial y}{\partial x_3}, \dots, \frac{\partial y}{\partial x_n}, \frac{\partial^2 y}{\partial x_1^2}, \frac{\partial^2 y}{\partial x_2^2}, \dots, \frac{\partial^2 y}{\partial x_n^2}, \dots, \frac{\partial^n y}{\partial x_n^n}\right) = 0$$

KdV, and non-linear KGE are examples of PDEs.

Dispersive KdV Equation:

$$u_t + \epsilon uu_x + \alpha u_{xxx} = f(x, t)$$

Non-linear KGE:

$$u_{tt} - u_{zz} + \mu u - \epsilon u^2 = m(z, t)$$

PDEs are extremely important because they link the physical and mathematical worlds. It is extremely useful in describing natural phenomena in science and engineering. The ICs and BCs of a PDE are used to perform many engineering computations. We discovered that it describes several processes, such as heat flow, wave propagation, and basic physics ideas from various perspectives. We study the vital role of PDEs in the diffusion of neutrons in nuclear reactors, study of population models, reactivity of chemical materials, fluid dynamics, quantum mechanics, and electricity.

1.1.3 Fractional Differential Equation:

FDEs have one or more than one independent variables and contain fractional derivatives with respect to the dependent variable.

$$F \left(x_1, x_2, x_3, \dots, x_n, y, \frac{\partial^{k_1} y}{\partial x_1^{k_1}}, \frac{\partial^{k_1} y}{\partial x_2^{k_1}}, \dots, \frac{\partial^{k_1} y}{\partial x_n^{k_1}} \right) = 0$$

Where $[k_1] < k_1 < [k_1 + 1] \forall n$

FDEs are the generalised form ODEs and PDEs. Some of the examples of this equations are Riccati equation, Kawahara equation.

Fractional Riccati Equation:

$$D^\alpha y(x) = -y^2(x) + 1$$

Fractional Vander Pol Equation:

$$D^\alpha y(m) + \frac{dy(m)}{dm} + y(m) + y^2(m) \frac{dy(m)}{dm} = F(m, y)$$

Fractional KE:

$$D_y^\mu \varphi(m, y) + k\varphi_z + \varphi_{zzz} - \varphi_{zzzz} = f(m, y)$$

FDEs have numerous uses within the realms of magnetism, fluid mechanics, heat transfer, the theory of viscoelasticity, the RLC electric circuit, wave propagation in the viscoelastic horn, and the cardiac tissue–electrode interface.

1.2 Fractional Calculus:

Fractional calculus (FC) has evolved into a highly valuable tool for elucidating intricate physical and chemical phenomena involving complex kinetics and microscopic structures. It has become more important over the past few decades as it has enormous significance in numerous fields like as in solid mechanics, signal processing, fluid flow, viscoelasticity, and statistics. The quantity of works describing the memory and intrinsic qualities of diverse substances using FEs that comprise derivatives and integrals of arbitrary order. The quantity of works describing the memory and intrinsic qualities of diverse substances using FEs that comprise derivative and integrals of arbitrary order. In a 1695 letter to Leibniz, L' Hospital sought clarification on a particular notation Leibniz had introduced a linear function whose derivative had n^{th} -order. Inquiring Leibniz to what would happen as if the value of n became half. Leibniz replied by stating that a puzzle is generated with important consequences in the future. Therefore, it was the first time that a fractional derivative was considered. Weierstrass-type functions are one example of a FD model with a non-differentiable but continuous solution [1]. OD or PD models cannot be used to explain these types of properties.

In the past, fractional calculus was primarily a mathematical concept with no apparent practical use. However, in today's world, fractional calculus has become immensely significant in the realms of science and technology due to its wide-ranging applications in areas such as thermo-elasticity theory [2], viscoelastic fluids [3], earthquake dynamics [4], fluid dynamics, and more [5]. In an experiment conducted on the movement of a rigid plate immersed in a Newtonian fluid by Bagley and Torvik, Surprisingly, the experiment demonstrated that the resisting force is directly linked to the displacement in the form of a fractional derivative in comparison to the velocity, as expected. Moreover, their experiment observations suggested that, in accurately predicting the properties of the same material, the fractional model is better than the previous ones. Furthermore, it has been experimentally observed, as well as confirmed through real-time observations, that numerous complex systems in the real-world exhibit anomalous dynamics. Examples of such systems include relaxation phenomena in viscoelastic materials, the diffusion of pollutants in the environment, and the transport of charges in amorphous semiconductors,

among others. The scientific community has shown significant interest in the enhanced efficiency and accuracy offered by FDEs in describing unusual system dynamics. These equations have extended numerous classical DEs, originally defined with integer orders, to generalized fractional forms, enabling a more comprehensive exploration of the associated physical models.

1.3 Definition of Fractional calculus:

FC introduces the notion of derivatives with real orders, even for complex and arbitrary values. Essentially, it serves as a generalized version of classical calculus. Many researchers are embracing FC definitions to introduce the concept of fractional-order derivatives and integrals. Within fractional derivatives, there exist various established definitions, such as the Riemann-Liouville definitions, Grunwald-Letnikov, and Caputo. Among these, the Riemann-Liouville definition is the most commonly used; however, it may not be suitable for addressing all types of physical models. Caputo proposed a definition in which ICs are specified in an integral order, unlike the Riemann-Liouville definition, where ICs are established in a fractional order. In contrast, the Grunwald-Letnikov method approaches the problem by defining the derivative itself. This particular approach is primarily employed in numerical algorithms and represents an extension of the derivative concept to fractional orders.

1.3.1 Mittag Leffler:

Mittag Leffler is general form of exponential function. As one-parameter function in the series it can be introduced in the form [1]:

$$E_p(z) = \sum_{n=0}^{\infty} \frac{z^n}{\Gamma(pn + 1)}, n > 0, p \in R, z \in C.$$

and in two-parameter function it is written as:

$$E_{p,q}(z) = \sum_{n=0}^{\infty} \frac{z^n}{\Gamma(pn + q)}, n > 0, p, q \in R, z \in C.$$

Some of the properties of Mittag Leffler function are:

$$E_{1,1}(n) = e^n$$

$$E_{2,1}(n^2) = \cosh(n)$$

$$E_{2,2}(n^2) = \frac{\sinh(n)}{n}$$

$$E_{\alpha,1}(n) = E_{\alpha}(n)$$

1.3.2 Reimann-Liouville fractional operator of order μ :

For the positive real numbers, μ , y across the interval $[m, n]$, the FDO established by the mathematician Riemann-Liouville is given by [1]:

$$d^\mu f(y) = \frac{1}{\Gamma(p - \mu)} \left[\frac{d}{dy} \right]^p \int_m^n f(z)(y - z)^{p-\mu-1} dz$$

where μ denotes the order of derivative and $y \in [m, n]$.

1.3.3 Caputo Fractional operator of order μ :

For positive real numbers, μ , y , the FDO developed by the Italian mathematician Caputo:

$$d^\mu f(y) = \frac{1}{\Gamma(p - \mu)} \int_m^n \left[\frac{d}{dy} \right]^p f(z)(y - z)^{p-\mu-1} dz$$

where μ denotes the order of derivative and $y \in [m, n]$.

1.4 Multi resolution analysis:

To ensure that the theory of wavelets and MRA develops smoothly, it is necessary to make modest assumptions about the refinement function. The structure of wavelets can be better understood via MRA. The general technique in wavelet analysis is to use an appropriate basis to transform a problem into its wavelet domain. To acquire the desired results, the issue is solved in the wavelet domain and then transformed back. The ability to show information in a hierarchical fashion is a key feature of wavelet analysis. Wavelets are a type of basis function that can represent a signal in both the time and in frequency domains. MRA is a useful tool for studying functions at different degrees of detail or resolution [6]. MRA relies on the mathematical idea of expressing a signal as a convergence of refined approximations. Each of these approximations refines the function further and corresponds to distinct resolution levels. As a result, MRA is a method for creating orthogonal wavelet bases that follows a set of principles and methods. The primary characteristic of this analysis lies in its use of mathematics to explain the exploration of signals or images across different scales. The notion of MRA is used in the $\phi_m(m \in Z)$ family of Haar wavelets, which entails a sequence of nested close

approximation subspaces. The increasing function $\{\phi\}_{m,n \in \mathbb{Z}}$ of a subset of $L^2(\mathbb{R})$ with a scaling function φ is called MRA if it satisfies the condition.

- I. $\dots \subset \phi_{-1} \subset \phi_0 \subset \phi_1 \subset \dots$ is known as Monotonicity.
- II. The spaces ϕ_j satisfies $\bigcap_{-\infty}^{\infty} \phi_n = 0$ and $\bigcup_{-\infty}^{\infty} \phi_n = L^2(\mathbb{R})$ is known as Separation.
- III. $f(t) \in \phi_0$ iff $f(2^n t) \in \phi_n$ for all $n \in \mathbb{Z}$ the space V_j are scaled version of the central space ϕ_0 is known as Dilation.
- IV. There exist $\varphi \in \phi_0$ such that $\{\varphi(t-k); k \in \mathbb{Z}\}$ is a Riesz basis in ϕ_0 is known as Existing of scaling.

1.5 Quasi-linearisation:

For obtaining numerical solutions to individual or systems of nonlinear DEs, a generalization of the Newton-Raphson method is used (ODEs or PDEs). The basis and advantage of this approach stem from the observation that linear equations can frequently be solved through analytical or numerical methods, whereas finding a comprehensive solution to a nonlinear DE in relation to a limited collection of precise solutions, lacks practical methods. In the Quasi-linearization method, nonlinear DEs are resolved iteratively through a sequence of linear DEs. This technique not only transforms the nonlinear equation into a linear form but also produces a sequence of functions that approaches the solution of the original nonlinear equation as it converges and makes it applicable in real-world scenarios. Basically, Quasilinearisation technique is generalized form of Newton-Raphson technique. It converges to the exact solution in its original form. Quadratically, it must show a monotone convergence [7].

1.6 Collocation Points:

The HW collocation approach has been employed in the literature to investigate and gain insight into a multitude of physical phenomena described by DEs. One of the prevalent discretization methods, known as the collocation approach, was introduced by Kantorovich in 1934 as part of the weighted residuals approach for solving DEs. In 1937, three years following its initial proposal by Frazer R.A. and his colleagues, the same approach was reintroduced for the identical objectives. In the collocation method, weighted truncated series expansions of basis functions are utilized to approximate the solution function at various points within the domain, referred to as collocation points. These weighted functions play a critical role in ensuring that a minimized set of basis functions can effectively satisfy the DEs. Consequently, the careful selection of appropriate weight functions is vital for obtaining an accurate AS with minimal residual errors when solving a DE.

1.7 Historical Background of Wavelets:

The core concept in wavelet studies involves analyzing data based on different scales. Many researchers in this field believe that employing wavelets represents a novel approach to data processing. Wavelets, which are functions meeting specific mathematical criteria, serve the purpose of representing data or other functions. Wavelet algorithms handle data at various scales or resolutions. Historically, scientists have approximated functions by expanding them into sine and cosine terms for several decades. According to this definition, these functions exhibit non-local characteristics, making them ineffective at approximating sharp spikes. However, wavelet analysis allows us to approximate functions within finite domains, making it well-suited for handling data with abrupt discontinuities.

Wavelet analysis utilizes a fundamental function called the mother wavelet. In temporal analysis, a compressed, high-frequency form of the prototype wavelet is employed, while frequency analysis utilizes an expanded, low-frequency version of the same wavelet. Given that the original signal can be expressed as a wavelet expansion, data manipulations can be conducted using the wavelet coefficients. Other applied fields that are making use of wavelets include astronomy, earthquake predictions, imaging, acoustics, human vision, neurophysiology, nuclear engineering, speech discrimination, magnetic resonance, sub-band coding, signal and image processing, optics, fractals, turbulence, radar, and pure mathematics applications such as solving PDEs. Recent years have witnessed an intense activity and interest in both the mathematical development of wavelets and their applications. The potential applications of wavelets appear limitless across various fields. Wavelets allow for the decomposition of intricate information, such as patterns, speech, music, and images, into fundamental building blocks at different scales and positions. These components can then be reconstructed with a high degree of accuracy [8]–[10]. Another area in which wavelets are gaining importance is the numerical analysis of DEs. In numerical analysis, wavelets have an enormous impact because of their inherent properties, computational efficiency, adaptivity. Additionally, the unidentified solution can be expressed through wavelets of varying resolutions, leading to a multigrid representation, which is much more compact and more comfortable for implementation. Wavelet-based thresholding techniques can transform the dense matrix produced by an integral operator into a sparse form, allowing for the achievement of any desired level of solution accuracy. Besides, the wavelet methods offer several advantages over the traditional numerical and semi-analytical methods.

There are numerous numerical methods for solving IVP and BVP that have been discussed. FE, FV, and FD are a few of them. However, these approaches have several limitations, such as high

cost and low order. These methods are effective in space localization, although they are inaccurate. Another semi-analytical technique produces an invalid series solution as a consequence of its analysis. In the spectral approach, a solution is approximated by using a set of indefinitely differentiable and nonvanishing basis functions throughout the entire domain. If the expected solution is in nature, spectral approaches have an exponential rate of convergence. However, the spatial localization is a discontinuous and non-smooth process. Spectral approaches offer a cost-effective solution, yet they are less effective for problems involving intricate geometries compared to FDM, FEM, and FVM, which operate with localized support. The methods work on local support such as FEM, FVM, and FDM, but the spectral technique works on global support. For complex problems with irregular geometry, spectral approaches have poor spatial localization, but they are more accurate and cause less error. FDM, FEM, and FVM, on the other hand, are less precise but have strong spatial localization. Each method has its own set of benefits and drawbacks.

In this scenario, wavelet-based methods emerge as a viable solution, as they enable us to incorporate the advantages of all these approaches into an estimate of an unknown solution. Because they are orthonormal, have compact support for translation, dilation, and multiresolution analysis, are computer-friendly, and are localized in both time and space, wavelets are able to handle a variety of issues in science and technology. To deal with more complicated problems, wavelet-based approaches can readily be expanded to higher dimensions. Wavelets are well-suited to establishing a link with well-established, fast, and highly accurate numerical algorithms. In the last few decades, wavelet has become a research topic for both pure and applied researchers. In domains such as time series analysis and numerical solutions of DEs using wavelet analysis, computations are more precise and time-efficient. Wavelet methods are acknowledged as one of the effective and rapidly developing techniques for solving ODEs and PDEs numerically, with increasing applications in science and engineering. With the passage of time, it develops into a strong weapon that can be used to solve a variety of situations. In general, wavelet decomposition analysis is used in signal processing for communication and signal identification. For functions with no smoothness but adequate to evaluate the behavior of a function around a point, Fourier series of functions with orthogonal functions can be employed. The wavelet transform is preferable to the Fourier series because it can study non-stationary, time localized events, whereas Fourier series can only provide exact solutions for time-independent events.

The term 'wavelet' describes a vanishing wave that oscillates within a limited time frame, enabling the representation of the time-frequency plane using atoms of varying time supports. A wavelet is a compact wave that can be modified in two distinct manners: translation, which involves shifting all of the wavelet's points in the same direction and for the same distance, and dilation, which involves stretching or decreasing the original wavelet.

$$\psi_{a,b}(t) = \frac{1}{\sqrt{|a|}} \psi\left(\frac{t-b}{a}\right)$$

where a is the dilation parameter and b is the translation parameter, A "mother wavelet," a function $\psi(t)$ confined within a finite interval, can serve as the foundation for generating a family of wavelets. $\psi_{a,b}(t)$ is known as Daughter wavelet are formed by translation of b and contraction or dilation of a .

1.7.1 Wavelet transform:

Wavelet transform is a real and complex valued function can be represented as:

$$w_{\psi}(f)(a, b)(t) = \int_{-\infty}^{\infty} f(t) \frac{1}{\sqrt{|a|}} \psi\left(\frac{t-b}{a}\right) dt$$

Which represents how much the scaled wavelet is like the function $f(t)$ at location $t=(b/a)$ where a is the dilation parameter and b is the translation parameter. It has a wider-applications in medical and scientific sectors for diagnosis and communication.

1.7.1.1 Orthonormal Wavelets:

Orthonormal wavelets are contemporary functions equipped with the capabilities of dilation and translation. These characteristics allow wavelet-based numerical algorithms to show a qualitative improvement over other-techniques.

1.7.1.2 $L_2(\mathbf{R})$ Space:

Vector space of square integral functions is $L_2(\mathbf{R})$ Space. To achieve finite coefficients for unknowns, it is crucial for the vector space to consist of square-integrable functions.

$$L_2(\mathbf{R}) = f: \mathbf{R} \rightarrow \mathbf{C}: \int_{-\infty}^{\infty} |f(t)|^2 dt < \infty$$

1.7.1.3 Inner Product Space:

In wavelet theory, an IPS is a vector space equipped with an inner product, which is a mathematical operation that takes two vectors as input and returns a scalar. The inner product measures the similarity or "closeness" of the two vectors and is typically denoted by a dot product. In the context of wavelet theory, an IPS is used to describe the properties of wavelet functions, which are functions that can be used to represent signals and other functions in terms of a set of basis functions. The IPS provides a framework for studying the properties of wavelet functions, including their orthogonality, completeness, and other important properties. By analyzing the properties of wavelet functions in an IPS, researchers can develop algorithms for signal processing, data compression, and other applications.

1.7.1.4 Translation and Dilation operator in $L_2(\mathbf{R})$ Space:

These operators are important in wavelet theory because they are used to generate the wavelet basis functions through a process called dyadic decomposition, which involves translating and dilating a single mother wavelet function to generate a family of wavelets with different scales and positions.

1.8 Types of Wavelets:

1.8.1 Continuous wavelet:

Continuous Wave Transform can effectively treat signals or functions that have multiple high-frequency components in their Fourier series. The translation and dilation parameters vary continuously. A wavelet function $\psi(t)$:

- continuous and the integral of $\int_{-\infty}^{\infty} \psi(t) dt = 0$
- square integrable $\int_{-\infty}^{\infty} |\psi(t)|^2 dt < \infty$

Then the Continuous wavelet transforms of a function $f \in L^2(\mathbf{R})$ is a function:

$$(W_f)(a, b)(t) = \int_{-\infty}^{\infty} f(t) \frac{1}{\sqrt{|a|}} \psi\left(\frac{t-b}{a}\right) dt$$

1.8.2 Discrete wavelet:

By discretizing the dilation and translation variables, stability in reconstruction can be achieved due to the redundancy inherent in continuous wavelet transform. Furthermore, a real orthonormal basis can be obtained. The scaling parameter 'a' is discretized using a logarithmic discretization. $a = a_0^m$ with m being an integer and a_0 is not equal to 1. For the translation

parameter 'b' it is chosen $b = nb_0a_0^m$ with m and n are integers. Then $\psi(a_0^m t - nb_0)$ covers the whole-time axis for any given scale a_0^m . Now the family of discrete wavelet functions is given by:

$$\psi_{mn}(t) = |a_0|^{\frac{m}{2}} \psi(a_0^m t - nb_0) , m, n \in Z$$

1.8.3 Haar Wavelets:

Wavelets are mathematical tools that have the potential and efficiency to break down data functions or operators into individual frequency components and scrutinizing each component at a resolution aligned with its scale. In the literature, various wavelets with distinct characteristics are available for analysing diverse types of data. However, the Haar wavelet (HW) being the most mathematically straightforward, computationally economical, is conceptually clear, and memory-efficient wavelet with compact support. The HW approach, which dates back to 1909 [11], is one of the simplest wavelet methods in contrast to others. The HW is a piecewise constant function with compact support as one of its properties. J. Morlett presented the wavelet notion to discuss his functions in the early 1980s, but it received little attention. However, Ingrid Daubechies transformed this tool into a formidable mathematical tool for solving various practical problems by demonstrating its application in several fields in 1980. We discovered that several forms of wavelets exist with various properties for signal processing, picture processing, data analysis, and communication in the literature. In 1982, Jean Morlet, an engineer, pioneered the concept of wavelets by exploring a family of functions generated through scaling and shifting a fundamental function, referred to as the mother wavelet.

$$\phi_{ab}(t) = \frac{1}{\sqrt{a}} \phi\left(\frac{t-b}{a}\right)$$

Here a represents dilation, whereas b represents translation. One of the simplest methods in comparison to others wavelet method is HWM. The technical disadvantage of the HW is that it is not continuous, and therefore not differentiable.

Because of its minimal computing demands, the Haar transform has primarily found applications in pattern recognition and image processing [5], [12]–[14]. Consequently, Haar transforms are highly efficient in the realm of 2-D image and signal processing due to their wavelet-like structure. It's widely recognized in this field that the most fundamental orthogonal wavelet system is often derived from the Haar scaling function and wavelet. Furthermore, wavelets are regarded as a broader application of Haar functions and transforms [15], [16]. This transform

finds practical applications in communication technology, including multiplexing, digital filtering and data coding [5], [17], [18]. For instance, the non-normalized Haar transform is employed in sequence division multiplex systems, as discussed in [19]. The paper presents an efficient bandwidth utilization method for multiplexed digital channels using the Haar transform. Additionally, real-time applications benefit from specialized hardware; fast Haar chips have been developed to support these functions. Various extensions of the Haar functions and transforms find applications in digital speech processing, voice-controlled computing devices and enabling functionalities in robotics. Reference [20] delves into a control system employing Haar spectrum for military airplanes. Additionally, [19] and [21] explore the applications of the Haar transform in control and communications. In [22], diverse Haar function forms are employed for approximate calculations of analytic functions. Furthermore, [5] provides a concise exploration of other applications where Haar and Walsh functions offer advantages over the Fourier transform.

One advantageous aspect of HW is their ability to be analytically integrated any number of times. Haar wavelets prove highly efficient in handling singularities, as they can serve as intermediary BCs. By reducing DEs to solving a system of algebraic equations, HW significantly simplify the problem.

The fundamental and simplest version of Haar wavelet is the Haar scaling function, which manifests as a square wave across the given interval, denoted with and generally written as $[0,1]$.

$$h_i(t) = \begin{cases} 1 & 0 \leq t < 1 \\ 0 & \text{else where} \end{cases}$$

The expression mentioned above, known as the Haar father wavelet, represents the initial level of wavelet analysis. It features neither displacement nor dilation, both being of unit magnitude.

The HWs have found applications in diverse fields, including image digital processing, physics (for characterizing Brownian motion and quantum field theory), numerical analysis, and more. In recent years, they have been utilized in a wide array of applications. The Haar transform stands as one of the earliest instances of what is now recognized as a dyadic, orthonormal, and compact wavelet transform. Haar functions appear very attractive in many applications as for example, edge extraction, binary logic design and image coding. In the realm of logic design, when applying the Haar wavelet (HW) transform, it is essential to have efficient approaches for computing the Haar spectrum from simplified representations of Boolean functions. These techniques have been introduced for deriving the Haar spectrum from disjoint cubes and various

types of decision diagrams. Furthermore, the field of optimal control theory has witnessed extensive use of HWs since their inception, primarily due to their capacity to model processes with long-term memory. Beyond control theory, these wavelets find applications in diverse domains such as structural dynamics, chemical engineering, space exploration, and economics.

There is considerable interest in diverse applications encompassing areas such as process and manufacturing, energy systems and management, environmental control, electric power generation and distribution, aerospace, defence, biomedical systems, chemical, petrochemical, industrial processes, socio-economic models, robotics and manufacturing systems, operations research, business, electrical, electronic systems, as well as healthcare and support services. These applications span a wide array of interdisciplinary and complex systems issues, where solutions often intelligent sensors, involve multi-agent software, and both dynamic and static optimization techniques.

Haar wavelets find common applications in signal processing. Digital images demand substantial storage due to their redundant data, making efficient processing crucial. Slow internet connections can significantly delay downloading large data sets. Wavelet transforms are instrumental in speeding up this process. Upon clicking to download an image, the computer retrieves the wavelet-transformed matrix from its memory. It then processes both approximations and detailed coefficients swiftly, enhancing the overall download experience. The development of the mathematical theory of wavelets initially caused certain excitement in the scientific computation community; however, we will show that not all applications of wavelets result in immediate advantages, particularly in terms of efficiency. Great care should be taken with respect to claims of efficiency.

1.8.4 Haar Scale 2 (HS2WM):

Wavelet family is expressed as in terms of mathematical form:

$$\text{Haar scaling function } \phi(t) = \begin{cases} 1 & 0 \leq t < 1 \\ 0 & \text{else where} \end{cases}$$

$$\text{Haar wavelet function } \varphi(t) = \begin{cases} 1 & 0 \leq t < 1/2 \\ -1 & 1/2 \leq t < 1 \\ 0 & \text{else where} \end{cases}$$

Haar wavelet family is defined as

$$h_i(t) = \psi(2^j t - k) = \begin{cases} 1 & \alpha_1(i) \leq t \leq \alpha_2(i) \\ -1 & \alpha_2(i) \leq t < \alpha_3(i), \\ 0 & \text{elsewhere} \end{cases} \quad i = 1, 2, 3, \dots, 2p$$

$$\alpha_1(i) = \frac{k}{p}, \alpha_2(i) = \frac{2k+1}{2p}, \alpha_3(i) = \frac{(k+1)}{p}, p = 2^j, j = 0, 1, 2, \dots, k = 0, 1, 2, \dots, p-1.$$

The wavelet number i is determined using the equation $i-1=p+k$, where J signifies the level of wavelet dilatation (with higher J values indicating reduced wavelet support), and k represents the wavelet's translation parameters. The term $h_1(t)$ is referred to as the father wavelet, while $h_2(t)$ is known as the mother wavelet. All other functions, such as $h_3(t)$, $h_4(t)$, $h_5(t)$, and so on, are derived through translation and dilation of the mother wavelet.

At $i = 2^{J+1}$, attains its maximum value,

$$h_1(t) = \begin{cases} 1, & t \in [0, 1) \\ 0, & \text{elsewhere} \end{cases}$$

The Haar function can be derived by discretizing the points into collocation points.

$$t = \frac{i - 0.5}{2M}$$

1.8.4.1 Integrals of HS2WM:

The generalized form of Haar wavelet integrals can be expressed as follows:

$$\phi_{1,s}(t) = \int_0^x h_{1,s}(t) dt$$

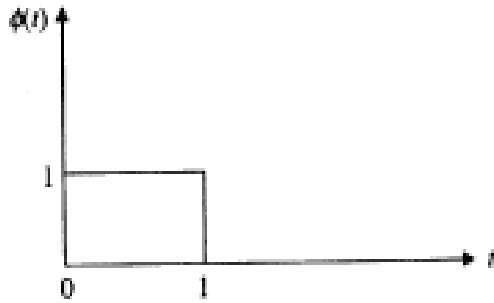
$$\phi_{1,s+1}(t) = \int_0^x \phi_{1,s}(t) dt$$

It can be written as:

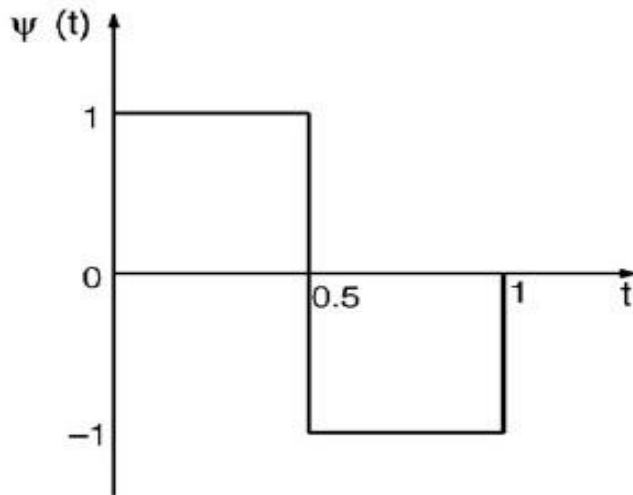
$$\phi_{i,s+1}(t) = \begin{cases} \frac{t^s}{\Gamma(s+1)} & , \quad \alpha_1 \leq t < \alpha_2 \\ 0 & \text{otherwise} \end{cases}$$

$$\varphi_{i,s+1}(t) = \begin{cases} \frac{[t - \mu_1(i)]^s}{\Gamma(s+1)} & ; \mu_1(i) \leq t < \mu_2(i) \\ \frac{[t - \mu_1(i)]^s - 2[t - \mu_2(i)]^s}{\Gamma(s+1)} & ; \mu_2(i) \leq t < \mu_3(i) \\ \frac{[t - \mu_1(i)]^s - 2[t - \mu_2(i)]^s + [t - \mu_3(i)]^s}{\Gamma(s+1)} & ; \mu_3(i) \leq t < \mu_4(i) \\ 0 & ; \text{otherwise} \end{cases}$$

1.8.4.2 Graphs of Haar Scale 2:



Haar Scaling Function



Haar Wavelet Function

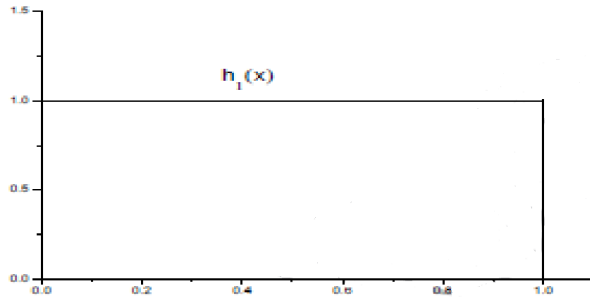
1.8.5 Haar Scale 3 (HS3WM):

Wavelet family with dilation factor three expressed in the form:

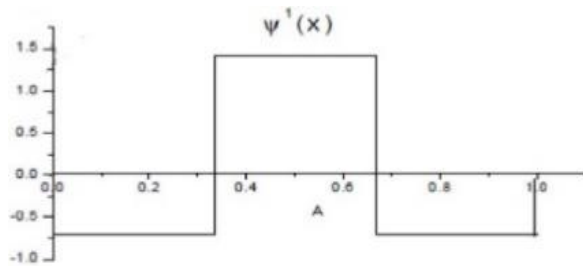
$$\text{Haar Scaling function } \phi(t) = \begin{cases} 1 & 0 \leq t \leq 1 \\ 0 & \text{otherwise} \end{cases}$$

$$\text{Haar Symmetric Wavelet function } \varphi^1(t) = \frac{1}{\sqrt{2}} \begin{cases} -1 & 0 \leq t \leq \frac{1}{3} \\ 2 & \frac{1}{3} \leq t \leq \frac{2}{3} \\ -1 & \frac{2}{3} \leq t \leq 1 \\ 0 & \text{otherwise} \end{cases}$$

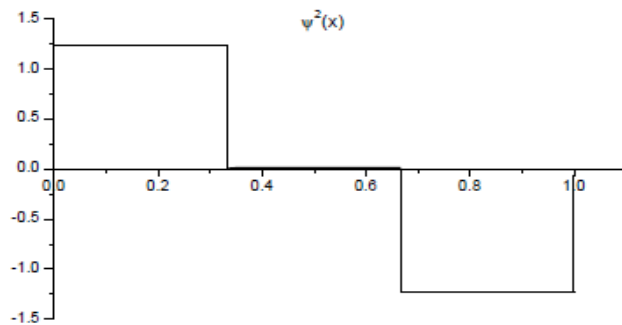
$$\text{Haar Anti-symmetric Wavelet function } \varphi^2(t) = \frac{1}{\sqrt{2}} \begin{cases} 1 & 0 \leq t \leq \frac{1}{3} \\ 0 & \frac{1}{3} \leq t \leq \frac{2}{3} \\ -1 & \frac{2}{3} \leq t \leq 1 \\ 0 & \text{otherwise} \end{cases}$$



Haar Scaling Function



Haar Wavelet φ^1



Haar Wavelet φ^2

$$h_i(t) = \phi(t) = \begin{cases} 1 & 0 \leq t \leq 1 \\ 0 & \text{otherwise} \end{cases} \text{ for } i = 1$$

$$h_i(t) = \varphi^1(3^j - k)(t) = \frac{1}{\sqrt{2}} \begin{cases} -1 & a_1 \leq t \leq a_2 \\ 2 & a_2 \leq t \leq a_3 \\ -1 & a_3 \leq t \leq a_4 \\ 0 & \text{otherwise} \end{cases} \text{ for } i = 2, 4, 6, \dots, 3p - 1$$

$$h_i(t) = \varphi^2(3^J - k)(t) = \sqrt{\frac{3}{2}} \begin{cases} 1 & a_1 \leq t \leq a_2 \\ 0 & a_2 \leq t \leq a_3 \\ -1 & a_3 \leq t \leq a_4 \\ 0 & \text{otherwise} \end{cases} \text{ for } i = 1, 3, 5, \dots, 3p$$

Where $a_1(i) = \frac{k}{p}$, $a_2(i) = \frac{3k+1}{3p}$, $a_3 = \frac{3k+2}{3p}$, $a_4 = \frac{k+1}{p}$, $p = 3^J$, $J = 0, 1, 2, 3, \dots$, $k = 0, 1, 2, \dots, p - 1$.

here i , J and k respectively, represents wavelet number, resolution level (dilation parameter) and translation parameter. Here $h_2(t)$ and $h_3(t)$ are mother wavelets and rest generated from mother wavelets are called daughter wavelets.

At $i = 3^{J+1}$, attained its maximum value,

$$h_1(t) = \begin{cases} 1, & t \in [0, 1) \\ 0, & \text{elsewhere} \end{cases}$$

The Haar function can be derived by discretizing the points into collocation points.

$$t = \frac{i - 0.5}{3M}$$

1.8.5.1 Integrals of HS3WM:

HW integrals in generalised form can be written as:

$$\phi_{1,s+1}(t) = \int_0^x \phi_{1,s}(t) dt$$

$$\varphi_{1,s+1}^1(t) = \int_0^x \varphi_{1,s}^1(t) dt$$

$$\varphi_{1,s+1}^2(t) = \int_0^x \varphi_{1,s}^2(t) dt$$

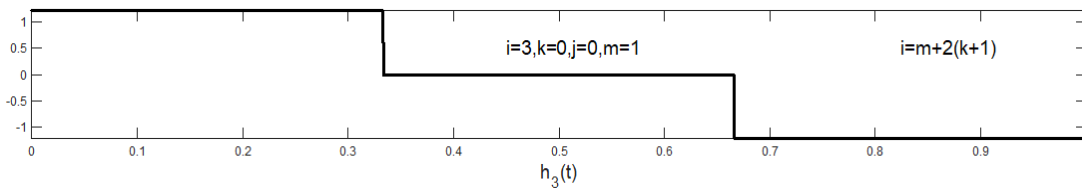
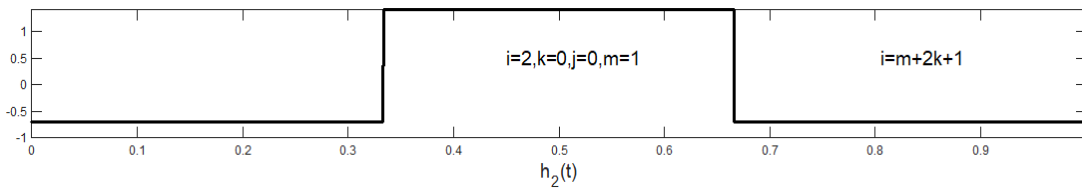
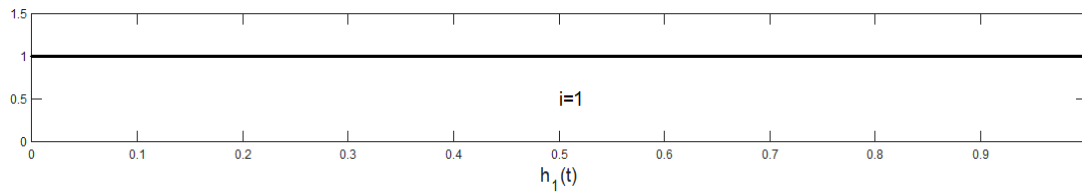
It can be written as:

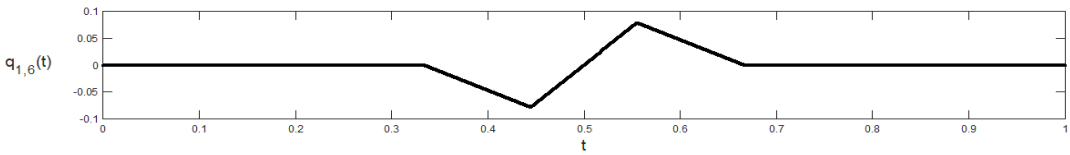
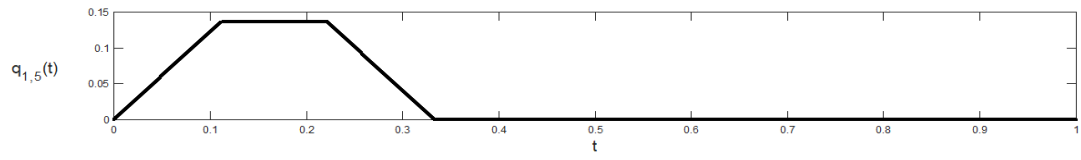
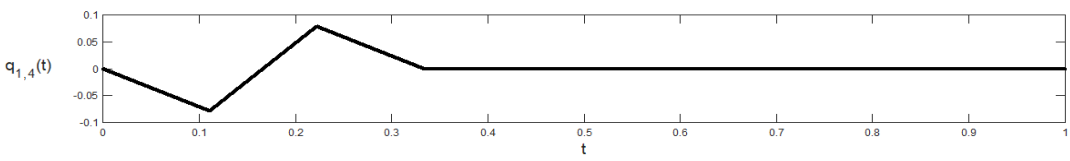
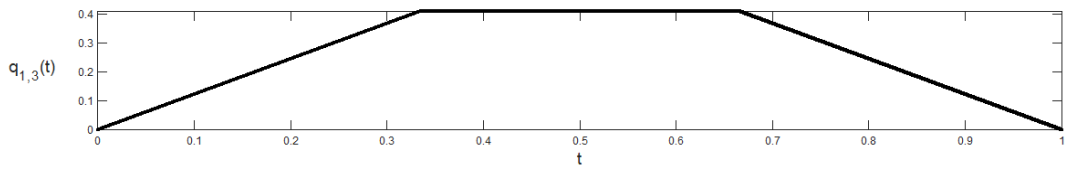
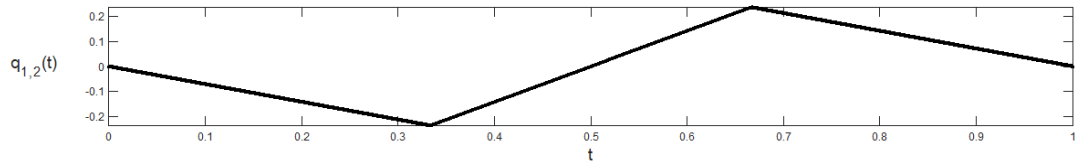
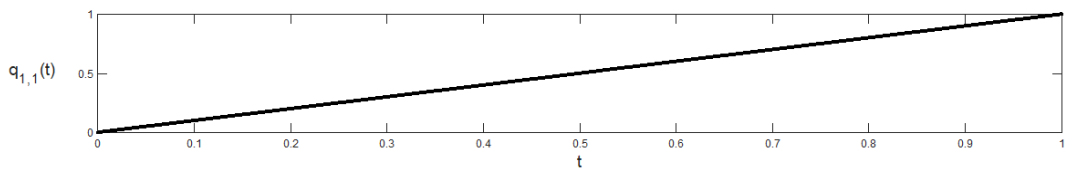
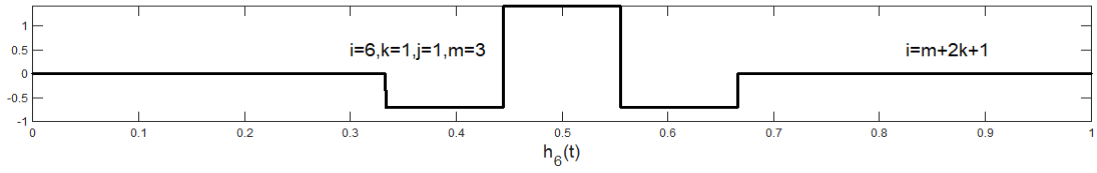
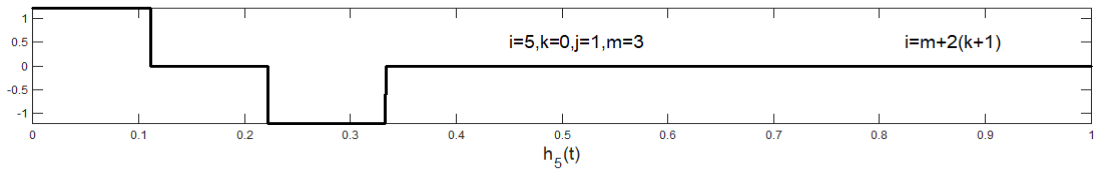
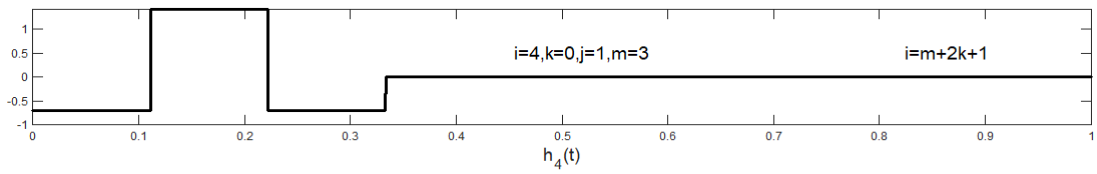
$$\phi_{i,s+1}(t) = \begin{cases} \frac{t^s}{\Gamma(s+1)} & , \quad \alpha_1 \leq t < \alpha_2 \\ 0 & \text{otherwise} \end{cases}$$

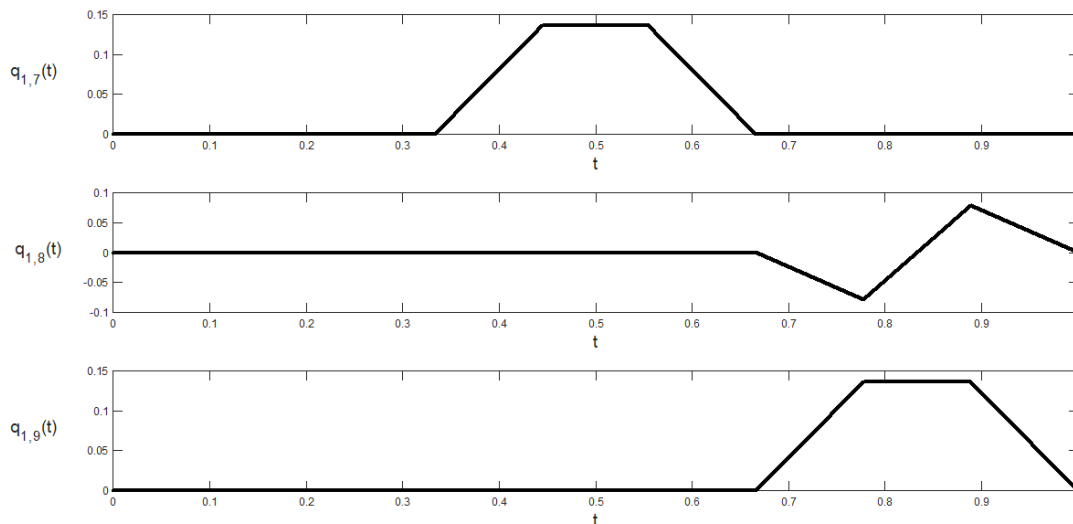
$$\varphi_{i,s+1}^1(t) = \frac{1}{\sqrt{2}} \begin{cases} 0 & ; 0 \leq t < \mu_1(i) \\ \frac{-[t - \mu_1(i)]^s}{\Gamma(s+1)} & ; \mu_1(i) \leq t < \mu_2(i) \\ \frac{3[t - \mu_2(i)]^s - [t - \mu_1(i)]^s}{\Gamma(s+1)} & ; \mu_2(i) \leq t < \mu_3(i) \\ \frac{3[t - \mu_2(i)]^s - 3[t - \mu_3(i)]^s - [t - \mu_1(i)]^s}{\Gamma(s+1)} & ; \mu_3(i) \leq t < \mu_4(i) \\ \frac{3[t - \mu_2(i)]^s - 3[t - \mu_3(i)]^s - [t - \mu_1(i)]^s + [t - \mu_4(i)]^s}{\Gamma(s+1)} & ; \mu_4(i) \leq t < 1 \end{cases}$$

$$\varphi_{i,s+1}^2(t) = \sqrt{\frac{3}{2}} \begin{cases} 0 & ; 0 \leq t < \mu_1(i) \\ \frac{[t - \mu_1(i)]^s}{\Gamma(s+1)} & ; \mu_1(i) \leq t < \mu_2(i) \\ \frac{[t - \mu_1(i)]^s - [t - \mu_2(i)]^s}{\Gamma(s+1)} & ; \mu_2(i) \leq t < \mu_3(i) \\ \frac{[t - \mu_1(i)]^s - [t - \mu_2(i)]^s - [t - \mu_3(i)]^s}{\Gamma(s+1)} & ; \mu_3(i) \leq t < \mu_4(i) \\ \frac{[t - \mu_1(i)]^s - 3[t - \mu_2(i)]^s - [t - \mu_3(i)]^s + [t - \mu_4(i)]^s}{\Gamma(s+1)} & ; \mu_4(i) \leq t < 1 \end{cases}$$

1.8.5.2 Graphs of Haar Scale 3 wavelet:







First integral of the first nine members of the HS3W family

1.9 Literature Review:

The origin of wavelets was introduced by Alfred Haar in his thesis in 1909 [11]. In each segment, the HW function is a constant function with the important characteristic of having a compact support. However, it has not received attention in the past few years due to its lack of continuous differentiability. But with the development of MRA by Mallat [6] and Meyer [23] in 1980, the field of wavelet analysis experienced significant growth. In the advancement of wavelet analysis, MRA played a beneficial role. MRA provides a valuable benefit by empowering researchers to create their own unique families of wavelets through mathematical techniques. Y. Meyer utilized MRA concepts to develop a novel collection of continuously differentiable wavelets. Meyer's wavelets did not possess compact support, unlike the HW. After several years, the concept introduced by Mallat and Meyer to create a novel set of wavelet bases was utilized by Daubechies [24], [25]. These developed wavelets were both orthonormal and had compact support, introducing them as a basic component of wavelet applications. After years of development and research, wavelets have evolved from being regarded as a scientific curiosity to an effective mathematical tool that can be used in a wide range of scientific disciplines. The Daubechies wavelet family is categorized by the number of vanishing moments it possesses. To achieve these vanishing moments, a system of simultaneous linear and non-linear algebraic equations was devised, resulting in the derivation of numerical coefficients. This straightforward approach gained acceptance in wavelet method development because it met the researchers' needs for understanding wavelet construction successfully. After this development, new wavelet families, including the coiflet and symlet wavelets, were introduced. These wavelets carried

attractive features such as continuity, differentiability, and compact support, which made them very useful in numerical analysis, image processing, and signal processing. Despite these benefits, a major drawback of these wavelets was that they lacked an explicit expression and were difficult to apply to discretization. As a result, analytical differentiation or integration for these wavelets is not practical because the construction of these wavelets depends on filter coefficients. When using these wavelets, it was difficult to compute integrals involving nonlinear functions because there wasn't an explicit expression. The idea of connection coefficients was developed as a solution to this problem. However, determining these connection coefficients meant performing a difficult process for every integral separately. Additionally, only simple equation nonlinearities, like quadratic equations, could be solved using this approach. Connection coefficients were successfully used by Mishra and Sabina [8] to solve DEs using the Galerkin method. However, some researchers started asking about the advantages of using the wavelet method over conventional methods due to the challenging nature of using wavelets to find solutions. Even more pessimistic opinions were expressed by Strang and Nguyen [9], who claimed that wavelets faced tough competition from other methods and that they did not believe wavelets would succeed.

Researchers investigated alternative solutions to this problem in order to address this skepticism. The problem of the HWs non-differentiability at the point of discontinuity was resolved in 1997 when researchers re-examined the existing wavelet families. Rather than approximating the solution function directly, Chen and Hsiao [26] proposed an approach of approximating the highest-order derivative using the HW series. The remaining derivatives and the solution function were subsequently derived through the integration of the HOD. This method continues to be widely employed by researchers due to its success in solving mathematical frameworks that involve integral, differential and intra-differential equations.

The work of Chen and Hsiao [26] was expanded upon by Lepik [10] by using wavelet transforms to examine the linear vibrations of systems with one and two degrees of freedom. Lepik used three distinct wavelet transformations and noticed that, for vibrations with one degree of freedom, all three wavelets produced results that were qualitatively comparable. In contrast to the third wavelet, the Morlet wavelet, the Mexican hat and HWs gave fundamentally different results for systems with degrees of freedom two. The HW was further used by Lepik and Tamme [27] to investigate the behavior of solutions to linear integral equations. We examined a number of integral equation types, such as the Fredholm and Volterra equations, the Integral-differential equations, and others. The solution obtained by using HWs outperformed traditional solutions

with the same step size, it was found. The convergence rate for the Fredholm and Volterra equations was specifically calculated to be $O(M^{-2})$. In order to investigate solutions for different kinds of ODEs and PDEs, Lepik [28] presented a novel method based on HWs. Lepik contrasted the segmentation and piecewise constant approximation methods with this approach, also known as the Chen and Hsiao method (CHM). Due to the wavelet matrices' increasing sparsity and the associated speed of computation, he noted that the CHM employing wavelets offered mathematical simplicity. However, it had difficulties approximating HOD accurately, resulting in instability of the proposed method. The HW approach was expanded by U. Lepik [29] to deal with nonlinear evolution problems. Burgers and SG equations were used to test the method's effectiveness in comparison to established classical techniques. Operational matrices for HWs were used by Chang and Piau [30] to solve ODEs. They optimized the procedure by executing computations using wavelets' integrals and their matrix representation. A technique based on HW was created by Lepik [31] to resolve various fractional integral equations. This approach proved to be fast and simple to use for solving these problems. The same year, Babolian and Shamsavaran [32] used error analysis to demonstrate the convergence of the HW approach, which was a significant problem at the time. Additionally, they managed nonlinearity for solving nonlinear Fredholm IEs. The use of the HW approach to solve nonlinear parabolic PDEs was expanded by Hariharan and Kannan [33]. They specifically evaluated the performance of the technique using well-known nonlinear PDEs. The proposed approach performed quite well, displaying its ability in dealing with nonlinearity. It was found that a large variety of nonlinear PDEs could be solved using this method. The same year, Hariharan [34] used the HWM to solve a physical model involving the deflection in a finite-length beam subject to a fourth-order ODE, as well as the BCs. In order to solve the model, the technique involved developing a generalised operation matrix and matrices for their integrals. The ES found in the literature was then compared to the results. The findings revealed that the HWM method outperformed other approaches by requiring less CPU time and delivering enhanced results with fewer degrees of freedom. With changes to the approximation method, Hariharan [35] expanded the use of the in HWM to solve the KGE and SGE. It was found that even with a limited set of points for collocation, the HW approach produces results that are more accurate, and that accuracy increases as the number of collocation points increases. The buckling of elastic beams was studied using the HW approach by Lepik [36]. The study explored various scenarios, such as simulating fractures, analysing beam vibrations on an elastic base, and studying beams with flexible cross-sections. The utilization of HW showcased several advantageous features, including remarkable accuracy with a minimal number of grid points, the application of shared

subprograms for addressing diverse problem areas, particularly in handling singularities within intermediate boundary conditions, and ease of implementation. By using several examples, the author also showed the method also used to solve problems with greater complexity. Kaur, Mishra, and Mittal [37] created an algorithm to solve different kinds of ODEs, IDEs, and IEs by combining HW with the collocation approach. To show the dependability and effectiveness of the developed method, numerical experiments were conducted. When dealing with problems of a similar form, the results showed that the wavelet-collocation approach is less time-taking and easier as compared to the Galerkin method. Two-dimensional HWs were used by Lepik [38] to solve PDEs, explaining their potential for being used for solving equations in higher dimensions. The Wave-Like Equation was successfully solved by Panchal et al., [39] via the HW technique. A HW approach for solving fractional KGEs was introduced by Hariharan [40]. The author developed wavelet operational matrices to formulate algebraic equations for the fractional KGE. The unknown coefficients of the HW series approximation of the solution were then discovered by converting these algebraic equations into a matrix system and solving them. The author claims that this approach works successfully for other differential and integral systems and is fast, simple, and versatile. Sekar [41] used a single-term HWM to solve Integro-Differential Equations and showed effectiveness by comparing the results with the LPR method. Berwal and Panchal [42] applied the HWM to the L-C-R problem to assess its effectiveness in comparison to the ES. The nonlinear Blasius problem was solved at uniform collocation points in the same year by Kaur et al. [43] using the Quasilinearization technique in conjunction with HW bases. An effective solution is needed for the important fluid mechanics problem known as the Blasius equation. The Quasilinearization method and HW approximation, according to the authors, make it simple to deal with nonlinearity without repeatedly iterating on specific collocation points.

The use of the HW series approximation method to solve fractional-order nonlinear oscillation equations was expanded by Saeed and Rehman [7]. They observed that the significant interval solutions were consistent with the Runge-Kutta technique of fourth order. The HW Quasilinearization method was used by Saeed and Rehman [44] to achieve an AS for the Heat Convection-Radiation Equations. The Quasilinearization technique was used by the author to first linearize the nonlinear heat transport equation. By approximating the DV and its derivatives the linear system was solved through a truncated convergent series of HW bases. Collocation points were used to solve the following algebraic equations, which produced a matrix system. The proposed scheme was applied to specific cases of nonlinear heat transfer equations. In their publication, the authors suggest that the HW Quasilinearization methodology is better than alternative techniques and closely approximates the exact answer. In order to study nonlinear

coupled Burgers' equations, a team of researchers lead by Mittal, Mishra and Kaur [45] used HWs and the collocation approach. Through this method, the set of equations was converted into a new set of ODEs, which were solved using the Runge Kutta method. The stability analysis of this hybrid approach by the researchers showed good results. They predict that other higher-order DEs can also be solved using similar approach. In the same year, Patel and Pradhan [46] used the Wavelet Galerkin strategy to solve nonlinear PDEs by combining Daubecheis wavelets with the Galerkin method. Using HW Matrices approaches, Arora, Brar, and Kumar [47] carried out a second study to identify numerical solutions to DEs.

In order to deal with fractional variational problems, Osama et al., [48] used the HW approach. Ray [49] compared and evaluated two potential methods for solving FDEs in the same year. The study compared the performance of the HWM to the OHAM using fractional Fisher type equations. Both approaches have been found to be reliable and suitable for solving these equations. However, when it came to results with a particular number of grid points, the OHAM performed better than the HWM. However, by adding more grid points, the accuracy of the HW approach could be improved. A new hybrid technique was introduced by Oruç et al., [50] for examining the solution of the modified Burgers' Equation. The algorithm used HW for spatial discretization and finite differencing for time discretization. The Quasilinearization method was employed to address the nonlinearities present in the equation. The developed method has been tested on three test problems and according to the authors, it is fast and computationally efficient. Kumar and Pandit [51] utilized an HWM-based approach to solve Fokker-Plank equations with both constant coefficients as well as variable coefficients. Additionally, Shiralashetti and Deshi [52] employed a collocation method utilizing HW bases to tackle multi-term fractional differential equations. In comparison to other methods, they observed that the HWCM is equally reliable, simple to use, and effective at approximating the solution.

Fallahpour et al., [53] introduced an approach based on HW to address the complexities of solving two-dimensional linear stochastic Volterra IEs involving multiple variables, a task exacerbated by inherent randomness. After subjecting the method to rigorous testing across different scenarios, the authors asserted its reliability, efficiency, and speed. However, they also suggested that its precision could be further enhanced by integrating additional numerical techniques. Shiralashetti et al., [54] expanded the utility of the HWCM to analyze systems governed by singular IVPs. Their research showcased the HWCM as a robust numerical technique capable of effectively addressing both linear and nonlinear singular IVPs. This method outperformed alternatives like the ADM and the VIM. Singh et al., [55] successfully tackled the

wave equation by employing the HWM, demonstrating its effectiveness compared to alternative approaches. Shiralashetti and colleagues, as detailed in reference [56], harnessed the HW technique for tackling the KGE, showcasing its superior performance when compared to traditional numerical approaches like the FDM. Moreover, in their study, Shah and colleagues [57] presented a specific version of the operational matrix for HWs, which was applied to tackle a range of both linear and non-linear FDEs. Through extensive testing on established benchmark problems, the authors asserted that their methodology demonstrated rapid convergence and superior accuracy. Patel and Pradhan [58] utilized the HW technique to analyze the advection-dispersion equation, a model describing the one-dimensional movement of contaminants within a porous medium. During that same year, Oruc et al., [59] introduced a hybrid approach incorporating HWs to investigate phenomena governed by the Regularized Long Wave Equation. Their technique involved discretizing the temporal derivatives using finite differencing and approximating the spatial derivatives through a truncated HW series. They applied this method to a range of test cases associated with solitary wave propagation and asserted its effectiveness in analysing such scenarios. Furthermore, Kaur and Kang [60] presented a time discretization scheme that incorporated HW series approximations along with the Quasilinearization approach to tackle established nonlinear PDEs. They employed the Quasilinearization method to address the nonlinearity within these equations. Moreover, a blend of the HWM and collocation technique was utilized to convert the given PDEs into a linear system of equations. This system was subsequently solved using the Thomas algorithm. Shiralashetti and a team of researchers [61] implemented an adaptive grid strategy. Notably, it showcased enhanced accuracy when compared to traditional HWCM and FDM approaches. Arbabi and her research team [62] utilized the two-dimensional HWM for solving sets of PDEs. They successfully showcased the method's convergence and stability while applying it to various test problems. Notably, the authors observed a significant level of correspondence between the results they obtained and the ES, affirming its accuracy and reliability.

Saeed [63] introduced an algorithm designed for the resolution of fractional LEEs. The algorithm involved approximating both the unknown solution and the nonlinear term within the DE using the ADM. By transforming the nonlinear equation into a system of linear FDEs, the author utilized the HWCM to solve these linear FDEs. Subsequently, the solutions obtained were reintroduced into the Adomian series, leading to the derivation of a series-based solution. In comparisons with other established methods, the author contended that this approach consistently yielded excellent results. Furthermore, it was emphasized that this method exhibited versatility in effectively addressing various forms of nonlinearities within DEs. Moreover,

Shiralashetti and fellow researchers [64] extended the application of the HWCM to address non-linear Volterra-Fredholm-Hammerstein integral equations. Majak and a team of researchers [65] presented an innovative HWT designed to address both integro-differential and DEs. They applied this method to a variety of such equations, with a particular emphasis on its utility in the analysis of FGM Structures. Their experimentation revealed that this novel approach demonstrated improved convergence rates and reduced error when compared to conventional methods. Furthermore, they underscored the method's adaptability, noting its capacity to be easily tailored for a broad spectrum of integro-differential and DEs with minimal modifications. Mittal and a team of researchers [66] introduced a novel approach utilizing HS3WM to address ordinary fractional dynamical systems. They assessed the method's validity through experimentation on several test problems and conducted a comparative analysis against the HS2WM. The results revealed that the HS3WM exhibited superior convergence rates when compared to the HS2WM method. Ahsan and his research team [67] utilized a hybrid approach that combined the HW-FDM in collaboration of Quasilinearization technique to find out the solution of both linear and nonlinear SEs. The authors noted that this combined approach successfully captured the physical behavior of the phenomena governed by the SEs. Nonetheless, it's worth mentioning that when applied to higher-dimensional SEs, this method might result in increased computational complexity. Additionally, when dealing with irregular domains, supplementary techniques may be necessary for effective implementation. Mittal and a group of researchers [68] introduced an innovative approach based on HS3WM for the solution of second-order ODEs characterized by singular coefficients and nonlinearity. They applied this newly proposed technique to a series of standard benchmark problems, demonstrating its superiority over other established methods, including the CSM, QSM, and HS2WM. The investigation further revealed that the HS3WM exhibited a more rapid convergence rate compared to the HS2WM. Ratas and fellow researchers [69] extended the application of the HOHWM to explore mathematical models governed by nonlinear EEs. They conducted a performance evaluation by comparing this method to the standard HWM and determined that both approaches exhibited equal competence in addressing these challenges. Nevertheless, they recommended employing HOHWM when higher levels of accuracy were essential, while HWM was suggested for scenarios where lower computational costs were preferred. Likewise, Pervaiz and a team of researchers [70] broadened the usage of the HWM to investigate nonlinear SEs featuring Dirichlet BCs. Their approach involved implementing the Crank-Nicolson scheme for time discretization and the HWCM for space discretization. Through extensive testing on a range of nonlinear Schrödinger equations with varying ICs and BCs, it became evident that the

proposed method consistently produced favorable outcomes for these specific problem scenarios.

1.10 Research Gap:

1. From the above study, we can observe that linear and non-linear DEs have been solved by using various methods, but under the consideration of HS3WM not much work has been done yet. However, some examples of linear and non-linear PDEs, such as Dispersive equation, KGE, Riccati equation, Vander-Pol equation etc are unsolved.
2. From the above discussion, we conclude that only a few DEs have been solved using FDM and Quasilinearization. But still, solution for many DEs using HS3WM is not explained.
3. From the literature review, we observe that non-linear DE with higher-order derivatives is still not much discussed under HS3W, equation such as KdV, LEE and fractional KE.

1.11 Objectives:

The utilization of wavelet methods has become popular due to their simple implementation, sparse computing costs, high accuracy with limited grid points, and other factors. In this research proposal, we aim to investigate the utilization of wavelet methods for solving DEs in diverse domains, including physics, economics, financial forecasting, image processing, environmental science, medicine, biology, chemistry, and beyond.

1. To explore the possibility of coupling the wavelet method with other legacy methods to frame a hybrid approach by varying the dilation factor.
2. To investigate the applicability of wavelet method in solving ordinary differential equations used in various fields.
3. To investigate the applicability of wavelet method in solving partial differential equations used in various fields.
4. To investigate the applicability of wavelet method in solving fractional differential equations used in various fields.

This thesis presents novel algorithms based on HS2WM and HS3WM for solving various types of linear and nonlinear DEs. The algorithms are applied to a wide range of numerical problems arising in different fields, such as BVPs, fractional KE, fractional Riccati equations, non-linear KGE, KdV, EFE, and LEE etc. These problems can be mathematically represented as ODEs, PDEs, and FDEs with ICs or BCs, and they are systematically treated using functional analysis, linear algebra, and approximation theory. The computations were carried out using MATLAB 20 software on a system equipped with an Intel Core i5 processor.

1.12 Layout of the thesis:

Chapter 2: A non-dyadic wavelet-based approximation method for the solution of higher-order ordinary differential equations that appear in Astrophysics with singularity at origin:

origin: In this chapter, we delve into the discussion of two ODEs that hold considerable importance in Astrophysics: LEE and the EFE. Both equations exhibit a singularity at the origin.

Throughout this study, we explore the implications of non-linearity and higher-order by employing a proposed method.

Chapter 3: A numerical analysis for solving various mathematical 2D-partial differential equations via scale 3 Haar wavelets:

Within this chapter, we address two distinct equations: the dispersion equation and the KGE. We thoroughly examine both linear and non-linear scenarios for each case and subsequently compare our findings with previously published results in the literature to assess the scheme's compatibility.

Chapter 4: An effective computational scheme for solving various mathematical fractional differential models via non-dyadic Haar wavelets:

Within this chapter, we explore FODEs to assess the method's applicability to fractional values. We explore various ODEs and PDEs, including the Riccati equation and the Vander-Pols equation. Furthermore, we address the fifth-order non-linear KE, a novel inclusion that has not been previously studied using any wavelet method, highlighting the uniqueness of our work.

Chapter 5: Conclusion and Future Scope

Chapter 2

A non-dyadic wavelet-based approximation method for the solution of higher-order ordinary differential equations that appears in Astrophysics with singularity at origin.

2.1 Introduction:

Numerous mathematicians and astrophysicists have become interested in finding out the solution of unique IVP in ODEs in recent years. The Lane Emden Equation (LEE) and Emden Fowler Equation (EFE), which have a singularity at the origin, are singularly perturbed equations that face computational difficulties in numerical processing [71]. For these kinds of problems convergence is directly affected by the small parameters. These equations are fundamentally important in the domain of stellar structure. It depicts the equilibrium density distribution in a self-gravitating polytropic isothermal gas sphere. Theoretical models of stellar structure and thermionic current depict a star as a gaseous sphere in thermodynamic and hydrostatic equilibrium. [72]. American astronomer Lane was the first to take this into account for determining the temperature and mass density on the surface as well as the thermal gradient of a spherical cloud of gas intervening under the mutual attraction of molecules. Second-order nonlinear singular boundary-value problems (SBVP) attracted Lane's interest. Following a thorough investigation, According to Lane and Emden, Poisson's equation for the gravitational potential of a star model is described by the second-order nonlinear SBVP in a dimensionless manner [73].

2.2 Lane Emden equation (LEE) for a Stellar structure:

Non-linear ODEs of the LEE have a semi-infinite domain. These equations explain how the spherical gas cloud temperature varies in accordance with the principles of classical thermodynamics and the molecules' attraction to one another. The polytropic theory of stars is primarily a result of thermodynamic considerations, which deal with the problem of transferring energy by moving materials across the layers of the star. These equations form a fundamental part of the theory of star structure.

We begin our study by considering a body of fluid that is sufficiently large and isolated that any force exerted on any component of the fluid is caused by the gravitational pull of the surrounding fluid components. Such a fluid entity is referred to as self-gravitating. A potential gradient can be used to represent the force F caused by gravity acting on this body.

At a distance of ' r ' from the centre of the spherical gas cloud ' $P(r)$ ' stands for the total pressure. The average pressure is influenced by both radiation and the usual gas pressure.

$$\mathcal{P} = \frac{1}{3}\eta T^4 + \frac{\mathcal{R}T}{\mathcal{V}}. \quad (2.1)$$

Here, η =radiation constant, \mathcal{V} =specific volume, \mathcal{R} =gas constant, T = temperature [3].

The Poisson equation and the hydrostatic equilibrium condition expressed as in the form of:

$$\frac{d\mathcal{P}}{dr} = -\frac{\mathbb{G}M(r)}{r^2}, \frac{dM}{dr} = 4\pi\rho r^2. \quad (2.2)$$

Let a sphere of radius ' r ' having mass ' $M(r)$ ' and ' \mathbb{G} ' the gravitation constant, ' ρ ' represents the density of the star from the centre of star at distance ' r '. While on combining these equations we get the equation in the form as:

$$\frac{1}{r^2} \frac{d}{dr} \left(\frac{r^2}{\rho} \frac{d\mathcal{P}}{dr} \right) = -4\pi\mathbb{G}\rho, \quad (2.3)$$

The LEE may be derived from these equations under the basic assumptions that the density just depends on while remaining are temperature independent. We analyse a relation in the form $\rho \sim \mathcal{P}^{\frac{3}{5}}$ where the pressure and density are for a degenerate electron gas. Assuming that there is a relationship of this type for several states of the star,

$$\mathcal{P} = a\rho^{1+\frac{1}{b}}, \quad (2.4)$$

where ' a ' and ' b ' are constants. It is important to remember that the polytropic index, which is connected with the ratio of particular temperatures in the gas that makes up the star, is referred to by the letter ' b ' in this sentence. With the use of these presumptions, we can use this relationship to add to the first equation we created to determine the hydrostatic equilibrium condition.

$$\left(\frac{a(b+1)}{4\pi\mathbb{G}} \eta^{\frac{1}{b}-1} \right) \frac{1}{r^2} \frac{d}{dr} \left(r^2 \frac{d\mathcal{Y}}{dr} \right) = -\mathcal{Y}^b. \quad (2.5)$$

In the above relation, η : central density of star, \mathcal{Y} : dimensionless quantity both are related to ' ρ '.

$$\rho = \eta y^{\ell}, \quad (2.6)$$

Furthermore, if we incorporate this finding into the Poisson equation, we get a DE for mass that depends on the polytropic index ' ℓ '. Although the DE appears to be challenging to solve, this issue can be partially alleviated by the addition of variable ' \mathcal{X} ' which is dimensionless, provided by the following.

$$r = \ell \mathcal{X}, \quad (2.7)$$

and

$$\ell = \left(\frac{a(\ell+1)}{4\pi G} \eta^{\frac{1}{\ell}-1} \right)^{1/2} \quad (2.8)$$

using these values in the above equations we obtained the LEE,

$$\frac{1}{x^2} \frac{d}{dx} \left(x^2 \frac{dy}{dx} \right) = -y^{\ell}. \quad (2.9)$$

On simplification of the above equations,

$$y'' + \frac{2}{x} y' + y^{\ell} = 0. \quad (2.10)$$

It is essential to provide the BCs at this point in order to take into consideration hydrostatic equilibrium and the normalising of the recently introduced values ' \mathcal{X} ' and ' y '. These are following boundary requirements on which BCs are based. If $r \rightarrow 0$ then $\mathcal{X}=0$, $\rho = \eta \rightarrow y(0)=1$ and this implies $y'(0) = 0$.

With initial conditions, $y(0) = 1$ and $y'(0) = 0$.

Similarly singular EFE is represented in the form:

$$y''(x) + k y'(x) + y(x) = 0. \quad (2.11)$$

With initial conditions: $y(0) = \alpha, y'(0) = 0$

A Higher order EFE is expressed as:

$$y^{IV}(x) + \frac{\kappa_1}{x} y'''(x) + \frac{\kappa_2}{x^2} y''(x) + \frac{\kappa_3}{x^3} y'(x) + \kappa_4 y(x) = F. \quad (2.12)$$

With ICs: $\mathcal{Y}(0) = \alpha$, $\mathcal{Y}'(0) = \beta$, $\mathcal{Y}''(0) = \eta$, and $\mathcal{Y}'''(0) = \gamma$ α, β, η and γ are constants in the above equation. $\kappa_1, \kappa_2, \kappa_3$ and κ_4 and F are constants and value of a function respectively [74].

Several methods have been presented for the solution of LEE by HFCM [75], [76], Legendre method [77], [78], HSCM [79]–[81], combination of homotopy perturbation and variational iteration [82], Taylors method [83], VIM [84], Green function and ADM [85], Laguerre polynomial [86], OHAM [87] and similarly different numerical solutions have been investigated by the researchers for the solution of EFE, HAM [88], and the Genocchi operational matrix for solving EFE [89]. It includes the quartic polynomial spline method, and fourth order B-spline method [90], [91], and modifies ADM, DTM, and VIM [74], [92]–[95]. In the research article, HSWM is discussed for obtaining the approximate solution of linear EFEs [96]. EFE is solved by using HSWM combined with the Newton-Raphson method and for solving nonlinearity. The Quasilinearisation technique is used and discussed in some special cases of EFE [97], Fourth-order EFE is discussed using HSWM and by converting the DE into a set of algebraic equations, and through various examples discuss the applicability of the proposed technique [98], Third order DEs are solved using HSWM, through different examples is discussed the effectiveness of the method for solving higher-order DEs [99], in the study, the author developed the solution to the HOBV problem using HSWM [100]. Fourth-order LEFE also described by two different methods: ADM and the quintic B-spline method [101].

After that, in 2018 Mittal and Pandit discussed non-dyadic wavelet-based methods and dealt with various kinds of DEs to examine the results [102]. As the dyadic wavelet discussed by Haar in 1910 [105], where as In 1995, Chui and Lian developed non-dyadic wavelet to discuss MRA [106] and found it better than the prior method. In recent years, a lot of work has been done using a non-dyadic (Haar scale -3) wavelet to discuss various kinds of DEs [102]–[104] by this proposed technique. After that R. Kumar discussed various equations using non-dyadic wavelets [107], [108]. But LEE and EFE are not yet discussed by the non-dyadic wavelet method, which motivates us to work on the solution of this equation. Our main objective is to study the LEE type and EFE using the HS3W approach.

2.3 Quasi-linearisation process

A generalized form of the Newton–Raphson method is the Quasilinearization strategy used for linearizing nonlinear DEs. Quadratically, it converges to the exact value. The fact that many nonlinear equations have no analytic solution but their solution is required as per their application in the physical world is a major motivation for employing this strategy. If we have a non-linear term, we must employ the recurrence relation shown below:

$$u^2 = f(u^2) = f(x, u^2)$$

$$[u^2]_{l+1} = [u^2]_l + [u_{l+1} - u_l] \left(\frac{\partial}{\partial u} (u^2) \right)_l$$

$$(u^2)_{l+1} = (u^2)_l + (u_{l+1} - u_l) 2u_l$$

$$(u^2)_{l+1} = (u^2)_l + 2u_{l+1}(u)_l - 2(u^2)_l$$

$$(u^2)_{l+1} = 2(u)_{l+1}u_l - (u^2)_l$$

2.4 Approximation of Emden Fowler differential equation (EFE) by Scale-3 Haar wavelet:

Theorem: Let $\chi(z)$ be any square integrable function over the interval $[\sigma_1, \sigma_2)$, whose highest derivative is expressible as a linear combination of HW family as $\chi^n(z) = \sum_{i=1}^{3p} a_k h_k(z)$.

Then all the derivatives of $\chi(z)$ of order less than n are given by [107] :

$$\chi^k(z) = \sum_{i=1}^{3p} a_i p_{n-k,i}(z) + \sum_{r=0}^{n-k-1} \frac{(z-Q)^r}{r!} \chi^{k+r}(Q); k = 0, 1, 2, 3, \dots, n-1. \quad (2.13)$$

Proof: Let us approximate the higher order derivative as:

$$\chi^n(z) = \sum_{i=1}^{3p} a_k h_k(z). \quad (2.14)$$

Integrating $\chi^n(z)$ w.r.t 'z' between z to Q we have,

$$\chi^{n-1}(z) = \sum_{i=1}^{3p} a_i p_{1,i}(z) + \chi^{n-1}(Q). \quad (2.15)$$

As per the rule of mathematical induction on $M = n - k$, Above, theorem is proved.

Take $M = 1 \Rightarrow k = n - 1$, by using $k = n - 1$ we have:

$$\chi^{n-1}(z) = \sum_{i=1}^{3p} a_i p_{1,i}(z) + \chi^{n-1}(Q). \quad (2.16)$$

It is same as the above calculated results, so for $m = 1$ it is true.

Assume the result is true for $M = n - k = s$

$$\chi^{n-s}(z) = \sum_{i=1}^{3p} a_i p_{s,i}(z) + \sum_{r=0}^{s-1} \frac{(z-Q)^r}{r!} \chi^{n-s+r}(Q). \quad (2.17)$$

Proof of the result at $M = s + 1$, integrating the above equations

$$\begin{aligned} \chi^{n-s-1}(z) &= \sum_{i=1}^{3p} a_i p_{s+1,i}(z) + \sum_{r=0}^{s-1} \frac{(z-Q)^{r+1}}{(r+1)!} \chi^{n-s+r}(Q) \\ &+ \chi^{n-s-1}(Q). \end{aligned} \quad (2.18)$$

$$\begin{aligned} \chi^{n-s-1}(z) &= \sum_{i=1}^{3p} a_i p_{s+1,i}(z) + \chi^{n-s-1}(Q) \\ &+ \left[\frac{(z-Q)^1}{1!} \chi^{n-s} + \frac{(z-Q)^2}{2!} \chi^{(n-s)+1} \right. \\ &\left. + \frac{(z-Q)^3}{3!} \chi^{(n-s)+2} + \dots + \frac{(z-Q)^s}{s!} \chi^{(n-s)+(s-1)}(Q) \right]. \end{aligned} \quad (2.19)$$

$$\begin{aligned} \chi^{n-s-1}(z) &= \sum_{i=1}^{3p} a_i p_{s+1,i}(z) + \frac{(z-Q)^0}{0!} \chi^{n-(s+1)} \\ &+ \left[\frac{(z-Q)^1}{1!} \chi^{(n-(s+1))+1} + \frac{(z-Q)^2}{2!} \chi^{(n-(s+1))+2} + \dots \right. \\ &\left. + \frac{(z-Q)^s}{s!} \chi^{(n-(s+1))+s}(Q) \right]. \end{aligned} \quad (2.20)$$

$$\chi^{n-(s+1)}(z) = \sum_{i=1}^{3p} a_i p_{s+1,i}(z) + \sum_{r=0}^{(s+1)-1} \frac{(z-Q)^r}{(r)!} \chi^{(n-(s+1))+r}(Q). \quad (2.21)$$

Hence the above result is verified for $M = (n - k) = s + 1$, therefore given result is valid for all derivative of $\chi(z)$ which satisfies the proof.

Since the members of family of non-dyadic HW have a property that they are orthogonal to each other, thus by using properties of wavelet and above theorem, over the interval $[0,1)$; any square integrable function $\chi(z)$ can be expressed as:

$$\chi(z) \approx \alpha_1 h_1(z) + \sum_{\text{even index } i \geq 2}^{\infty} \alpha_i \varphi_i^1(z) + \sum_{\text{odd index } i \geq 3}^{\infty} \alpha_i \varphi_i^2(z). \quad (2.22)$$

Here α_i 's coefficients of HW can be calculated as:

$$\alpha_i = \int_0^1 \chi(z)h_i(z)dz, i = 1, 2, 3, \dots, 3p. \quad (2.23)$$

Considering terms in finite number, for first $3p$ terms, where $p = 3^j, j = 0, 1, 2, \dots$ to approximate the function $\chi(z)$ we get,

$$\chi(z) \approx \chi_{3p} = \sum_{i=1}^{3p} a_i h_i(z). \quad (2.24)$$

2.5 Methods for the solution of LEE and EFE:

Approximation Technique

Step 1: Consider an ODE known as LEE and EFE.

Step 2: Approximate the higher derivatives of the existing equation.

Step 3: By integrating the higher derivatives, other lower derivatives can be obtained which are present in the equation.

Step 4: After finding all the derivatives and values of the function by the approximation method, substitute all the values it into the given mathematical equation.

Step 5: By using proposed methodology, an ODE is converted into algebraic equation.

Step 6: By applying the MATLAB algorithm to a given equation, an approximate solution to the given problem is obtained, and then the exact solution and solution existing in the literature are compared with the results obtained for a mathematical equation.

Step 7: Results are obtained in the form of tables and graphs, and it has been observed that our results are better than the existing results in the literature.

Consider a LEE:

$$y'' + \frac{2}{x}y' + y^b = 0 \quad (2.25)$$

With BCs, $y(0) = 1$ and $y'(0) = 0$, for $b = 1$

$$y''(x) = \sum_{\tau=1}^{3M} \mu_{\tau} h_{\tau}(x) \quad (2.26)$$

On integrating w.r.t x

$$y'(x) = \sum_{\tau=1}^{3M} \mu_{\tau} P_{1,\tau}(x) + y'(0)$$

$$y(x) = \sum_{\tau=1}^{3M} \mu_{\tau} P_{2,\tau}(x) + xy'(0) + y(0)$$

$$y(x) = \sum_{\tau=1}^{3M} \mu_{\tau} P_{2,\tau}(x) + 1 \quad (2.27)$$

Using all values in above equation,

$$\sum_{\tau=1}^{3M} \mu_{\tau} h_{\tau}(x) + \frac{2}{x} \sum_{\tau=1}^{3M} \mu_{\tau} P_{1,\tau}(x) + \sum_{\tau=1}^{3M} \mu_{\tau} P_{2,\tau}(x) + 1 = 0 \quad (2.28)$$

$$\sum_{\tau=1}^{3M} \mu_{\tau} [h_{\tau}(x) + \frac{2}{x} P_{1,\tau}(x) + P_{2,\tau}(x)] = -1$$

Similarly, EFE is solved by approximating the higher derivatives and finding the other values and results are further discussed using numerical examples.

2.6 Error analysis with test problems

Above scheme is applied on LEE and EFE to validate the competency of the scheme and accuracy level gained by the recent technique. L_2 – error, L_{∞} – error and absolute errors has been found which can written as.

$$\text{Absolute Error} = |u_{exact}(x_r) - u_{num}(x_r)|. \quad (2.29)$$

$$L_{\infty} = \max_r |u_{exact}(x_r) - u_{num}(x_r)|. \quad (2.30)$$

$$L_2 = \frac{\sqrt{\sum_{l=1}^{3p} |u_{exact}(x_r) - u_{num}(x_r)|^2}}{\sqrt{\sum_{l=1}^{3p} |u_{exact}(x_r)|^2}}. \quad (2.31)$$

where x_r represents the collocation points of the domain and calculated by the relation.

$$x_r = a + (b - a) \frac{m - 0.5}{3p}; m = 1, 2, 3, \dots, 3p \quad (2.32)$$

2.7 Numerical Observations:

2.7.1 Fourth non-order linear EFE:

$$u^{iv}(z) + \frac{12}{z} u'''(z) + \frac{36}{z^2} u''(z) + \frac{24}{z^3} u'(z) + 60(7 - 18z^4 + 3z^8)u^9 = 0. \quad (2.33)$$

With IC,

$$u(0) = 1, u'(0) = u''(0) = u'''(0) = 0. \quad (2.34)$$

ES of the given equation:

$$u(z) = \frac{1}{\sqrt{1+z^4}}. \quad (2.35)$$

$$u(z) = \sum_{i=1}^{3p} a_i h_i(z) + \frac{12}{z} P_{1,i}(z) + \frac{36}{z^2} P_{2,i}(z) + \frac{24}{z} P_{2,i}(z) + 60(7 - 18z^4 + 3z^8)(9u_{r+1}u_r^8 - 8u_r^9)$$

Table 2.1 shows a comparative study of absolute error of proposed methods with other methods and whereas Table 2.2 represents a comparative study at LOR J=2 and Table 2.3 signifies value of L_2 and L_{∞} error at different LOR. In Figure 2.1, comparative study is discussed between the AS and ES derived by proposed method and Figure 2.2 signifies the value of absolute error at different collocation points.

Table 2.1 A comparison study of Absolute errors of proposed method with other methods.

z	Absolute error by VIM [74].	Absolute error by HS2WM [98].	Absolute error by HS3WM
0.930	4.5E-02	1.1E-02	1.32E-05
0.943	6.2E-02	1.3E-02	1.35E-05
0.961	8.5E-01	1.5E-02	1.42E-05
0.977	1.2E-01	1.7E-02	1.48E-05
0.992	1.6E-01	2.0E-02	1.53E-05

Table 2.2 A comparison study of Absolute errors by proposed method at different points for LOR $J=2$.

z	ES	AS by HS3WM	Absolute Error by HS3WM	Absolute Error by ADM [101]	Absolute Error by QBSM [101]
0.1	0.999858843193092	0.999858845358450	2.165E-09	1.1713E-05	2.9749E-06
0.2	0.999140153146428	0.999140184430897	3.128E-08	-	-
0.3	0.995124236352257	0.995124652439060	4.160E-07	-	-
0.4	0.983937555332222	0.983940019395591	2.464E-06	6.5734E-06	1.7577E-06
0.5	0.970136312766435	0.970142500145332	6.187E-06	5.2624E-07	4.7039E-07
0.6	0.936785055989435	0.936803613298913	1.855E-05	7.5805E-06	3.9870E-06
0.7	0.886591328782529	0.886633635115172	4.230E-05	-	-
0.8	0.821293712001356	0.821369965673296	7.625E-05	-	-
0.9	0.771883253099228	0.771983726870444	1.004E-04	3.6837E-05	1.0483E-05

Table 2.3 Value of the L_2 and L_∞ errors at different LOR:

LOR	L_2 error at HS3WM	L_∞ error at HS3WM
$J=1$	4.85313E-04	1.05739E-03
$J=2$	5.15079E-05	1.21669E-04
$J=3$	5.69559E-06	1.37822E-05
$J=4$	6.32507E-07	1.54229E-06
$J=5$	7.02744E-08	1.71784E-07
$J=6$	7.80821E-09	1.91028E-08

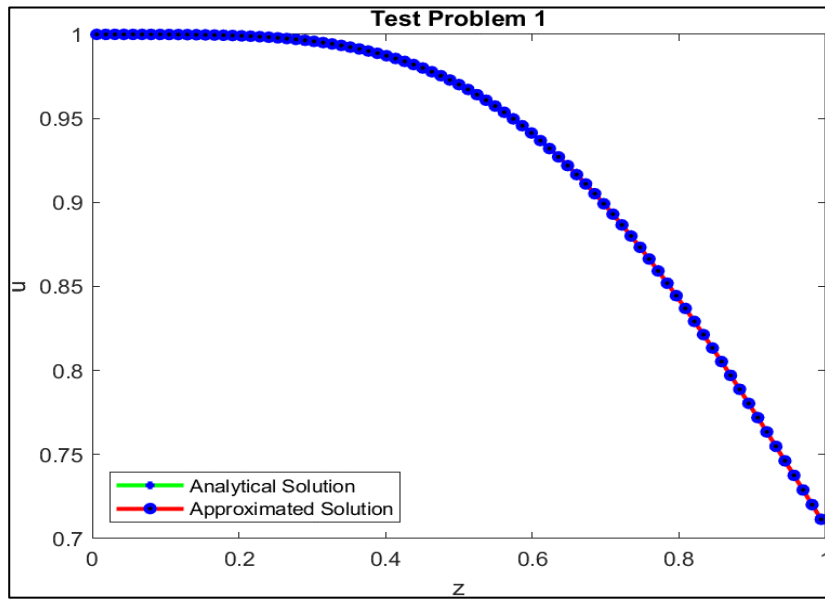


Figure 2.1 For NE no. 2.7.1, graphical presentation of ES and AS of $u(z)$ at distinct point of z .

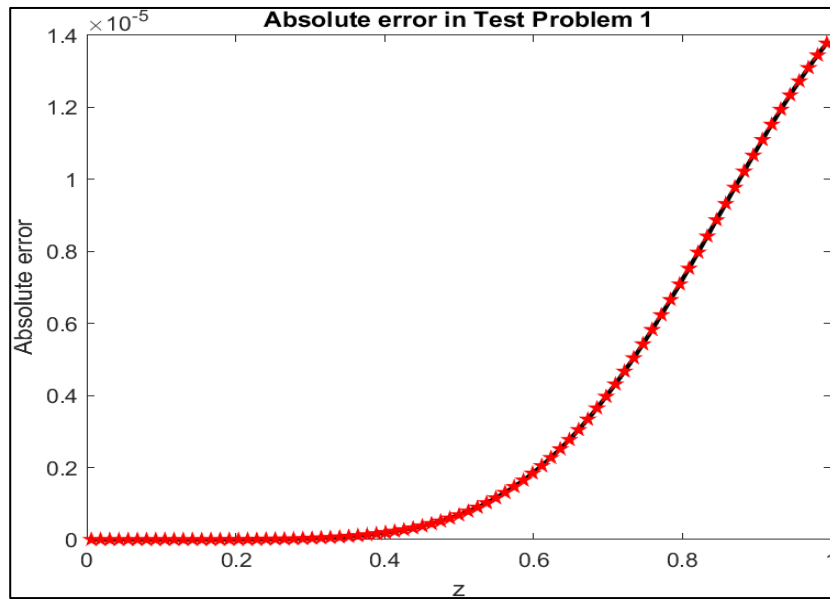


Figure 2.2 For NE no. 2.7.1, Value of Absolute error for different values of z .

2.7.2 Third order non-linear ODE (EFE)

$$u'''(z) + \frac{3}{z}u''(z) = u^3(z) + 24e^z + 36ze^z + 12z^2e^z + z^3e^z - z^9e^{3z}. \quad (2.36)$$

With IC,

$$z(0) = 0, z(1) = e, z'(0) = 0. \quad (2.37)$$

ES of the given equation:

$$u(z) = z^3 e^z. \quad (2.38)$$

$$u(z) = \sum_{i=1}^{3p} a_i h_i(z) + \frac{3}{z} a_i P_{1,i}(z) - (3u_{r+1}u_r^2 - 2u_r^3) - (24e^z + 36ze^z + 12z^2e^z + z^3e^z - z^9e^{3z})$$

Table 2.4 shows a comparative study of absolute error of proposed methods with other methods at LOR J=3 and Table 2.5 signifies value of L_2 and L_∞ error at different LOR. In Figure 2.3, comparative study is discussed between the AS and ES derived by proposed method and Figure 2.4 signifies the value of absolute error at different collocation points.

Table 2.4 A comparison study of Absolute errors of proposed method with other methods at resolution level J=3.

z	ES	AS by HS3WM	Absolute error by HS3W
0.104	0.001283440775195	0.001282586360785	8.54E-07
0.203	0.010362491097857	0.010359072316960	3.41E-06
0.302	0.037445865503173	0.037437985358077	7.88E-06
0.401	0.096482597073391	0.096468138911095	1.44E-05
0.50	0.206090158837516	0.206066773523318	2.33E-05
0.611	0.420496827502144	0.420460286063230	3.65E-05
0.709	0.727518335078141	0.727467043686249	5.12E-05
0.808	1.187018782746865	1.186949558412363	6.92E-05
0.907	1.851351961228259	1.851261220832432	9.07E-05

Table 2.5 Value of the L_2 and L_∞ error at different LOR

LOR	L_2 Error by HS2W[109]	L_∞ error by HS2W[109]	L_2 error by HS3W	L_∞ error by HS3W
$J=1$	1.8840E-02	2.9323E-02	4.14486E-03	7.8944E-03
$J=2$	2.1377E-02	1.0697E-02	4.70304E-04	9.8452E-04
$J=3$	8.1855E-03	2.8254E-03	5.23755E-05	1.1305E-04
$J=4$	2.9917E-03	7.1846E-04	5.82097E-06	1.2693E-05

$J=5$	1.0737E-03	1.8035E-04	6.46793E-07	1.4152E-06
$J=6$	3.8237E-04	4.5133E-05	7.18663E-08	1.5742E-07

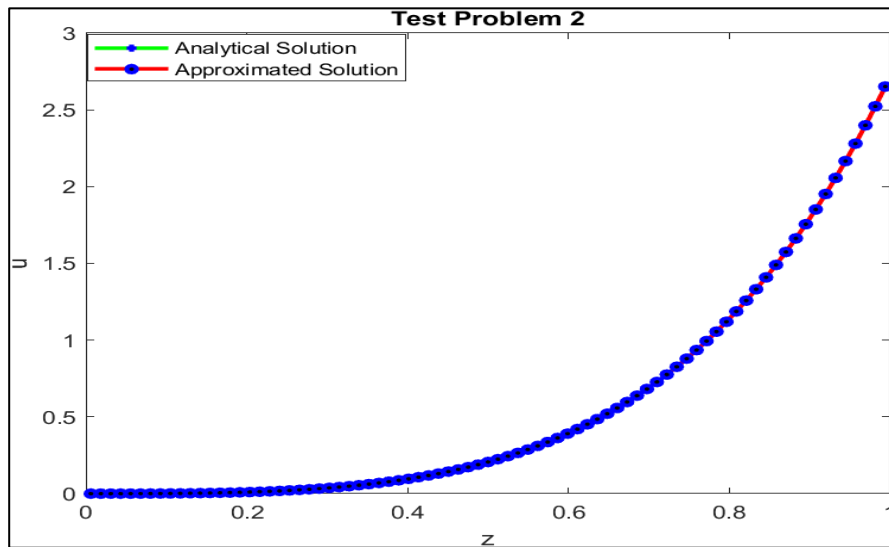


Figure 2.3 For NE no. 2.7.2, graphical presentation of ES and AS of $u(z)$ at distinct point of z .

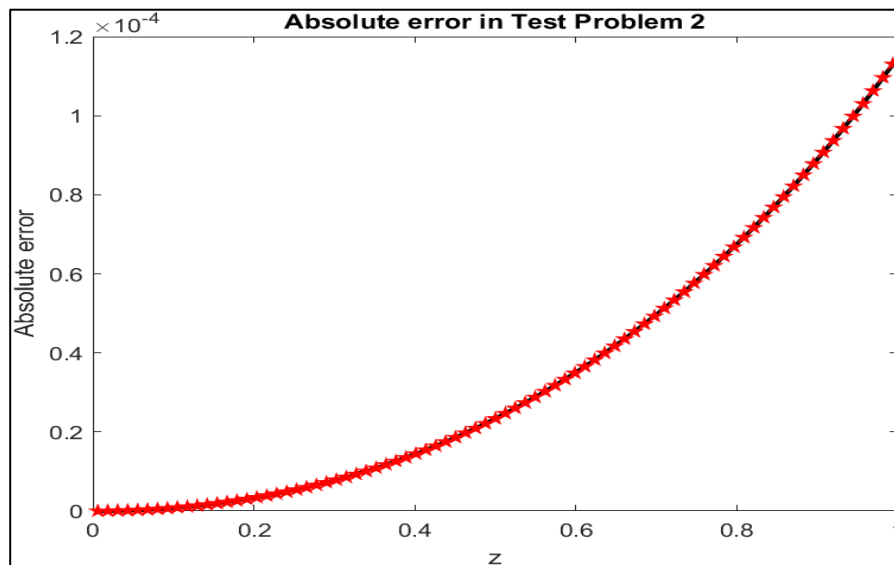


Figure 2.4 For NE no. 2.7.2, Value of Absolute error for different values of z .

2.7.3 A Fourth order linear ODE:

$$u^{iv}(z) + \frac{9}{z}u'''(z) + \frac{18}{z^2}u''(z) + \frac{6}{z^3}u'(z) - 32(15 + 75z^4 + 54z^8 + 8z^{12})u = 0. \quad (2.39)$$

With IC,

$$u(0) = 1, u'(0) = u''(0) = u'''(0) = 0. \quad (2.40)$$

ES of the given equation:

$$u(z) = e^{z^4} \quad (2.41)$$

$$u(z) = \sum_{i=1}^{3p} a_i h_i(z) + \frac{9}{z} P_{1,i}(z) + \frac{18}{z^2} P_{2,i}(z) + \frac{6}{z^3} P_{3,i}(z) + 32(15 + 75z^4 + 54z^8 + 8z^{12})P_{4,i}(z).$$

Table 2.6 shows a comparative study of absolute error of proposed methods with other methods and whereas Table 2.7 represents a comparative study at resolution level $J=2$ and Table 2.8 signifies value of L_2 and L_∞ error at different LOR. In Figure 2.5, comparative study is discussed between the AS and ES derived by proposed method and Figure 2.6 signifies the value of absolute errors at different collocation points.

Table 2.6 A comparison study of Absolute errors of proposed method with other methods at resolution level $J=3$.

z	ES	AS by VIM [74]	AS by HS2WM [98]	AS by HS3WM
0.504	1.0667142	1.01574	1.06660	1.0667141
0.605	1.1453966	1.03202	1.14384	1.1453962
0.707	1.2840731	1.05733	1.28388	1.2840730
0.801	1.5117446	1.08968	1.50862	1.5117443
0.902	1.4512819	1.13321	1.94051	1.9459544

Table 2.7 A comparison study of Absolute errors by proposed method at different points for LOR $J=2$.

z	ES	AS by HS3WM	Absolute Error by HS3WM
0.1	1.000282406409751	1.000282408938148	2.528E-08
0.2	1.001723294678824	1.001723334769213	4.009E-07
0.3	1.009870313695018	1.009870867313081	5.536E-06
0.4	1.033454757045220	1.033458183478689	3.426E-05
0.5	1.064485414542223	1.064494458917860	9.044E-05
0.6	1.149633526509271	1.149664285482661	3.075E-05

0.7	1.312594689586376	1.312681132438711	8.644E-05
0.8	1.619507358288849	1.619719662482946	2.123E-04
0.9	1.969508640506898	1.969871146748689	3.625E-04

Table 2.8 Value of the L_2 and L_∞ error at different LOR:

LOR	L_2 error by HS3WM	L_∞ error at HS3WM
$J=1$	1.11181E-03	3.93567E-03
$J=2$	1.34148E-04	5.83032E-04
$J=3$	1.50753E-05	7.03277E-05
$J=4$	1.67720E-06	8.00930E-06
$J=5$	1.86383E-07	8.96960E-07
$J=6$	2.07096E-08	9.99204E-08

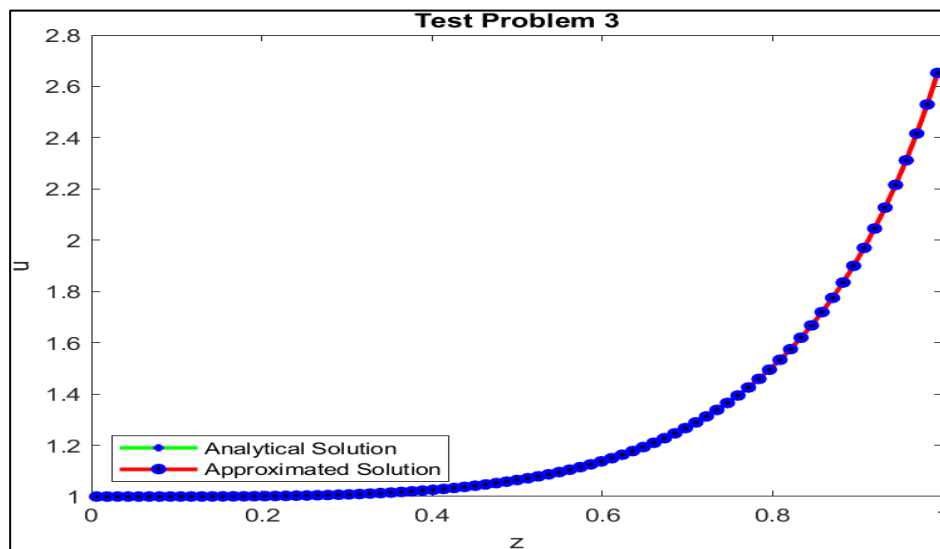


Figure 2.5: For numerical Experiment no. 2.7.3, graphical presentation of ES and AS of $u(z)$ at distinct point of z .

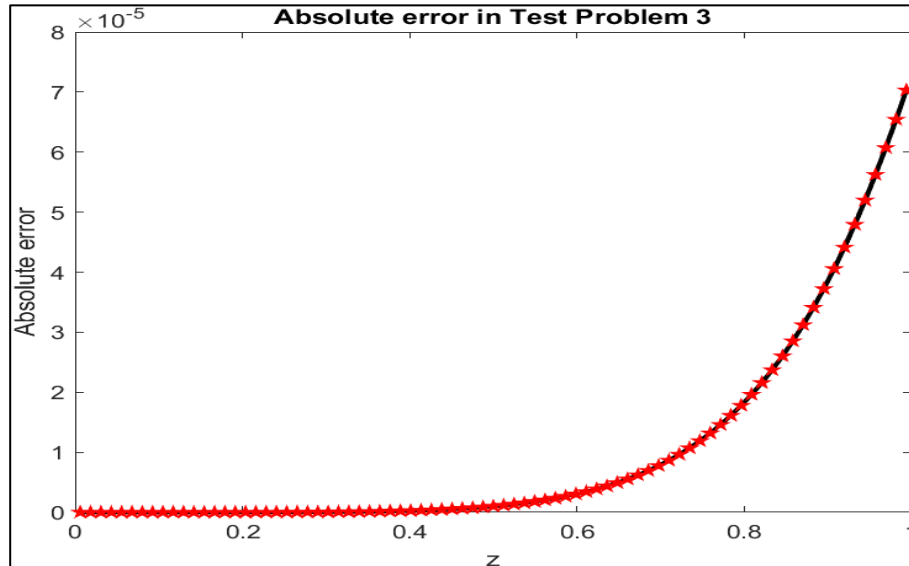


Figure 2.6 For NE no. 2.7.3: Value of Absolute error for different values of z .

2.7.4 For $\mu(\mathcal{X}) = 1$ and $\lambda(y) = y^{\mathcal{b}}$ the fundamental LEE introduced to analyze the thermal behavior of a gas cloud that was spherical.

With BC: $y(0) = 0, y'(0) = 0$, here $\mathcal{b} \geq 0$, there are different cases for different

$$y'' + \frac{2}{x}y' + y^{\mathcal{b}} = 0 \quad (2.42)$$

values of \mathcal{b} .

Case a: for $\mathcal{b} = 0$, equation's ES given as: $y(\mathcal{X}) = 1 - \frac{x^2}{6}$

Case b: for $\mathcal{b} = 1$, equation's ES given as: $y(\mathcal{X}) = \frac{\sin \mathcal{X}}{x}$

Case c: for $\mathcal{b} = 5$, equation's ES given as: $y(\mathcal{X}) = \left(1 + \frac{x^2}{3}\right)^{-\frac{1}{2}}$

For $\mathcal{b} = 0$, equation becomes:

$$y'' + \frac{2}{x}y' + 1 = 0 \quad (2.43)$$

With BC,

$$y(0) = 0, y'(0) = 0 \quad (2.44)$$

ES:

$$y(x) = 1 - \frac{x^2}{6} \quad (2.45)$$

Table 1 and table 2 shows a comparative study of absolute error of proposed methods with other methods and whereas table 3 represents a comparative study at LOR J=2 and table 3 signifies value of L_2 and L_∞ error at different LOR. In figure 1, comparative study is discussed between the AS and ES derived by proposed method for case (a) and (b).

Table 2.9 A comparative study of Absolute errors obtained using proposed method with methods available in the literature.

x	Absolute error by HS2W[79]	Absolute error by HS3W
0.24	5.55E-17	0
0.36	5.55E-17	0
0.49	0	0
0.61	5.55E-17	0
0.74	0	0
0.86	2.78E-17	0
0.99	0	0

For $\ell = 1$, equation becomes:

$$y''(x) + \frac{2}{x}y'(x) + y(x) = 0 \quad (2.46)$$

With BC,

$$y(0) = 0, y'(0) = 0, \quad (2.47)$$

ES:

$$y(x) = \frac{\sin x}{x} \quad (2.48)$$

Table 2.10 A comparative study of Absolute errors obtained using proposed method with methods available in the literature.

x	J=5 [76]	HSWM3	J=6 [76]	HSWM3
0.2	4.79E-06	1.05E-10	1.63E-07	1.16E-11
0.4	9.51E-06	4.19E-10	2.79E-07	2.00E-11
0.6	1.12E-05	9.36E-10	3.11E-07	1.04E-10
0.8	1.17E-05	1.65E-09	3.19E-07	1.84E-10

Table 2.11 A comparative study of Errors obtained using proposed method at different LOR.

LOR	$L_2 - error$	$L_\infty - error$
$J=0$	5.81E-05	9.20E-05
$J=1$	7.82E-06	1.49E-05
$J=2$	8.87E-07	1.80E-06
$J=3$	9.88E-08	2.05E-07
$J=4$	1.09E-08	2.30E-08
$J=5$	1.22E-09	2.56E-09

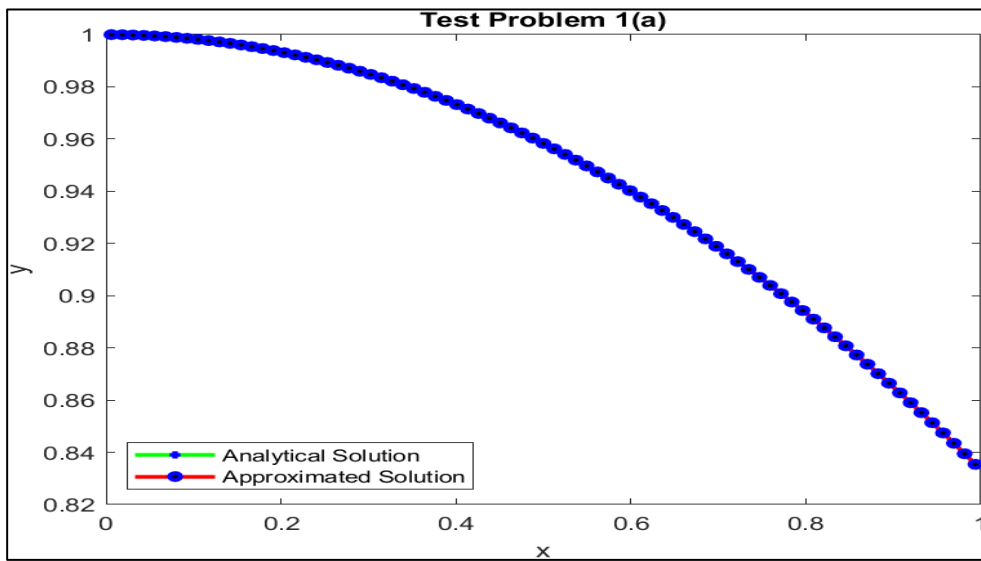


Figure 2.7 Graphical depiction of AS and ES for NE no. 2.7.4 for case (a)

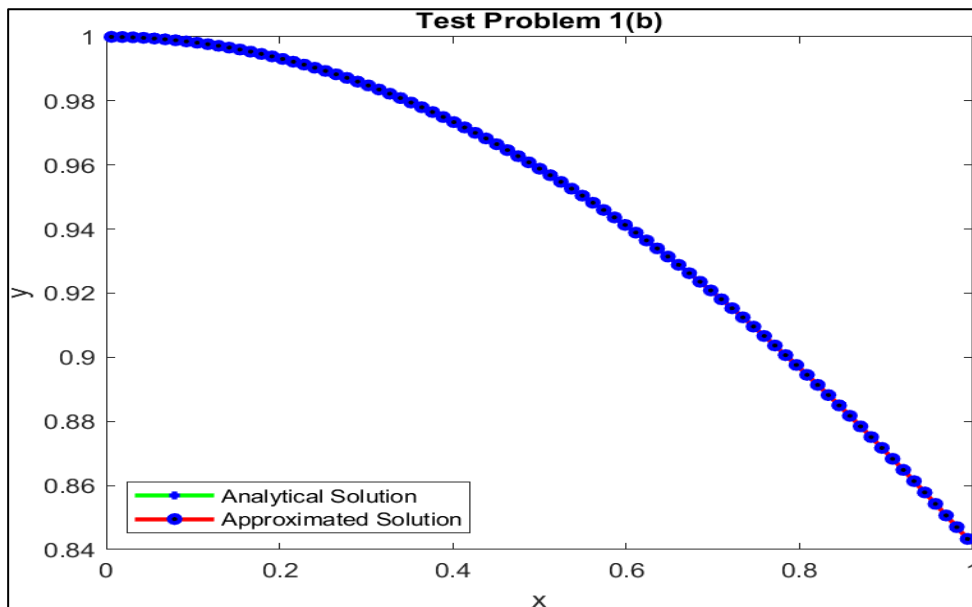


Figure 2.8 Graphical depiction of AS and ES for NE no. 2.7.4 for case (b).

2.7.5 For $\ell = 5$, equation becomes:

$$y'''(x) + \frac{2}{x}y'(x) + y^5(x) = 0 \quad (2.49)$$

With BC,

$$y(0) = 0, y'(0) = 0 \quad (2.50)$$

ES:

$$y(x) = \left(1 + \frac{x^2}{3}\right)^{-\frac{1}{2}} \quad (2.51)$$

Table 2.12 shows a comparative study of absolute error of proposed methods with other methods and whereas Table 2.13 signifies value of L_2 and L_∞ error at different LOR. In Figure 2.9, comparative study is discussed between the AS and ES derived by proposed method and absolute error value for case (c).

Table 2.12 A comparative study of Absolute errors obtained using proposed method with methods available in the literature.

x	TWM [83]	VIM [84]	IDM [85]	HS3WM
0.1000	6.4E-06	6.2E-03	3.1E-03	7.9E-10
0.2000	6.3E-06	6.1E-03	2.9E-03	3.1E-09
0.3000	6.0E-06	5.8E-03	2.6E-03	6.8E-09
0.4000	5.7E-06	5.5E-03	2.2E-03	1.1E-08
0.5000	5.3E-06	5.0E-03	1.8E-03	1.7E-08
0.6000	4.8E-06	4.5E-03	1.4E-03	2.4E-08
0.7000	4.3E-06	3.8E-03	9.8E-04	3.2E-08
0.8000	3.8E-06	2.8E-03	6.0E-04	4.0E-08
0.9000	3.2E-06	1.6E-03	2.7E-04	4.8E-08

Table 2.13 A comparative study of Errors obtained using proposed method at different resolution levels.

LOR	$L_2 - error$	$L_\infty - error$
$J=0$	1.70E-03	2.61E-03
$J=1$	1.91E-04	3.43E-04
$J=2$	2.13E-05	4.02E-05
$J=3$	2.36E-06	4.55E-06

$J=4$	2.63E-07	5.09E-07
$J=5$	2.92E-08	5.66E-08

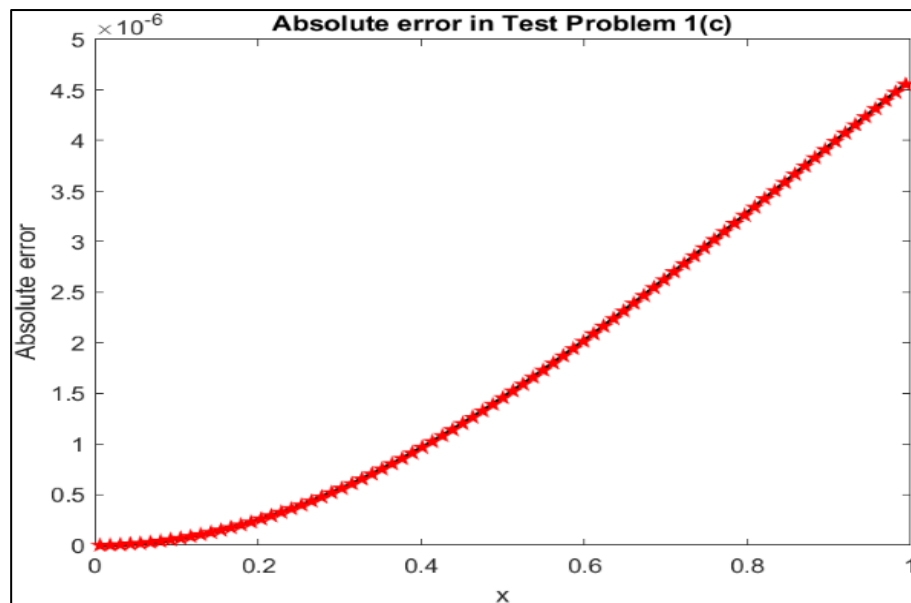
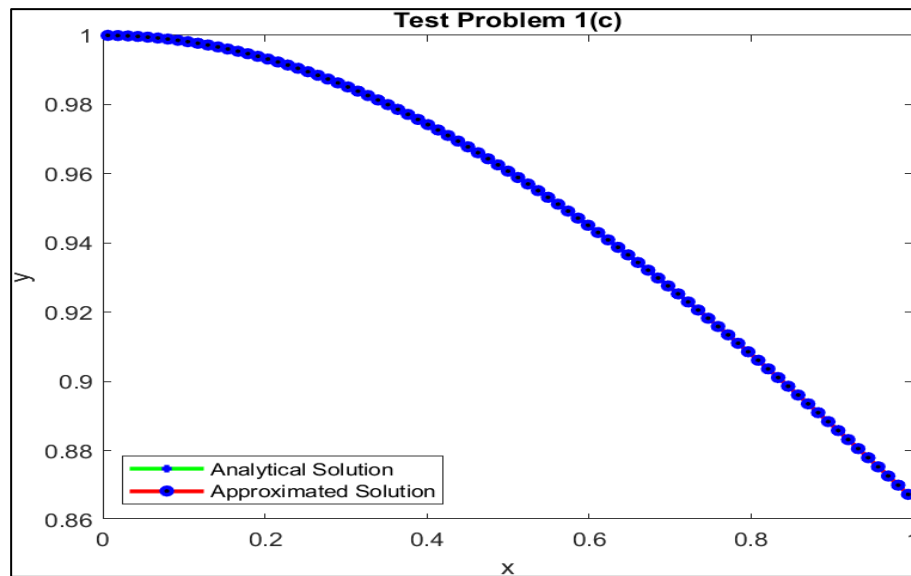


Figure 2.9 Graphical depiction of ES, AS and Absolute error for NE no. 2.7.5 for case (c).

2.7.6 Basic LEE:

For $\mu(x) = -2(2x^2 + 3)$ and $\lambda(y) = y$ then the equation

$$y''(x) + \frac{2}{x}y'(x) - 2(2x^2 + 3)y(x) = 0 \quad (2.52)$$

With BC,

$$y(0) = 1, y'(0) = 0, \quad (2.53)$$

ES:

$$y(x) = e^{x^2} \quad (2.54)$$

Table 2.14 shows a comparative study of absolute error of proposed methods with other methods and whereas Table 2.15 signifies value of L_2 and L_∞ error at different LOR. In Figure 2.10, comparative study is discussed between the AS and ES derived by proposed method and absolute error value.

Table 2.14 A comparative study of Absolute errors obtained using proposed method with methods available in the literature.

\mathcal{X}	Error by Absolute error [110]	Absolute Error Gürbüz and Sezer [86]	Absolute error HSWM
0.1	3.73E-07	9.27E-04	1.75E-10
0.2	2.91E-07	1.66E-03	6.91E-10
0.3	3.97E-07	2.02E-03	1.53E-09
0.4	4.85E-07	2.29E-03	2.66E-09
0.5	3.99E-07	2.58E-03	4.00E-09
0.6	5.43E-07	2.93E-03	5.38E-09
0.7	6.52E-07	3.36E-03	6.50E-09
0.8	6.24E-07	3.92E-03	6.80E-09
0.9	9.22E-07	4.66E-03	5.22E-09

Table 2.15 A comparative study of Errors obtained using proposed method at different LOR.

LOR	$L_2 - error$	$L_\infty - error$
$J = 0$	1.99E-03	5.06E-03
$J = 1$	1.21E-04	3.18E-04
$J = 2$	1.71E-05	4.37E-05
$J = 3$	1.95E-06	4.98E-06
$J = 4$	2.17E-07	5.54E-07
$J = 5$	2.42E-08	6.16E-08

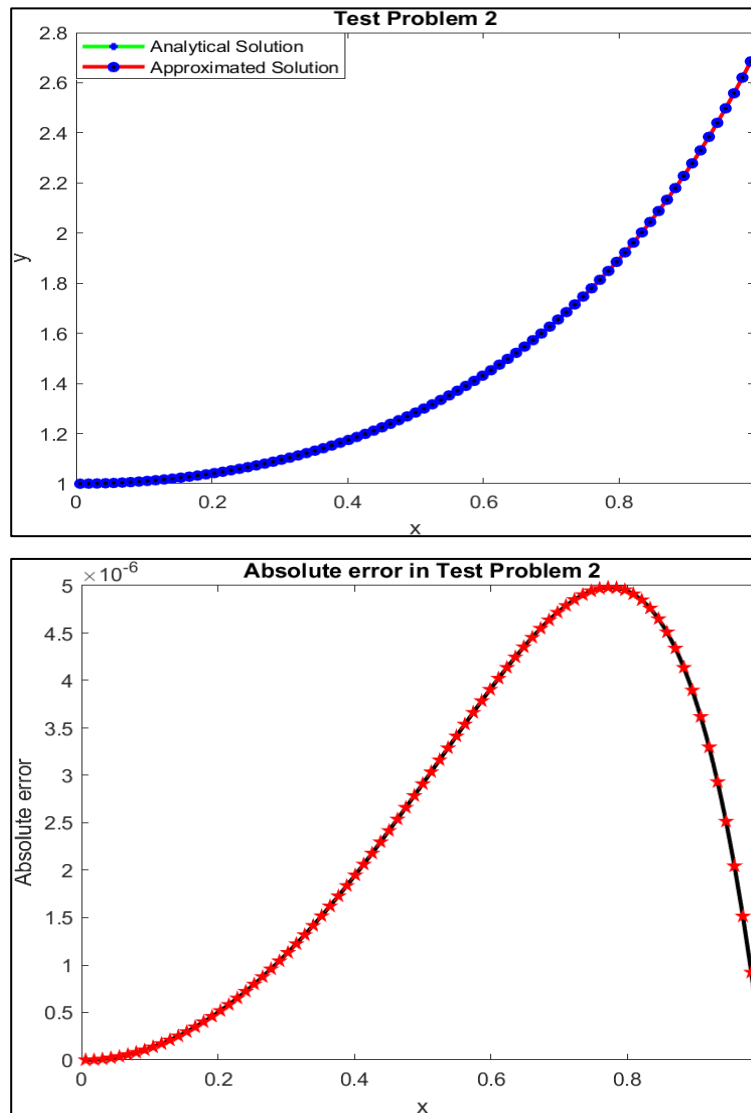


Figure 2.10 Graphical depiction of ES, AS, Absolute error for NE no. 2.7.6.

2.7.7 Lane Emden equation:

For $\mu(x) = 1$, $\lambda(y) = y$ and $\varphi(x) = 6 + 12x + x^2 + x^3$

$$y''(x) + \frac{2}{x}y'(x) + y(x) = 6 + 12x + x^2 + x^3 \quad (2.55)$$

With BC,

$$y(0) = 0, y'(0) = 0, \quad (2.56)$$

ES:

$$y(x) = x^2 + x^3 \quad (2.57)$$

Table 2.16 shows a comparative study of absolute error of proposed methods with other methods and whereas Table 2.17 signifies value of L_2 and L_∞ error at different LOR. In Figure 2.11, comparative study is discussed between the AS and ES derived by proposed method and absolute error value.

Table 2.16 A comparative study of Absolute errors obtained using proposed method with methods available in the literature.

χ	Absolute error by HS3W at LOR J=4	Absolute error by HS3W at LOR J=5
0.1	4.259E-07	4.738E-08
0.2	8.591E-07	9.421E-08
0.3	1.270E-06	1.405E-07
0.4	1.675E-06	1.862E-07
0.5	2.073E-06	2.303E-07
0.6	2.476E-06	2.739E-07
0.7	2.850E-06	3.161E-07
0.8	3.211E-06	3.568E-07
0.9	3.571E-06	3.957E-07

Table 2.17 A comparative study of Errors obtained using proposed method at different LOR.

LOR	Absolute error by HS2W[43]	Absolute error by HS3W
$J = 4$	5.434E-04	2.073E-06
$J = 5$	3.427E-05	2.303E-07

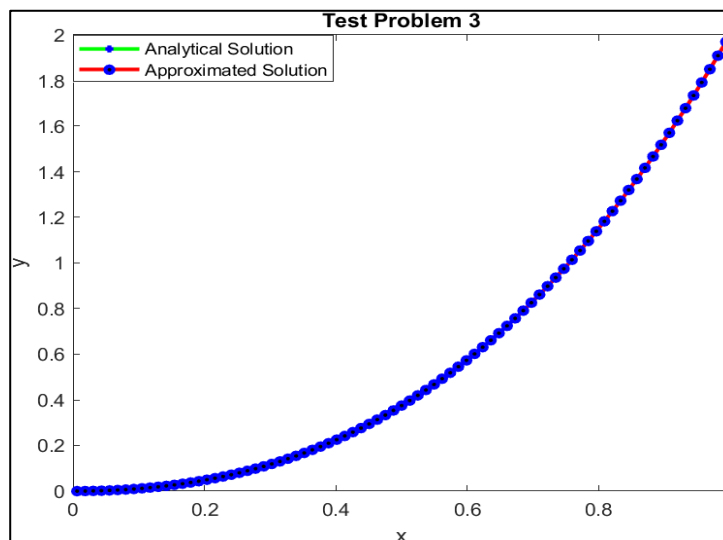




Figure 2.11 Graphical depiction of ES, AS, Absolute error for NE no.2.7.7.

2.7.8 Basic LEE:

For $\mu(x) = x$, $\lambda(y) = y$ and $\varphi(x) = x^5 - x^4 + 44x^2 - 30x$, then the equation is the basic LEE

$$y''(x) + \frac{8}{x}y'(x) + xy(x) = x^5 - x^4 + 44x^2 - 30x \quad (2.58)$$

BC,

$$y(0) = 0, y'(0) = 0 \quad (2.59)$$

ES:

$$y(x) = x^4 - x^3 \quad (2.60)$$

Table 2.18 shows a comparative study of absolute error of proposed methods with other methods and whereas Table 2.19 signifies value of L_2 and L_∞ error at different LOR. In Figure 2.12, comparative study is discussed between the AS and ES derived by proposed method and absolute error value.

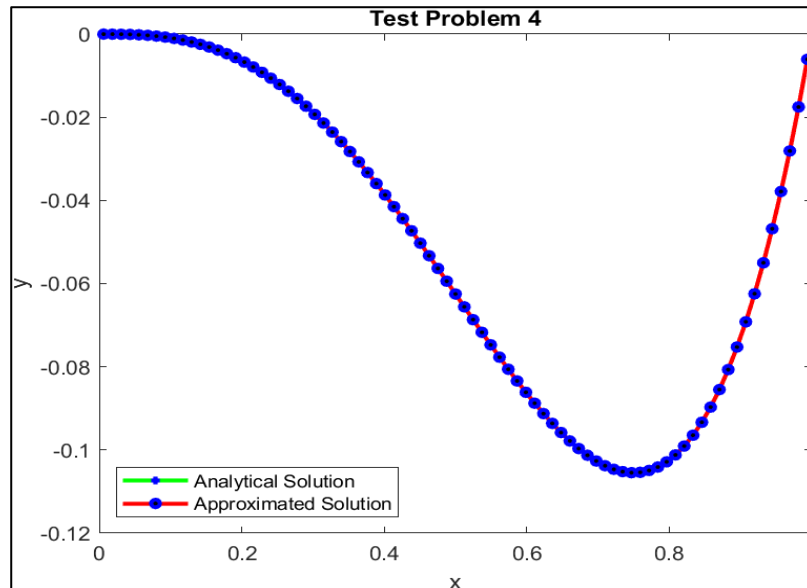
Table 2.18 A comparative study of Absolute errors obtained using proposed method with methods available in the literature.

x	ES	Absolute error by HS3W at LOR	Abs. Error for OHAM (0 th order) [87].
0.1	-0.0009	4.426E-09	1.180E-08
0.2	-0.0064	7.200E-09	6.899E-07
0.3	-0.0189	8.357E-09	7.114E-06

0.4	-0.0384	7.877E-09	3.579E-05
0.5	-0.0625	5.775E-09	1.206E-04
0.6	-0.0864	2.036E-09	3.125E-04
0.7	-0.1029	3.326E-09	6.679E-04
0.8	-0.1024	1.029E-08	1.220E-03
0.9	-0.0729	1.880E-08	1.932E-03

Table 2.19 A comparative study of Errors obtained using proposed method at different LOR.

LOR	$L_2 - error$	$L_\infty - error$
$J = 0$	9.34E-02	9.17E-03
$J = 1$	9.66E-03	1.33E-03
$J = 2$	1.07E-03	1.76E-04
$J = 3$	1.19E-04	2.05E-05
$J = 4$	1.33E-05	2.32E-06
$J = 5$	1.48E-06	2.59E-07



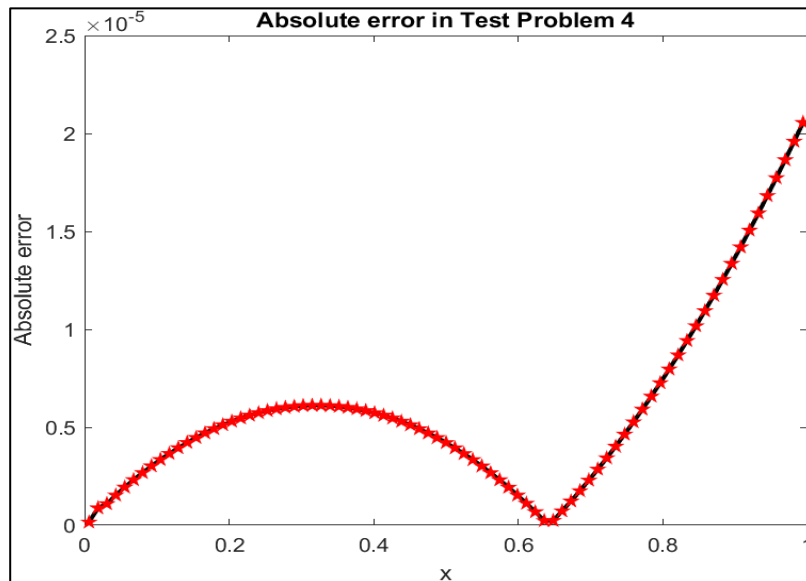


Figure 2.12 Graphical depiction of the ES, the AS, and the absolute error for NE no. 2.7.8

2.7.9 LEE:

For $\mu(\mathcal{X}) = \mathcal{X}$, $\lambda(\mathcal{Y}) = \mathcal{Y}$ and $\varphi(x) = -n^2 \cos(n\mathcal{X}) - \frac{2n}{x} \sin(n\mathcal{X})$, then the equation is the basic LEE

BC,

$$y(0) = 2, y'(0) = 0 \quad (2.62)$$

ES:

$$y(\mathcal{X}) = 1 + \cos(n\mathcal{X}) \quad (2.63)$$

Table 2.20 shows a comparison between absolute error of proposed method by other methods.

In Figure 2.13, shows a comparison between the AS and ES derived by proposed method.

Table 2.20 A comparative study of Absolute errors obtained using proposed method with methods available in the literature.

\mathcal{X}	ES	Absolute error by HS3W at LOR	Abs. Error for IEM [111].
0.2	1.8253	4.5355E-07	1.500E-02
0.1	1.9553	1.052E-07	9.800E-03
0.05	1.9887	2.926E-08	2.800E-05
0.02	1.9882	1.411E-10	8.400E-06

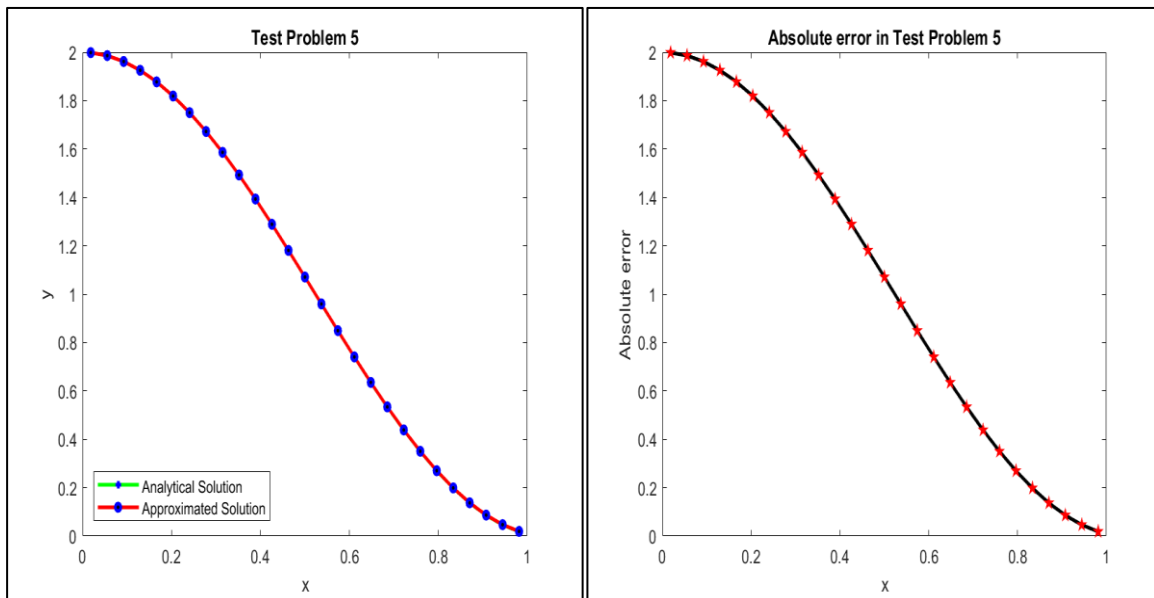


Figure 2.13 Graphical depiction of the ES, the AS, and the absolute error for NE no. 2.7.9

2.8 Conclusion:

After going through the results obtained for numerical experiments with the proposed technique, we observed that, in comparison to other methods, a higher-order non-linear EFE and LEE can be easily solved by using HS3WM with less computational cost and high accuracy. With the use of the MATLAB subprogram, AS of EFE is attained. The solution obtained accuracy results with a higher LOR at a small number of collocation points by HS3WM in comparison to HS2WM and other existing methods available in the literature. Even at same LOR HS3WM provides the less value of error in comparison to HS2WM.

Therefore, by observing the performance of the method on different numerical experiments, it is concluded that, in the future the proposed computational method will be extended to solve numerous higher order complex ODEs of the same kind with singularities, which has great importance in the fields of applied mathematics and astrophysics. While the Haar scale 3 wavelet family offers advantages, its discontinuity at partition points poses a challenge. This discontinuity prevents the direct use of differentiation for calculating wavelet weight coefficients. Consequently, integration becomes the preferred method for determining these coefficients. Otherwise this method is appropriate for solving different kinds of ODEs.

Chapter 3

A numerical analysis for solving various mathematical 2D-partial differential equations via scale 3 Haar wavelets.

3.1 Introduction:

In various fields such as plasma physics, solid-state physics, fluid physics, chemical kinetics, and mathematical biology, non-linear phenomena play a vital role in discussing the solutions to the physical problems developed in these fields, which are represented in terms of PDEs. To deal with these kinds of difficulties, different numerical and analytical methods are used for finding the solution to these equations. As per the literature review, it was observed that wavelet-based methods are one of the compatible tools for searching the solutions of these kinds of real-life problems. As it is enough sufficient to tackle with these kinds of complexities. Several articles have already published to discuss the applicability of the wavelet method for evaluating the solution non-linear and higher order complex DEs. Nonlinear dispersive equations are predominantly occurring whenever dispersion leads to dissipation, such as in plasma physics, nonlinear fiber optics, electrical transmission line behavior, communication theory, transport in porous media, and even blood pressure etc. In the world of waves, strong dispersion is the inherent property of waves arising in the natural real medium, except for some exclusion of non-dispersive light and sound. This fact has strongly motivated the research community to conduct the deep analysis of phenomena governed by nonlinear dispersive equations. In the framework of the theory of nonlinear dispersive equations, the KdV equation has gotten huge attention from the scientific community. One-dimensional nonlinear lattice, long-wave motion in shallow water, hydrodynamics, quantum mechanics, plasma physics, and optics are all discussed by the generalized KdV equation [112]–[116]. The KdV equation's wave-soliton solutions explain why our pulse can be felt all over our body, which is caused by a localized pressure wave in our arteries and survives despite changes in local circumstances and artery shape [117], [118]. Similarly, a nonlinear KGE is a second order PDE, and it has applications in the sector of applied physics, such as phenomena of field theory and quantum mechanics. Basically, KGE belongs to family of a wave equations used to study the behavior of particles in motion at high velocities with high energy.

Because of some mathematical complications in treating these equations, finding the solution to these types of equations becomes a big challenge, as there is no established analytic method to solve this kind of problems. As a result, many researchers are working on developing numerical and semi-analytic schemes for solving problem governed by these PDEs, such as GT[119], DM[120], Collocation and RBF [121], HP[122], VIM[123], FDM[124], LM [125] and dyadic wavelet [126]–[128], quadratic and cubic non-linearity [129], ADM [130], [131], Decomposition method [132], [133], VIM [74], [134], HPM [135], AEM [136], Polynomial wavelets [137], Legendre wavelet [138], [139], HWOM[140], Laguerre wavelet [141], CWM [142], HWCM [56].

The wavelet method is applicable in different fields, such as image denoising [143], [144] finding variance, correlation, and covariance in BSE [145]. But the use of HS2WM is common in the literature. Mittal and Pandit devised the HS3W-based technique to achieve a numerical approximation of order two beginning and problems with boundary value recently. They also demonstrated that the scale-3 Haar wavelet convergence rate is higher than the dyadic wavelets [66], [68]. H. Kaur et al. discussed the Bagley-Torvik equation by using a HW, and the results obtained are good in comparison to existing solutions in the literature [146]. R. Kumar et al. suggested a solution to higher-order linear and non-linear boundary problems using the Haar scale [147] and further demonstrated a hybrid method for solving BVPs. The results obtained are better than the previous results [107]. R. Kumar discussed the historical development of the Haar scale and also devised the construction of non-dyadic wavelet families with their integrals [148]. This gives us reason to believe that developing a new hybrid approach using HS3WM for the dispersive equations, would lead to an improved solution for these problems.

The prime objective of the current work is to provide a better solver for the third-order KdV equation and second order non-linear KGE by developing a new numerical technique using two-dimensional HS3W bases.

The KdV equation has the following mathematical form. i.e.

$$u_t + \epsilon uu_x + \alpha u_{xxx} = f(x, t), \quad a \leq x \leq b, \quad t > 0, \quad \epsilon > 0$$

$$\text{with ICs, } u(x, 0) = k_1(x), a \leq x \leq b \quad \text{and}$$

$$\text{BCs: } u(0, t) = \rho_1, \quad u_x(0, t) = \rho_2, \quad u_{xx}(0, t) = \rho_3.$$

where are k_1, ρ_1, ρ_2 and ρ_3 assumed to be continuous functions, t is time variable, and x is space variable.

Nonlinear KGE expressed as:

$$\frac{\partial^2 u}{\partial t^2} - \frac{\partial^2 u}{\partial x^2} + \mu u - \epsilon u^2 = m(x, t), \quad (x, t) \in [0, 1] \times [0, T] \quad (3.1)$$

Having IC as,

$$u(x, 0) = \eta_1(x) \quad (3.2)$$

$$\frac{\partial u}{\partial t}(x, 0) = \eta_2(x) \quad (3.3)$$

and the BC,

$$u(0, t) = \gamma_1(t), \quad t \in [0, T] \quad (3.4)$$

$$u(1, t) = \gamma_2(t), \quad t \in [0, T] \quad (3.5)$$

Where μ, ϵ, m are known constants, $\eta_1(x), \eta_2(x), \gamma_1(t), \gamma_2(t), m(x, t)$ are the given functions and here value of $u(x, t)$ is to be determined.

3.2 Haar Scale-3 Wavelet:

The HS3W integral approach is used to solve third-order non-linear PDEs, in which the DEs highest order derivative is elaborated into HS3W, and the derivatives of lower order are assessed by integrating the DEs. The HS3WM as more accuracy and converges faster than the HS2W.

$$f(x) \approx k_1 \phi_1(x) + \sum_{\text{even index } n \geq 2}^{\infty} k_n \phi_n^1(x) + \sum_{\text{odd index } n \geq 3}^{\infty} k_n \phi_n^2(x)$$

3.3 Discretization Scheme for second and third order partial differential equation:

For solving PDE of the kind, we discussed the concept of time and space discretisation.

$$u_t + \epsilon u u_x + \alpha u_{xxx} = f(x, t) \quad (3.6)$$

$$u_t^\alpha + \epsilon u u_x + u_{xx} + \mu u_{xxx} = f(x, t) \quad (3.7)$$

For $\epsilon = 0$ and $\alpha = 1$, for a non – homogenous equation $f(x, t) = F(x, t)$ above equation becomes linear.

$$u_t + u_{xxx} = f(x, t) \quad (3.8)$$

For $\epsilon = 1$ and $\alpha = 1$, $\mu = 1$, we get,

$$u_t + uu_x + u_{xxx} = f(x, t) \quad (3.9)$$

For solving the non-linearity of the above function Quasilinearisation technique is used.

For linear dispersive equation:

$$u_t + u_{xxx} = f(x, t) \quad (3.10)$$

With subject to ICs:

$$u(x, 0) = g(x); 0 \leq x \leq 1 \quad (3.11)$$

With subject to BCs:

$$u(0, t) = \varphi_0(t), u_x(0, t) = \varphi_1(t); 0 \leq t \leq T \quad (3.12)$$

$$u_{xx}(0, t) = \varphi_2(t). \quad (3.13)$$

Here α, ϵ are known constants. $g(x), \varphi_0(t), \varphi_1(t)$ and $\varphi_2(t)$ are the given functions. The value of $u(x, t)$ is to be determined.

Let us consider,

$$u_{txxx}(x, t) = \sum_{i=1}^{3p} \sum_{x=1}^{3p} a_{iz} H_i(x) H_z(t) \quad (3.14)$$

Integrating equation (3.14), w.r.t to t between 0 to t

$$u_{xxx}(x, t) = \sum_{i=1}^{3p} \sum_{x=1}^{3p} a_{ix} H_i(x) Q_{1,x}(t) + u_{xxx}(x, 0) \quad (3.15)$$

$$u_{xxx}(x, t) = \sum_{i=1}^{3p} \sum_{x=1}^{3p} a_{ix} H_i(x) Q_{1,x}(t) + [g(x)]_{xxx} \quad (3.16)$$

On integrating with respect to x,

$$u_{xx}(x, t) - u_{xx}(0, t) = \sum_{i=1}^{3p} \sum_{x=1}^{3p} a_{ix} Q_{1,i}(x) Q_{1,x}(t) + [u_{xx}(x, 0) - u_{xx}(0, 0)] \quad (3.17)$$

$$u_{xx}(x, t) = \sum_{i=1}^{3p} \sum_{x=1}^{3p} a_{ix} Q_{1,i}(x) Q_{1,x}(t) + [u_{xx}(x, 0) - u_{xx}(0, 0)] + u_{xx}(0, t) \quad (3.18)$$

Integrating with respect to x,

$$u_x(x, t) - u_x(0, t) \quad (3.19)$$

$$= \sum_{i=1}^{3p} \sum_{x=1}^{3p} a_{ix} Q_{2,i}(x) Q_{1,x}(t) + [u_x(x, 0) - u_x(0,0)] - x u_{xx}(0,0) + x u_{xx}(0, t)$$

$$u_x(x, t) = \sum_{i=1}^{3p} \sum_{x=1}^{3p} a_{ix} Q_{2,i}(x) Q_{1,x}(t) - x u_{xx}(0,0) + x u_{xx}(0, t) + [u_x(x, 0) - u_x(0,0)] + u_x(0, t) \quad (3.20)$$

$$u_x(x, t) = \sum_{i=1}^{3p} \sum_{x=1}^{3p} a_{ix} Q_{2,i}(x) Q_{1,x}(t) + [g_x(x, 0) - g_x(0,0)] - x \varphi_2(0) + x \varphi_2(t) + \varphi_1(t) \quad (3.21)$$

Again, integrating with respect to x .

$$u(x, t) - u(0, t) = \sum_{i=1}^{3p} \sum_{x=1}^{3p} a_{ix} Q_{3,i}(x) Q_{1,x}(t) + [u(x, 0) - u(0,0)] - x u_x(0,0) - \frac{x^2}{2} u_{xx}(0,0) + \frac{x^2}{2} u_{xx}(0, t) + x u_x(0, t) \quad (3.22)$$

$$u(x, t) = \sum_{i=1}^{3p} \sum_{x=1}^{3p} a_{ix} Q_{3,i}(x) Q_{1,x}(t) + [u(x, 0) - u(0,0)] - x u_x(0,0) - \frac{x^2}{2} u_{xx}(0,0) + \frac{x^2}{2} u_{xx}(0, t) + x u_x(0, t) + u(0, t) \quad (3.23)$$

On differentiating w.r.t to t we get,

$$u_t(x, t) = \sum_{i=1}^{3p} \sum_{x=1}^{3p} a_{ix} Q_{3,i}(x) H_x(t) + [\frac{x^2}{2} u_{xx}(0, t)]_t + x [u_x(0, t)]_t + [u(0, t)]_t \quad (3.24)$$

BCs we get,

$$u(x, t) = \sum_{i=1}^{3p} \sum_{x=1}^{3p} a_{ix} Q_{3,i}(x) Q_{1,x}(t) + [g(x) - g(0)] + \frac{x^2}{2} [\varphi_2(t) - \varphi_2(0)] + x [\varphi_1(t) - \varphi_1(0)] + \varphi_0(t) \quad (3.25)$$

$$u_t(x, t) = \sum_{i=1}^{3p} \sum_{x=1}^{3p} a_{ix} Q_{3,i}(x) H_x(t) + \frac{x^2}{2} [\varphi_2(t)]_t + x [\varphi_1(t)]_t + [\varphi_0(t)]_t \quad (3.26)$$

$$u_x(x, t) = \sum_{i=1}^{3p} \sum_{x=1}^{3p} a_{ix} Q_{2,i}(x) Q_{1,x}(t) + [g_x(x, 0) - g_x(0,0)] + x [\varphi_2(t) - \varphi_2(0)] + \varphi_1(t) \quad (3.27)$$

$$u_{xxx}(x, t) = \sum_{i=1}^{3p} \sum_{x=1}^{3p} a_{ix} H_i(x) Q_{1,x}(t) + u_{xxx}(x, 0) \quad (3.28)$$

$$u_t + \alpha u_{xxx} = F(x, t) \quad (3.29)$$

$$\sum_{i=1}^{3p} \sum_{x=1}^{3p} a_{ix} Q_{3,i}(x) H_x(t) + \left[\frac{x^2}{2} \varphi_2(t) \right]_t + [x\varphi_1(t)]_t + [\varphi_0(t)]_t \quad (3.30)$$

$$+ \alpha \left[\sum_{i=1}^{3p} \sum_{x=1}^{3p} a_{ix} H_i(x) Q_{1,x}(t) + [g(x)]_{xxx} \right] \\ = F(x, t)$$

$$\sum_{i=1}^{3p} \sum_{x=1}^{3p} a_{ix} \{ Q_{3,i}(x) H_x(t) + \alpha [H_i(x) Q_{1,x}(t)] \} \quad (3.31)$$

$$= F(x, t) - [x\varphi_1(t)]_t - [\varphi_0(t)]_t - \left[\frac{x^2}{2} \varphi_2(t) \right]_t - \alpha [g(x)]_{xxx}$$

Similarly, For approximating Space and time variables containing HOD in the KGE are approximated with the help of HS3WM as explained below:

$$u_{xxtt}(x, t) = \sum_{i=1}^{3p} \sum_{n=1}^{3p} a_{in} h_i(x) h_n(t) \quad (3.32)$$

To perform integration with respect to x , the lower limit is set to zero, while the upper limit is x , the above equation converted in to:

$$u_{xxtt}(x, t) = \sum_{i=1}^{3p} \sum_{n=1}^{3p} a_{in} P_{1,i}(x) h_n(t) + \varphi_{xxtt}(0, t) \quad (3.33)$$

Again, integration with respect to x , the lower limit is set to zero, while the upper limit is 1, the value of $u_{xxtt}(0, t)$ is given by

$$u_{xxtt}(0, t) = (u_{tt}(1, t) - u_{tt}(0, t)) - \sum_{i=1}^{3p} \sum_{n=1}^{3p} a_{in} P_{2,i}(1) h_n(t) \quad (3.34)$$

and equation becomes,

$$u_{x\tau\tau}(x, \tau) = \sum_{i=1}^{3p} \sum_{n=1}^{3p} a_{in} \left(P_{1,i}(x) - P_{2,i}(1) \right) h_n(\tau) + (u_{\tau\tau}(1, \tau) - u_{\tau\tau}(0, \tau)) \quad (3.35)$$

Again, integration with respect to x , the lower limit is set to zero, while the upper limit is x

$$u_{\tau\tau}(z, \tau) = \sum_{i=1}^{3p} \sum_{n=1}^{3p} a_{in} \left(P_{2,i}(z) - z P_{2,i}(1) \right) h_n(\tau) + z u_{\tau\tau}(1, \tau) + (1 - z) u_{\tau\tau}(0, \tau) \quad (3.36)$$

between the limit 0 to τ , integrating w.r.t t and after that on applying the BC, we get

$$u_{\tau}(x, \tau) = \sum_{i=1}^{3p} \sum_{n=1}^{3p} a_{in} \left(P_{2,i}(x) - x P_{2,i}(1) \right) P_{1,n}(\tau) + x (u_{\tau}(1, \tau) - \eta_2(1)) + (1 - x) (u_{\tau}(0, \tau) - \eta_2(0)) + \eta_2(x) \quad (3.37)$$

Integrate w.r.t τ in between the given limit implies:

$$u(x, \tau) = \sum_{i=1}^{3p} \sum_{n=1}^{3p} a_{in} \left(P_{2,i}(x) - x P_{2,i}(1) \right) P_{2,n}(\tau) + x(\gamma_2(\tau) - \gamma_2(0)) - x \tau \eta_2(1) + (1 - x)(\gamma_1(\tau) - \gamma_1(0)) - (1 - x) \tau \eta_2(0) + \tau \eta_2(x) \quad (3.38)$$

On Differentiating the above equation with respect x two times,

$$u_{xx}(x, \tau) = \sum_{i=1}^{3p} \sum_{n=1}^{3p} a_{in} h_i(x) P_{2,n}(\tau) + \tau (\eta_2)_{xx}(x) \quad (3.39)$$

$$\begin{aligned} & \sum_{i=1}^{3p} \sum_{n=1}^{3p} a_{in} \left(P_{2,i}(z) - x P_{2,i}(1) \right) h_n(\tau) + x(\gamma_2(\tau))_{\tau\tau} + (1 - x)(\gamma_1(\tau))_{\tau\tau} + \\ & \alpha \left(\sum_{i=1}^{3p} \sum_{n=1}^{3p} a_{in} \left(P_{2,i}(x) - x P_{2,i}(1) \right) P_{2,n}(\tau) + x(\gamma_2(\tau) - \gamma_2(0)) - x \tau \eta_2(1) \right. \\ & \quad \left. + (1 - x)(\gamma_1(\tau) - \gamma_1(0)) - (1 - x) \tau \eta_2(0) + \tau \eta_2(x) \right) \end{aligned} \quad (3.40)$$

$$= \sum_{i=1}^{3p} \sum_{n=1}^{3p} a_{in} h_i(x) P_{2,n}(t) + t(\eta_2)_{xx}(x) + m(x, t)$$

$$\begin{aligned} \sum_{i=1}^{3p} \sum_{n=1}^{3p} a_{in} \left[\left(P_{2,i}(x) - x P_{2,i}(1) \right) h_n(t) + \alpha \left(\left(P_{2,i}(x) - x P_{2,i}(1) \right) P_{2,n}(t) \right) - \right. \\ \left. h_i(x) P_{2,n}(t) \right] = m(x, t) + t(\eta_2)_{xx}(x) - \left(x(\gamma_2(t))_{tt}, + (1-x)(\gamma_1(t))_{tt} \right) - \\ \alpha \left(x(\gamma_2(t) - \gamma_2(0)) - x t \eta_2(1) + (1-x)(\gamma_1(t) - \gamma_1(0)) - (1-x) t \eta_2(0) + \right. \\ \left. t \eta_2(x) \right) \end{aligned} \quad (3.41)$$

Now discretizing the variable as $x \rightarrow x_r$, $t \rightarrow t_s$ where $x_r = \frac{2r-1}{6p}$, $t_s = \frac{2s-1}{6p}$, $r, s = 1, 2, \dots, 3p$ in the above equations we get the following system of algebraic equations:

$$\sum_{i=1}^{3p} \sum_{n=1}^{3p} a_{in} R_{i,n,r,s} = F(r, s)$$

Where,

$$\begin{aligned} R_{i,n,r,s} = \left[\left(P_{2,i}(x_r) - x_r P_{2,i}(1) \right) h_n(t_s) + \alpha \left(\left(P_{2,i}(x_r) - x_r P_{2,i}(1) \right) P_{2,n}(t_s) \right) - \right. \\ \left. h_i(x_r) P_{2,n}(t_s) \right] \\ F(r, s) = m(x_r, t_s) + t(\eta_2)_{xx}(x_r) - \left(x_r(\gamma_2(t_s))_{tt}, + (1-x_r)(\gamma_1(t_s))_{tt} \right) - \\ \alpha \left(x_r(\gamma_2(t_s) - \gamma_2(0)) - x_r t_s \eta_2(1) + (1-x_r)(\gamma_1(t_s) - \gamma_1(0)) - (1-x_r) t_s \eta_2(0) + \right. \\ \left. t_s \eta_2(x_r) \right) \end{aligned}$$

The system mentioned above is simplified into a system of algebraic equations, which is then reduced to the following set of 4D-arrays.

$$A_{3p \times 3p} R_{3p \times 3p \times 3p \times 3p} = F_{3p \times 3p}$$

Using the given transformations, the aforementioned system of arrays is transformed and reduced to the following matrix system.

$$a_{i\ell} = b_\lambda \text{ and } F_{rs} = G_\mu$$

$$B_{1 \times (3p)^2} S_{(3p)^2 \times (3p)^2} = G_{1 \times (3p)^2}$$

Where $\lambda = 3p(i - 1) + l$ and $\mu = 3p(r - 1) + s$

The values of b_λ can be calculated for various n values ($n = 1, 2, \dots$) using MATLAB program and the Thomas algorithm to solve the SOE mentioned above. By applying the transformation mentioned earlier, the original wavelet coefficients $a_{i\ell}$ can be retrieved. To obtain the final solution of the problem, these coefficients will be utilized in the equations for different t_n values ($n = 0, 1, 2, \dots$).

3.4 Numerical Methods:

The MATLAB computer language was used to do numerical calculations and generate graphical outputs. A discrete form of the HS3W series is required to determine the numerical solution of a PDE using the HS3WM. There are a range of methods to do this, but we'll stick to the collocation method in the meantime. The HS3W is discontinuous. Therefore, to avoid the collocation point at the point of continuity, the approach given in the equations is applied for the selection of collocation points of the HS3W matrix for the initial LOR $J = 2$.

3.4.1 Linear homogeneous equation

$$u_t + \alpha u_{xxx} = 0, 0 \leq x \leq 1, t \geq 0, \alpha > 0 \quad (3.42)$$

With IC, (3.43)

$$u(x, 0) = \cos x, 0 \leq x \leq 1 \text{ and}$$

$$u(0, t) = \cos at \quad (3.44)$$

$$u_x(0, t) = -\sin at$$

$$u_{xx}(0, t) = -\cos at, t \geq 0.$$

ES, (3.45)

$$u(x, t) = \cos(x + at)$$

$$u(x, t) = \sum_{i=1}^{3p} \sum_{x=1}^{3p} a_{ix} Q_{3,i}(x) Q_{1,x}(t) + u(0, t) + x[u_x(0, t) - u_x(0,0)] \quad (3.46)$$

$$+ \frac{x^2}{2} [u_{xx}(0, t) - u_{xx}(0,0)] + [u(x, 0) - u(0,0)]$$

Table 3.1 Comparison of results achieved for test problem 3.4.1 with ES.

x	t	AS	ES	Absolute Error
0.0555555555556	0.0555555555556	0.97541008539	0.97541008538	2.30E-10
0.1666666666667	0.1666666666667	0.94495691696	0.94495694631	1.87E-09
0.2777777777778	0.2777777777778	0.90284957492	0.90284966935	2.69E-09
0.3888888888889	0.3888888888889	0.84960735580	0.8496075628	2.19E-08
0.5000000000000	0.5000000000000	0.78588689733	0.78588726077	1.19E-08
0.6111111111111	0.6111111111111	0.71247409841	0.71247462453	3.92E-08
0.7222222222222	0.7222222222222	0.68600257950	0.68600314569	6.32E-08
0.8333333333333	0.8333333333333	0.65859016536	0.65859075501	9.24E-08
0.9444444444444	0.9444444444444	0.63027446253	0.63027505092	1.26E-07

The application of boundary conditions to the equation results in the solution being presented through tables and figures. Figure 3.1 described the clear agreement in the ES and AS. Table 3.1 is depicting the performance of present method in comparison with the ES existing in the recent literature. We observed that the proposed method is running well. Further, it has been observed that the error norms decrease with an increase in collocation points which ensures that the proposed scheme is stable.

Table 3.2 L_2 and L_∞ errors at different values of J for test problem 3.4.1.

LOR	J=1	J=2	J=3
L_2 error (HS3WM)	3.962E-04	4.420E-05	4.928E-06
L_2 error [15]	3.867E-03	4.015E-04	4.1837E-05
L_∞ (HS3WM)	8.838E-04	1.052E-04	1.423E-05

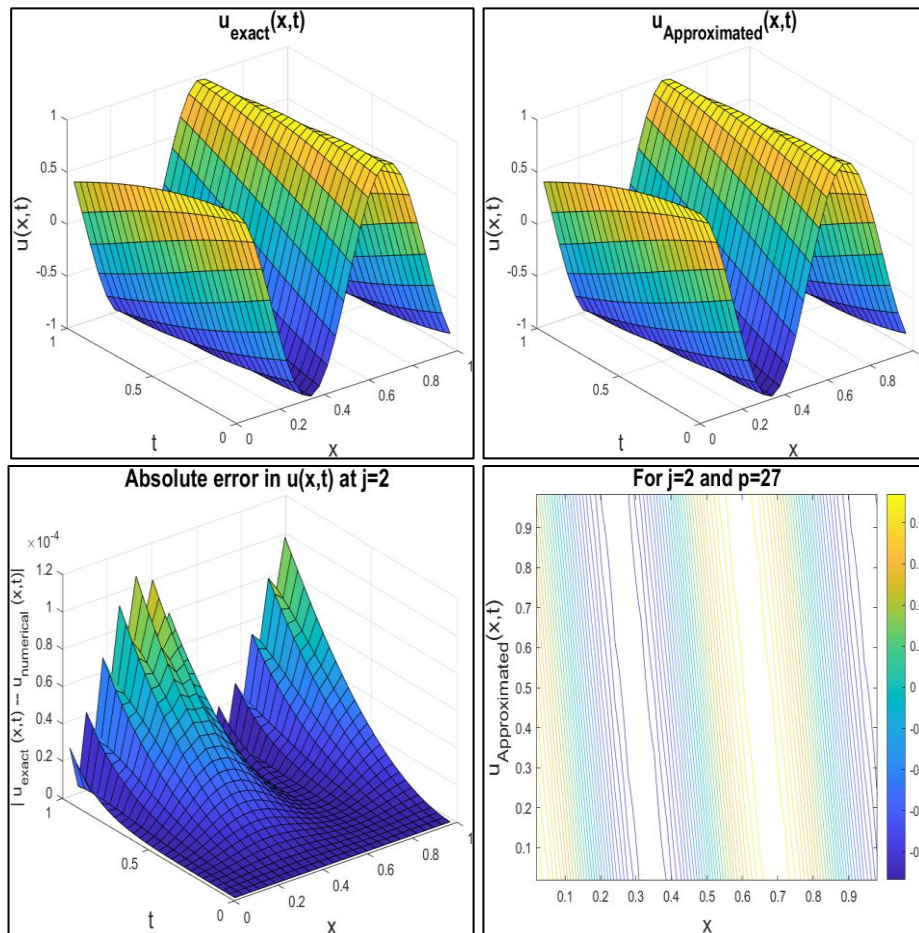


Figure 3.1 Graphical Representation of Numerical Problem: Above Figure shows a graphical representation of ES and AS for Numerical Problem. Illustrate that the exact and numerical findings for $J=2$ are compatible.

3.4.2 Linear Non-homogeneous Equation

$$v_t + \alpha v_{xxx} = -\pi^3 \cos(\pi x) \cos t - \sin(\pi x) \sin t, 0 \leq x \leq 1, t \geq 0, \alpha > 0 \quad (3.47)$$

ES,

With ICs,

$$v(x, 0) = \sin \pi x, 0 \leq x \leq 1 \text{ and } v(0, t) = 0 \quad (3.48)$$

$$v_x(0, t) = \pi \cos t, v_{xx}(0, t) = 0, t \geq 0$$

$$v(x, t) = \sin(\pi x) \cos t \quad (3.49)$$

$$v(x, t) = \sum_{i=1}^{3p} \sum_{x=1}^{3p} a_{il} Q_{3,i}(x) Q_{1,x}(t) + v(0, t) + \frac{x^2}{2} [v_{xx}(0, t) - v_{xx}(0, 0)] + x[v_x(0, t) - v_x(0, 0)] + [v(x, 0) - v(0, 0)] \quad (3.50)$$

With the help of surface plots, results and tables obtained by the proposed scheme have been explained. It is clear from Figure 3.2 that the results achieved and the analytic solution with the proposed scheme are roughly coinciding. By increasing the number of collocation points the solution achieved can further be improved. Table 3.3, in comparison with the ES error obtained by the discussed scheme, are presented.

Table 3.3 Comparison of results achieved for test problem 3.4.2 with ES.

z	t	AS	ES	Absolute Error
0.05555	0.05555	0.058134859223	0.05813485923	8.24E-12
0.16666	0.16666	0.058055122235	0.05805512231	8.47E-11
0.27777	0.27777	0.057895757626	0.05789575784	7.74E-11
0.38888	0.38888	0.057656983977	0.05765698439	6.13E-10
0.50000	0.50000	0.057339128788	0.05733912948	4.19E-10
0.61111	0.61111	0.056942628022	0.05694262905	4.99E-09
0.72222	0.72222	0.056468025517	0.05646802695	3.38E-08
0.83333	0.83333	0.173618403368	0.17361840345	1.22E-08
0.94444	0.9444	0.173618403368	0.17338027100	1.21E-08

Table 3.4 L_2 and L_∞ errors at different values of J for test problem 3.4.2.

LOR	J=1	J=2	J=3
L_2 error (HS3WM)	2.344E-03	2.765E-04	2.907E-04
L_2 error [15]	1.442E-02	1.489E-03	1.5000E-03
L_∞ (HS3WM)	5.491E-03	8.791E-04	1.345E-03

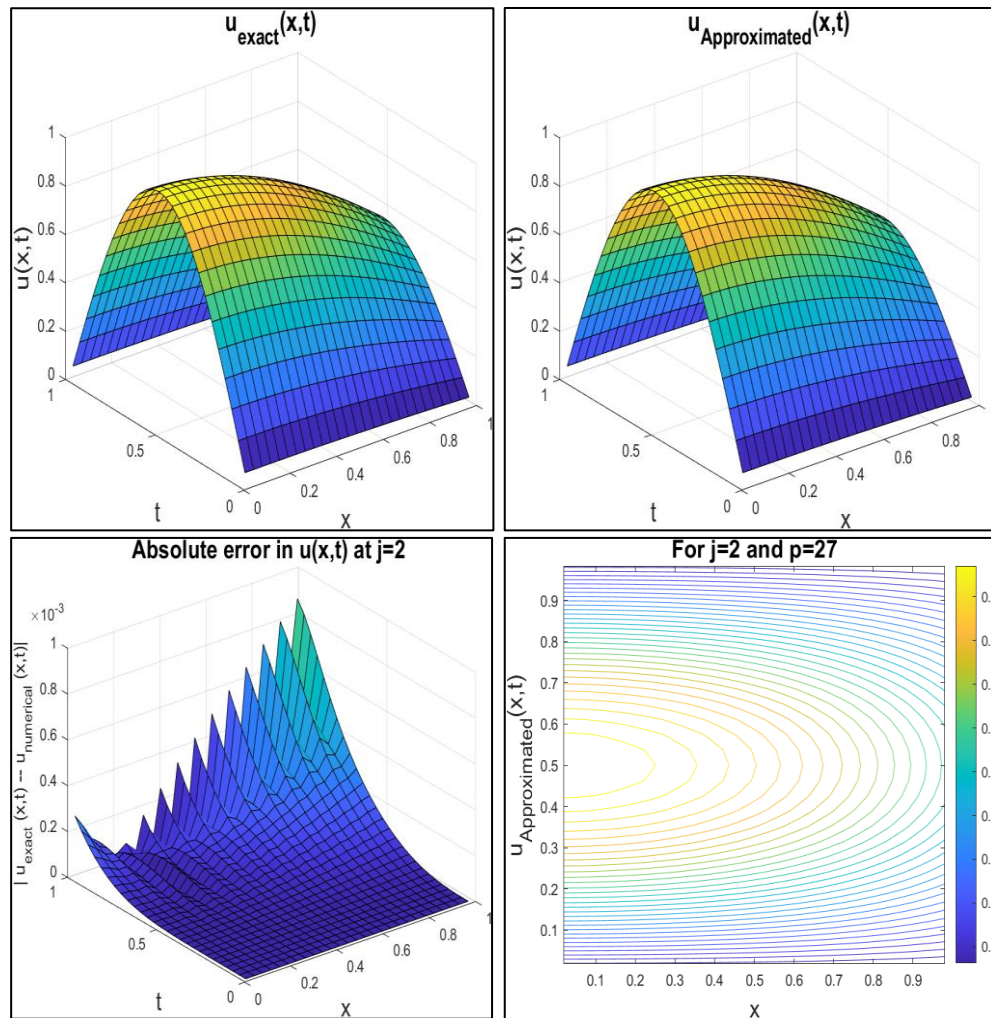


Figure 3.2 Graphical Representation of Numerical Problem: Above Figure shows a graphical representation of ES and AS for Numerical Problem. Illustrate that the exact and numerical findings for $J=2$ are compatible.

3.4.3 Non-Linear KdV Equation

$$w_t^\alpha + ww_x + w_{xxx} = 2 \frac{\sqrt{t}e^x}{\Gamma(1/2)} + t^2e^{2x} + te^x \quad (3.51)$$

With subject to IC

$$w(x, 0) = 0. \quad (3.52)$$

With subject to BC,

$$(3.53)$$

$$w(0, t) = t, w_x(0, t) = t, w_{xx}(0, t) = t$$

For this above problem we consider for $\alpha = 1$,

ES of the given statement in the literature

$$w(x, t) = t e^x$$

$$w^{\alpha}_t + w w_x + w_{xxx} = 2 \frac{\sqrt{t} e^x}{\Gamma(1/2)} + t^2 e^{2x} + t e^x \quad (3.54)$$

$$w(x, t) = \sum_{i=1}^{3p} \sum_{x=1}^{3p} a_{il} Q_{3,i}(x) Q_{1,x}(t) + w(0, t) + \frac{x^2}{2} [w_{xx}(0, t) - w_{xx}(0, 0)] \quad (3.53)$$

$$+ x [w_x(0, t) - w_x(0, 0)] + [w(x, 0) - w(0, 0)]$$

Table 3.5 Comparison of AS and ES with Absolute error for numerical problem

x	t	AS	ES	Absolute error
0.0555555555556	0.0555555555556	0.05870679949	0.05872931915	6.83E-08
0.1666666666667	0.1666666666667	0.17616794218	0.17618795746	2.05E-08
0.2777777777778	0.2777777777778	0.29362739612	0.29364659576	3.41E-08
0.3888888888889	0.3888888888889	0.41108608457	0.41110523407	4.78E-07
0.5000000000000	0.5000000000000	0.52854439875	0.52856387238	6.15E-07
0.6111111111111	0.6111111111111	0.64600237955	0.64602251068	7.51E-07
0.7222222222222	0.7222222222222	0.76346019728	0.76348114899	8.82E-07
0.8333333333333	0.8333333333333	0.06502208135	0.06563113404	1.02E-07
0.9444444444444	0.9444444444444	0.19634933254	0.19689340214	1.16E-07

The application of boundary conditions to the equation results in the solution being presented through tables and figures. Figure 3.3 described the clear agreement in the ES and AS. Table 3.5 is depicting the performance of present method in comparison with the ES existing in the recent literature. We observed that the proposed method is running well. Further, it has been observed that the error norms decrease with an increase in collocation points which ensures that the proposed scheme is stable.

Table 3.6 L_2 and L_∞ errors at different values of J for test problem 3.4.3.

LOR	$J=1$	$J=2$	$J=3$
L_2 error (HS3WM)	1.3780E-04	1.5385E-05	1.7103E-06
L_2 error [16]	5.0822E-04	1.0454E-04	2.6384E-05
L_∞ error (HS3WM)	4.5581E-04	5.6298E-05	6.5662E-06

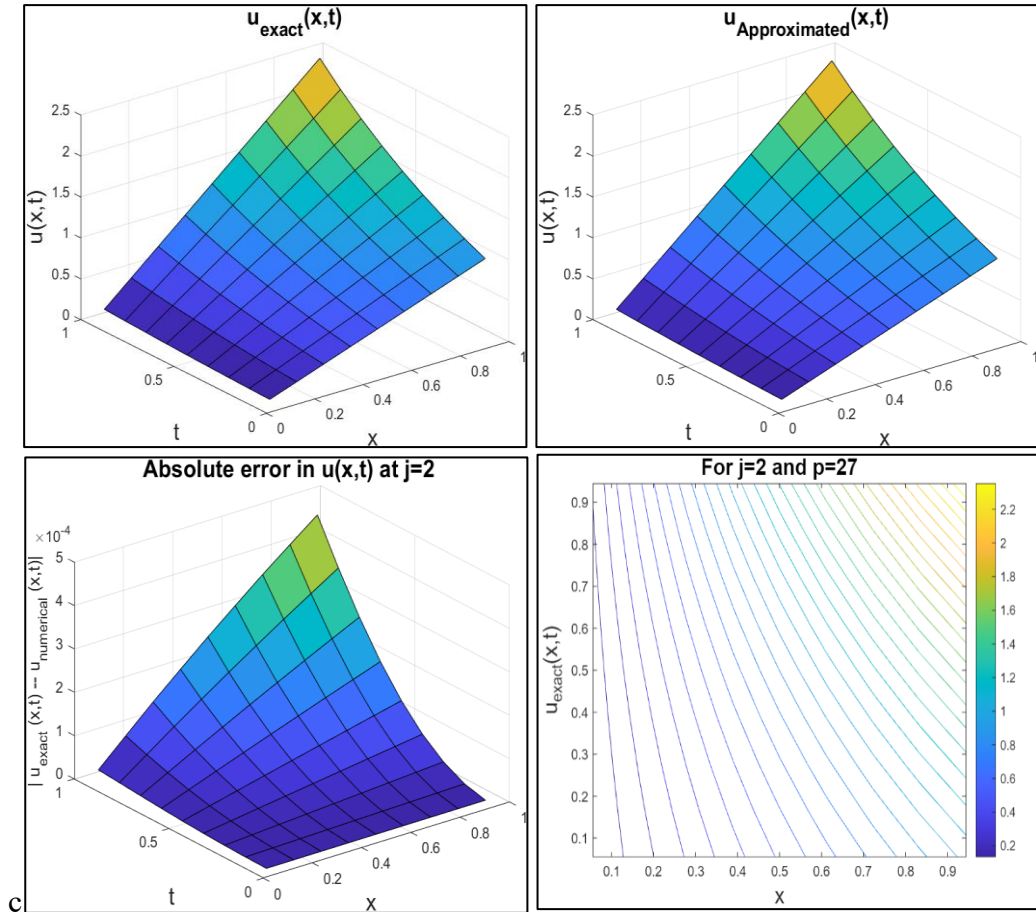


Figure 3.3 Graphical Representation of Numerical Problem: Above Figure shows a graphical representation of ES and AS for Numerical Problem. Illustrate that the exact and numerical findings for $J=2$ are compatible.

3.4.4 “A Non-linear KGE”:

With IC,

$$\frac{\partial^2 u}{\partial t^2} - \omega \frac{\partial^2 u}{\partial z^2} + \mu u - \epsilon u^2 = m(z, t), (z, t) \in [0,1] \times [0, T], \quad (3.54)$$

$$u(z, 0) = 0 \quad z \in [0,1], \quad \frac{\partial u}{\partial t}(z, 0) = 0, z \in [0,1] \quad (3.55)$$

and the BC,

$$u(0, t) = 0 \quad , \quad u(1, t) = t^3 \quad t \in [0, T] \quad (3.56)$$

With

$$\omega = -1, \mu = 0, \epsilon = 1 \text{ \& } m(z, t) = 6zt(z^2 - t^2) + z^6t^6$$

Using current scheme, proposed the numerical solution in the following form:

ES for the problem:

$$u(x, t) = z^3t^3 \quad (3.57)$$

$$u(z, t) = \sum_{i=1}^{3p} \sum_{l=1}^{3p} a_{il} \left(P_{2,i}(z) - z P_{2,i}(1) \right) Q_{2,l}(t) - z t u_t(1,0) + z (u(1, t) - u(1,0)) + (1 - z)(u(0, t) - u(0,0)) - (1 - z) t u_t(0,0) + t u_t(z, 0) + u(z, 0) \quad (3.58)$$

Table 3.7 At different of 'J', value L_2 and L_∞ errors for Test problem 3.4.4

LOR	$J = 1$	$J = 2$	$J = 3$	
L_2 -error	2.6933e-03	2.9622e-04	3.2876e-05	2.5e-04 [149]
L_∞ -error	7.6259e-04	8.5589e-05	9.5212e-06	9.7e-05 [149]

Table 3.8 Comparison of ES for Test problem 3.4.4 with results achieved

z	t	AS	ES	Value of Absolute error	Error value [149].
0.05	0.05	0.000014553615258	0.000014444806667	1.07e-09	-
0.1	0.1	0.003815423325686	0.003900097800132	7.16e-09	3.1e-04
0.2	0.2	0.017939826726911	0.018056008333945	1.34e-08	3.5e-04
0.3	0.3	0.049416386100151	0.049545686868345	1.67e-08	1.8e-04
0.4	0.4	0.034562837292023	0.034563423922912	1.62e-08	3.7e-04
0.5	0.5	0.105175840987305	0.105302640603567	1.60e-08	2.5e-04
0.6	0.6	0.192148930569310	0.192260376739845	1.24e-08	3.7e-04
0.7	0.7	0.317266350484410	0.317352402477415	7.40e-08	3.6e-04
0.8	0.8	0.487458705981956	0.487512225016511	2.80e-08	2.2e-04
0.9	0.9	0.709656476255199	0.709673351557369	2.84e-09	4.5e-04

Applying boundary conditions to the equation yields a solution best visualized through tables and figures. Figure 3.4 demonstrates the good agreement between the ES and AS. Table 3.8 compares the performance of our method against existing ES methods from recent literature.

The results show that our method performs well, with decreasing error norms as the number of collocation points increases, indicating the scheme's stability.

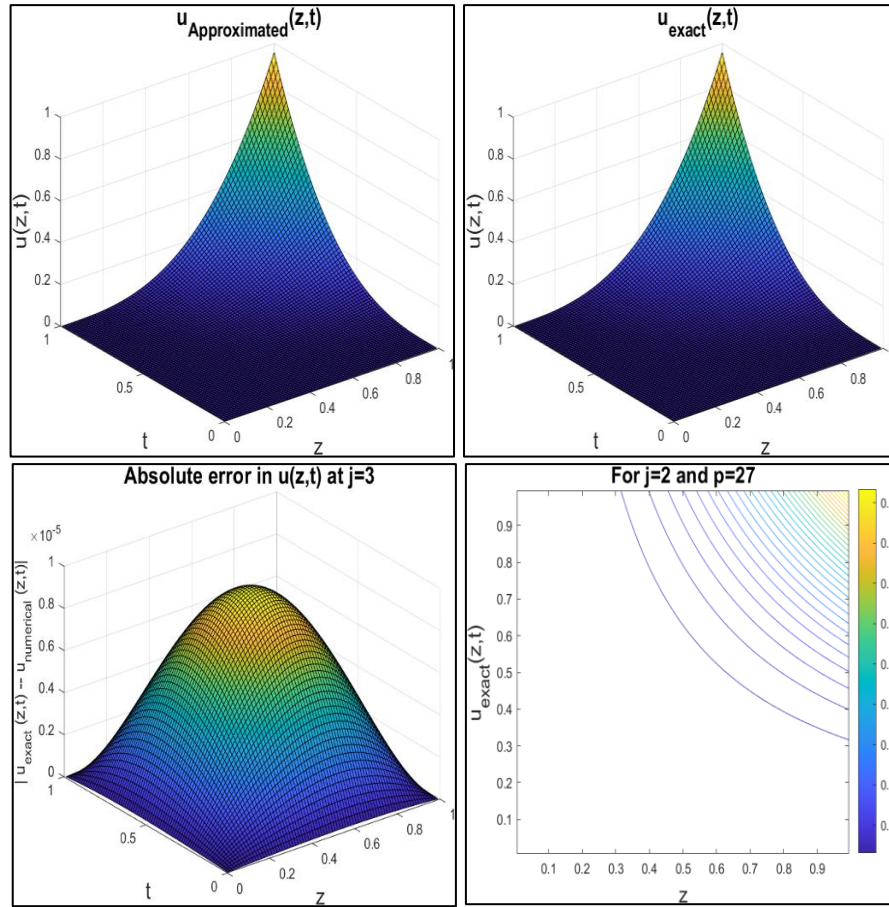


Figure 3.4 The solution for numerical Experiment no. 3.4.4 includes four graphical representations: ES, AS, contour view of the ES, and absolute error.

3.4.5 Numerical Experiment:

$$\frac{\partial^2 u}{\partial t^2} - \omega \frac{\partial^2 u}{\partial z^2} + \mu u - \epsilon u^2 = m(z, t), \quad (z, t) \in [0,1] \times [0, T] \quad (3.59)$$

With IC,

$$\begin{aligned} u(z, 0) &= z, \quad z \in [0,1] \\ \frac{\partial u}{\partial t}(z, 0) &= 0, \quad z \in [0,1] \end{aligned} \quad (3.60)$$

and the BC,

$$u(0, t) = 0, \quad t \in [0, T] \quad (3.61)$$

$$u(1, t) = \cos t, \quad t \in [0, T]; \quad \text{with } \omega = -1 \quad \text{and } m(z, t) = -z \cos t + z^2 \cos^2 t$$

ES for the problem:

$$u(z, t) = z \cos t \quad (3.62)$$

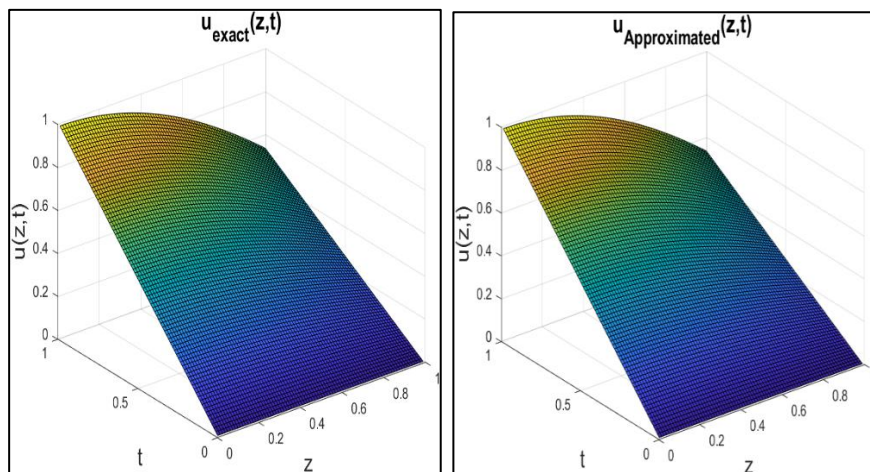
Using current scheme, proposed the numerical solution in the following form:

$$\begin{aligned}
 u(z, t) = & \sum_{i=1}^{3p} \sum_{l=1}^{3p} a_{i\ell} \left(P_{2,i}(z) - z P_{2,i}(1) \right) Q_{2,\ell}(t) - z \tau u_t(1,0) + z (u(1, t) \\
 & - u(1,0)) + (1 - z)(u(0, t) - u(0,0)) - (1 - z) \tau u_t(0,0) \\
 & + \tau u_t(z, 0) + u(z, 0)
 \end{aligned} \tag{3.63}$$

Surface plots effectively illustrate the results and tables generated by our proposed scheme. Figure 3.5 visually confirms the close agreement between the solution obtained using our scheme and the analytical solution. Increasing the number of collocation points can further refine the solution. Table 3.10 presents the error comparison between our scheme and the established ES.

Table 3.9 At different of 'J', value L_2 and L_∞ errors for Test problem 3.4.5

LOR	L_∞ -error (FDM)	L_∞ -error (HSWM2) [56]	L_∞ -error (MFDCM) [149]	L_∞ -error (CM) [149]	L_∞ -error (HSWM3)
3	1.1474E-01	2.2466E-08	5.7e-11	3.3e-04	0
4	1.2236E-01	5.9080E-10	5.8e-12	8.3e-05	0
5	1.2433E-01	6.4369E-11	-	-	0



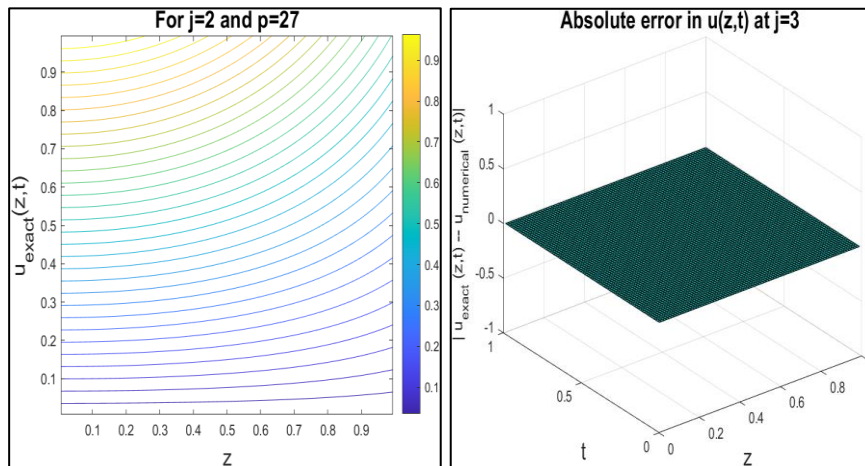


Figure 3.5 The solution for numerical Experiment no. 3.4.5 includes four graphical representations: ES, AS, contour view of the ES, and absolute error.

Table 3.10 Comparison of ES for Test problem 3.4.5 with results achieved

z	t	AS	ES	Value of Absolute Error	Error value [150].
0.1	0.1	0.0061388829	0.0061388829	0	$4.9593E - 8$
0.2	0.2	0.0060452101	0.0060452101	0	$5.6542E - 7$
0.3	0.3	0.0058926166	0.0058926166	0	$1.8493E - 6$
0.4	0.4	0.0056825896	0.0056825896	0	$3.2841E - 6$
0.5	0.5	0.0054171763	0.0054171763	0	$3.8373E - 6$
0.6	0.6	0.0050556234	0.0050556234	0	$4.6197E - 6$
0.7	0.7	0.0046817428	0.0046817428	0	$1.4141E - 5$
0.8	0.8	0.0042622308	0.0042622308	0	$5.6879E - 5$
0.9	0.9	0.0038011762	0.0038011762	0	$1.8571E - 4$

3.5 Discussion:

Using the HS3WM, we convert DEs into set of linear algebraic equations. A NM is proposed by using Quasilinearisation and collocation methods for solving the linear and non-linear PDEs. By dealing with different numerical experiments, a comparison is made between numerical results derived from the discussed HS3WM and other existing numerical methods to test their compatibility.

3.6 Conclusion

From the outcomes we obtained from the results of NM performed on three numerical problems with the discussed technique, we conclude that:

- 2D PDE of order two and three containing non-linearity can easily be solved with high accuracy and less computational cost by the discussed scheme.
- To solve distinct types of PDEs the MATLAB subprograms are used to make it more computer-friendly.
- The proposed scheme for a limited collocation points becomes a strong solver for PDEs of these forms, and good accuracy is obtained.
- In comparison to the classical HS2WM, numerical findings indicate that Quasilinearization using HS3WM converges rapidly, even for small numbers of grid points.

Figure 3.1 to 3.5 demonstrates excellent agreement between the solution from our scheme and the analytical solution. Further refinement can be achieved by increasing the number of collocation points. Therefore, by observing the techniques performance, we observed that the discussed method can be extended to solve DEs of distinct kinds, such as ODEs, PDEs, FDEs, IDEs, and IEs. By using MATLAB, all the calculations have been done.

Chapter 4

An effective computational scheme for solving various mathematical fractional differential models via non-dyadic Haar wavelets.

4.1 Introduction:

In recent years, the usage of FOD has exploded in engineering and biological sciences, as well as other fields of study. Modeling and controlling of numerous dynamic systems is one of the biggest advantages of using FDEs. Fractional derivatives and integrals are more useful and cost-effective than conventional derivatives in the formulation of specific electrochemical applications [151]. This discovery stimulated their curiosity not only in the applications of the concepts of integrals and derivatives of arbitrary order but also, in the fundamental mathematical features of these interesting operators [152]. Many physical phenomena, such as the behavior of biological and mechatronic systems, rheology, complicated viscoelasticity, anomalous diffusion, and so on, cannot be well defined and justified based on partial calculus, due to which it attracted the researchers [153]–[155]. In the distinct fields such as science and engineering, FDEs have many practical applications. Numerous substantial and technical structures, such as dielectric polarisation methods, viscoelastic systems, and electrode-electrolyte polarisation are modelled using fractional derivatives [156], [157]. As, a result of the expanding applications, many numerical approaches for the solution of these equations have been developed including the wavelet method [158], generalized DTM, VIM, and FDM[159], and so on. Nonlinear phenomena may be seen in several scientific fields, including fluid dynamics, plasma physics, solid-state physics, and chemical kinetics, in engineering, and other fields. The mathematical technique of wavelet analysis is well-known and extensively applied. Wavelets are a set of expressions that have been combined to generate basic functions in summation form, and to generate these basic functions, a mother wavelet is translated and compressed. Therefore, it produces locality and smoothness properties. The use of wavelets has aroused researcher's interest in solving conventional ODEs and PDEs numerically, For solutions to these equations numerous traditional wavelet techniques have recently expanded by the researchers. Numerical solutions and numerical integration of fractional ODEs and PDEs are two further wavelet applications in practical mathematics. For the time being, wavelets such as B-spline, Legendre wavelet, the HW, Daubechies and Boubaker wavelets are used [160]. Many studies have employed the HSW, a

wavelet that is orthonormal with compact support [161][7]. A FDE is converted into an algebraic structure with finite variables using HWs [162]. In 2018, Mittal and Pandit used HS3W to solve a variety of DE, and expressed that many various types of mathematical models controlled by DEs, such as dispersive equations [108] and, second-order linear integro-differential equations [163], can be equally capable of being solved by using these wavelet bases [164]. They also depicted that, in terms of convergence the HS3WM is more rapidly convergent than the HS2WM. Furthermore, the attributes of the solution to the nonlinear FDE are yet to be investigated using HS3WM. This inspires us to introduce a new technique for analysing the behavior of FE-governed systems by employing the HS3WM. The following types of DEs are used to assess the applicability of modified HS3W [107].

$$Du^\alpha(z) = G(z, u(z), u'(z), u''(z)) \quad (4.1)$$

With the set of ICs and BCs,

(a) ICs:

$$u(0) = \mu_1 \text{ and } u'(0) = \mu_2 \quad (4.2)$$

(b) Dirichlet BCs:

$$u(0) = \mu_3 \text{ and } u(1) = \mu_4 \quad (4.3)$$

4.2 Basic definition of fractional calculus:

In the given section, we discussed the basic definitions of Fractional Differentiation and Integration.

- Reimann Liouville Fractional differential operator of order α : For the positive real numbers, α, t across the interval $[m, n]$, the FDO established by the Riemann-Liouville is given by [1]:

$$d^\alpha f(t) = \frac{1}{\Gamma(p - \alpha)} \left[\frac{d}{dt} \right]^p \int_m^n f(x) (t - x)^{p - \alpha - 1} dx$$

where α denotes the order of derivative and $t \in [m, n]$.

- Caputo fractional differential operator of order α : For positive real numbers, α, t , the FDO developed by the Caputo, an Italian mathematician is [162]:

$$d^\alpha f(t) = \frac{1}{\Gamma(p - \alpha)} \int_m^n \left[\frac{d}{dt} \right]^p f(x) (t - x)^{p - \alpha} dx$$

where α denotes the order of derivative and $t \in [m, n]$.

4.3 Quasilinearisation technique:

Basically, QT is generalised form of Newton-Raphson technique. It converges to solution in its exact form. Quadratically, it must show a monotone convergence [44]. Here consider a non-linear second order DE:

$$\psi''(v) = k(v, \psi(v)) \quad (4.4)$$

With BC:

$$\psi(a_1) = \theta_1, \psi(b_1) = \theta_2; a_1 \leq v \leq b_1 \quad (4.5)$$

Here k is in terms of $\psi(v)$. Let us choose approximation at initial step of solution $\psi(v)$. Let us say $\psi_0(v)$. k can be expanded around $\psi_0(v)$ is written in the form:

$$k(\psi(v), v) = k(\psi_0(v), v) + (\psi(v) - \psi_0(v)) k_{\psi_0(v)}(\psi_0(v), v) \quad (4.6)$$

$$\psi''(v) = k(\psi_0(v), v) + (\psi(v) - \psi_0(v)) k_{\psi_0(v)}(\psi_0(v), v) \quad (4.7)$$

After that

$$\psi''(v) = k(\psi_1(v), v) + (\psi(v) - \psi_1(v)) k_{\psi_1(v)}(\psi_1(v), v) \quad (4.8)$$

The form of a recurrence relationship is:

$$\psi_{s+1}''(v) = k(\psi_s(v), v) + (\psi(v) - \psi_s(v)) k_{\psi_s(v)}(\psi_s(v), v) \quad (4.9)$$

for obtaining $\psi_{s+1}(v)$ here use $\psi_s(v)$, whose value is already known. a non-linear DE with required conditions is given as,

$$\psi_{s+1}(v) = \alpha, \psi_s(v) = \beta. \quad (4.10)$$

Now consider the non-linear second order DE of the form;

$$\psi''(v) = k(\psi'(v), \psi(v), v) \quad (4.11)$$

$$\begin{aligned} \psi_{s+1}''(v) = & k(\psi'(v), \psi(v), v) + (\psi'_{s+1}(v) \\ & - \psi'_s(v)) k_{\psi'_s(v)}(\psi'_s(v), \psi_s(v), v) + (\psi_{s+1}(v) \\ & - \psi_s(v)) k(\psi'_s(v), \psi_s(v), v) \end{aligned} \quad (4.12)$$

With BCs

$$\psi_{s+1}(v) = \alpha, \psi_s(v) = \beta. \quad (4.13)$$

Follow the same technique to establish the recurrence relation for higher order non-linear DEs.

$$L^j \psi_{s+1}(v) = k(\psi_s(v), \psi'_s(v), \dots, \psi_s^{j-1}(v), v) + \sum_{p=0}^{n-1} (\psi_{s+1}^p(v) - \psi_s^p(v)) k_{\psi^p}(\psi'_s(v), \psi_s(v), \dots, \psi_s^{j-1}(v), v) \quad (4.14)$$

The order of the DE is j , the above equation is linear, and it can be solved recursively $\psi_s(v)$ if $\psi_s(v)$ is having a known value and can use it to get value of $\psi_{s+1}(v)$.

4.4 Applications of Fractional differential equation

In this part, the HS3WM is used to solve certain numerical problems for solving linear as well as non-linear FDEs and to showcase the method's compatibility, compare the outcomes with those obtained using existing methods in the literature.

4.4.1 Numerical Experiment: Fractional Riccati Equation.

Riccati equation is a non-linear ODEs which has applications in various fields such as diffusion problems, optimal control, and random processes.

$$D^\alpha y(x) = -y^2(x) + 1, \text{ for } x \geq 0, 0 \leq \alpha \leq 1 \quad (4.15)$$

Subject to IC,

$$y(0) = 0. \quad (4.16)$$

ES at $\alpha = 1$,

$$y(x) = \frac{e^{2x} - 1}{e^{2x} + 1} \quad (4.17)$$

Solution: Applying QT on non-linear term of equation

$$D^\alpha y_{s+1}(x) + 2 y_s(x) y_{s+1}(x) = y_s^2 + 1, x \geq 0 \quad (4.18)$$

With ICs $y_{s+1}(0) = 0$; we apply HS3WM to (4.15), we approximate the term containing highest derivatives by HWS as:

$$D^\alpha y_{s+1}(x) = \sum_{i=1}^{3M} c_i h_i(x) \quad (4.19)$$

On integrating the above equation (4.19) we obtained the lower derivatives and by using the IC we have,

$$y_{s+1}(x) = \sum_{l=1}^{3M} c_l P_{\alpha,l}(x) \quad (4.20)$$

Now substituting equations (4.19) and (4.20) in equation (4.18) we get

$$\sum_{l=1}^{3M} c_l [h_l(x) + 2 y_s(x) P_{\alpha,l}(x)] = y_s^2(x) + 1 \quad (4.21)$$

For $\alpha = 1$, we assign the differential order to equation (4.15) and at J=2 resolution level. Table 4.1 and 4.2 shows the comparative study of the ES and AS as well as value of errors respectively derived using the HS3W technique and graphical results are shown in Figure 4.1. The absolute inaccuracy decreases as the number of iterations increases. Using the QT at a given LOR, the precise answer at $\alpha = 1$ and the HW resolution at various α 's which varies from 0.2 to 0.8 and it is described by the graph when the values of parameter approach to 1 the AS approaches to ES which shows competency of the method that are demonstrated in Figure 4.2.

Table 4.1 Comparison of ES and AS at different values of x . Discussion of Absolute Error by HS3WM with HSW.

For different value of x	ES	AS	Absolute Error by HS3WM	Absolute Error by HSW [160].
0.1	0.018516401922	0.0185121722129	4.229709e-06	6.11e-05
0.2	0.055498470109	0.0554858503623	1.261974e-05	1.16e-04
0.3	0.0923288861517	0.0923080825640	2.080356e-05	1.12e-04
0.4	0.1289083852227	0.1288797350278	2.865019e-05	8.34e-04
0.5	0.1651404129246	0.1651043750530	3.603787e-05	6.69e-03
0.6	0.2009321223245	0.2008892648997	4.285742e-05	6.64e-03
0.7	0.2361952879391	0.2361462731435	4.901479e-05	6.24e-04
0.8	0.2708471185167	0.2707926854500	5.443306e-05	5.86e-03
0.9	0.3048109541868	0.3047519003975	5.905378e-05	1.48e-04
1.0	0.3380168376494	0.3379540000363	6.283761e-05	5.89e-04

Table 4.2 Comparison of value of Error of HS3WM at different levels of resolution.

LOR	J=3	J=4	J=5
HSWM3 L_2 error	1.1896e-05	1.3217e-06	1.5412e-07
HSWM3 L_∞ error	7.7184e-06	8.5760e-07	9.7023e-08

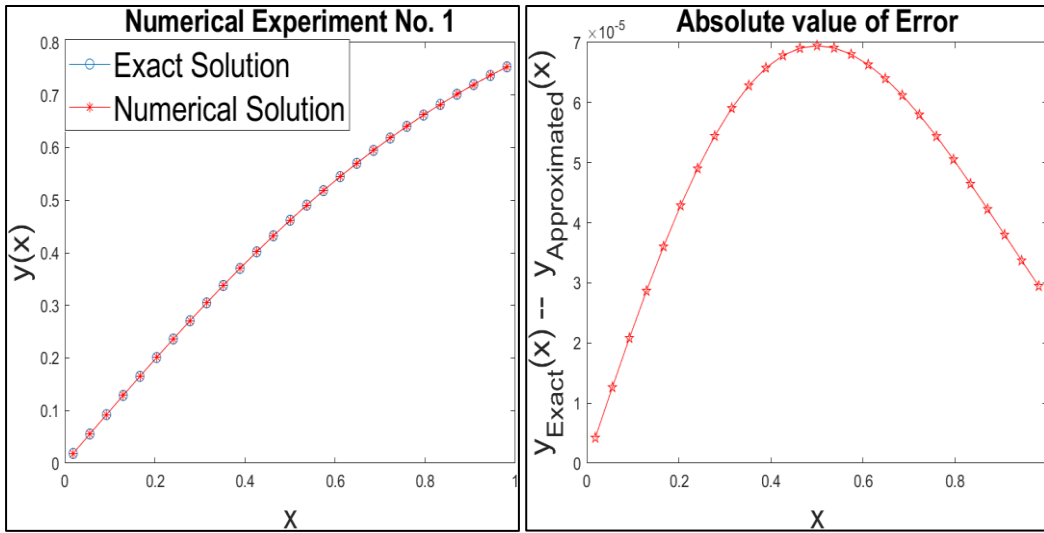


Figure 4.1 Graphical representation of ES and AS at $\alpha = 1$.

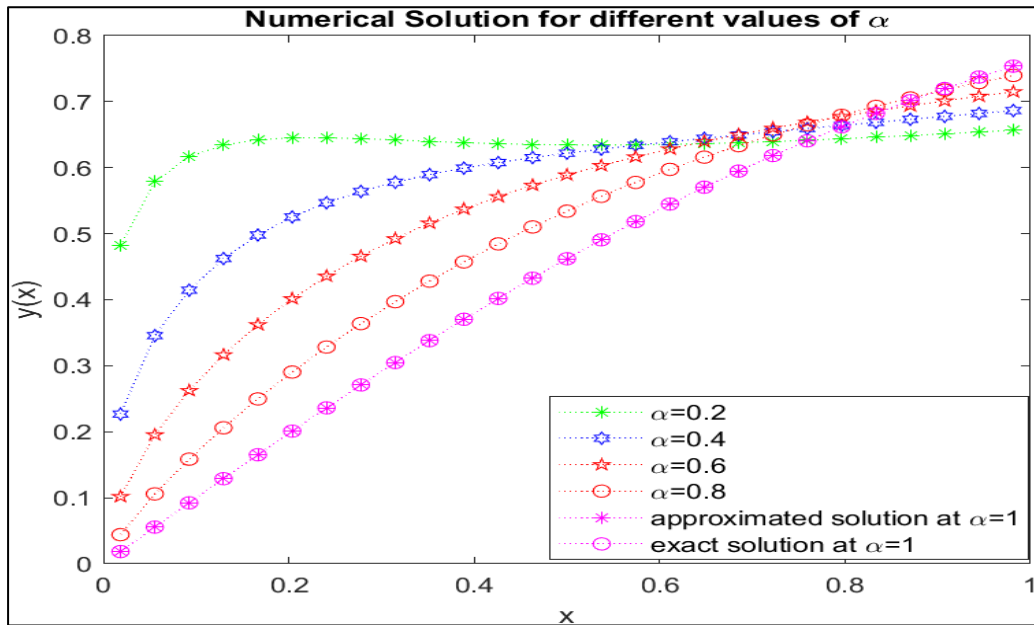


Figure 4.2: Graphical representation exact and approximate value for different values of α lies between 0 and 1. At J=2 resolution level.

4.4.2 Numerical Experiment: Fractional Vander-Pol Oscillator Problem

$$D^\alpha y(x) + \frac{dy(x)}{dx} + y(x) + y^2(x) \frac{dy(x)}{dx} = 2 \cos(x) - \cos^3(x), \quad (4.22)$$

$$1 \leq \alpha \leq 2$$

Subject to IC,

$$y(0) = 0, y'(0) = 1 \quad (4.23)$$

At $\alpha = 2$, the precise answer exists in literature is given by:

$$y(x) = \sin(x) \quad (4.24)$$

Solution:

After applying QT to equation (19) we get,

$$D^\alpha y_{s+1}(x) + (1 + 2y_s(x)y_s'(x))y_{s+1}(x) + (1 + y_s^2(x))y_{s+1}'(x) = \quad (4.25)$$

$$2y_s'(x)y_s^2(x) + 2\cos(x) - \cos^3(x), 1 \leq \alpha \leq 2$$

With ICs, $y_{s+1}(0) = 0, y_s'(0) = 1$; we apply HS3WM to (4.22), we approximate the term which has highest derivatives by HWS as:

$$D^\alpha y_{s+1}(x) = \sum_{l=1}^{3M} c_l h_l(x) \quad (4.26)$$

On integrating the above equation (4.26) we obtained the lower derivatives and by using the ICs we have,

$$y_{s+1}(x) = \sum_{l=1}^{3M} c_l P_{\alpha,l}(x) \quad (4.27)$$

Now substituting equations (4.26) and (4.27) in equation (4.22) we get

$$\sum_{l=1}^{3M} c_l [h_l(x) + (1 + 2y_s(x)y_s'(x))P_{\alpha,l}(x) + (1 + y_s^2(x))P_{\alpha-1,l}(x)] = 2y_s^2(x)y_s'(x) - (1 + 2y_s'(x)y_s(x))x - \quad (4.28)$$

$$1 - y_s^2(x) + 2\cos(x) - \cos^3(x)$$

With initial approximations

$$y_0(x) = 0, y_0'(x) = 1 \quad (4.29)$$

We assign the differential order to Eq. (4.22) for $\alpha = 2$, and the LOR to $J=2$. Table 4.3 and 4.4 shows the comparative study of the ES and AS as well as value of errors respectively derived using the HS3W technique and graphical results are shown in Figure 4.3. With more iterations,

the absolute error reduces. The precise solution at $\alpha = 1$ and the HWS at distinct α 's are represented in Figure 4.4 via QT at a fixed LOR. The HW resolution at various α 's which varies from 1.2 to 1.8 and it is described by the graph when the values of parameter approach to 2 the AS approaches to ES which shows competency of the method.

Table 4.3 Comparison of ES and AS at different values of x . Discussion of Absolute Error by HS3WM with HSW.

For different value of x	ES	AS	Value by HS2WM [63].	Absolute Error by HS3WM
0.1	0.0998334166	0.0998334056	0.0998333872	2.89934e-06
0.2	0.1986693308	0.1986693108	0.1986692768	8.67113e-06
0.3	0.2955202067	0.2955202012	0.2955201331	1.44070e-05
0.4	0.3894183423	0.3894182990	0.3894182543	2.01071e-05
0.5	0.4794255386	0.4794255100	0.4794254413	2.57714e-05
0.6	0.5646424734	0.5646423900	0.5646423719	3.13998e-05
0.7	0.6442176872	0.6442176329	0.6442175863	3.69924e-05
0.8	0.7173560909	0.7173560600	0.7173559950	4.25492e-05
0.9	0.7833269096	0.7833268874	0.7833268225	4.80701e-05
1.0	0.8414709848	0.8414709675	0.8414709106	5.35553e-05

Table 4.4 Comparison of value of Error of HS3WM at different LOR.

LOR	J=2	J=3	J=4
HSWM3 L_2 error	6.33395260e-05	7.03695009e-06	7.81873793e-07
HSWM3 L_∞ error	4.12718973e-05	4.58592395e-06	5.09566047e-07

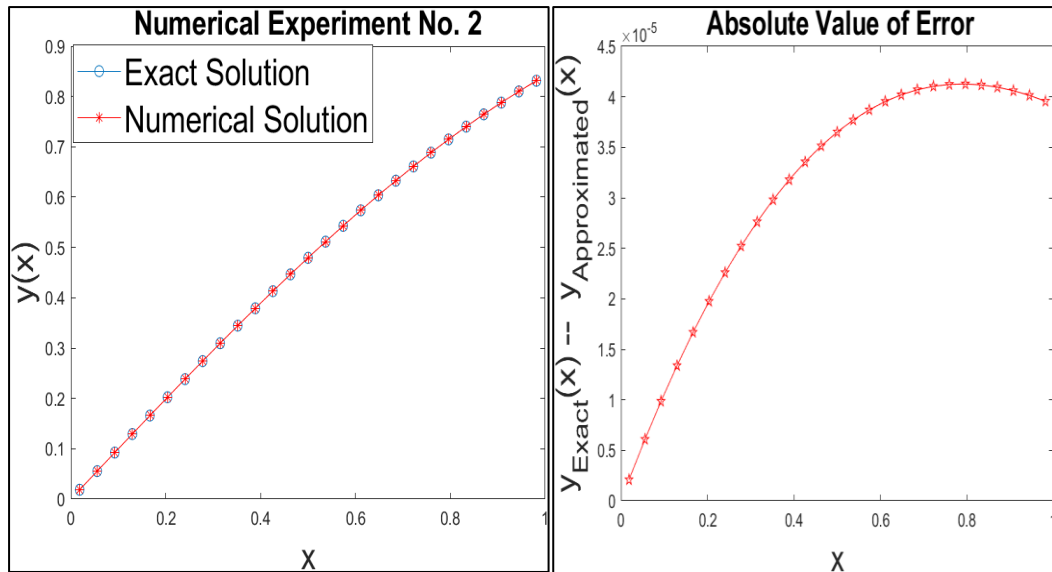


Figure 4.3 Graphical representation of ES and AS

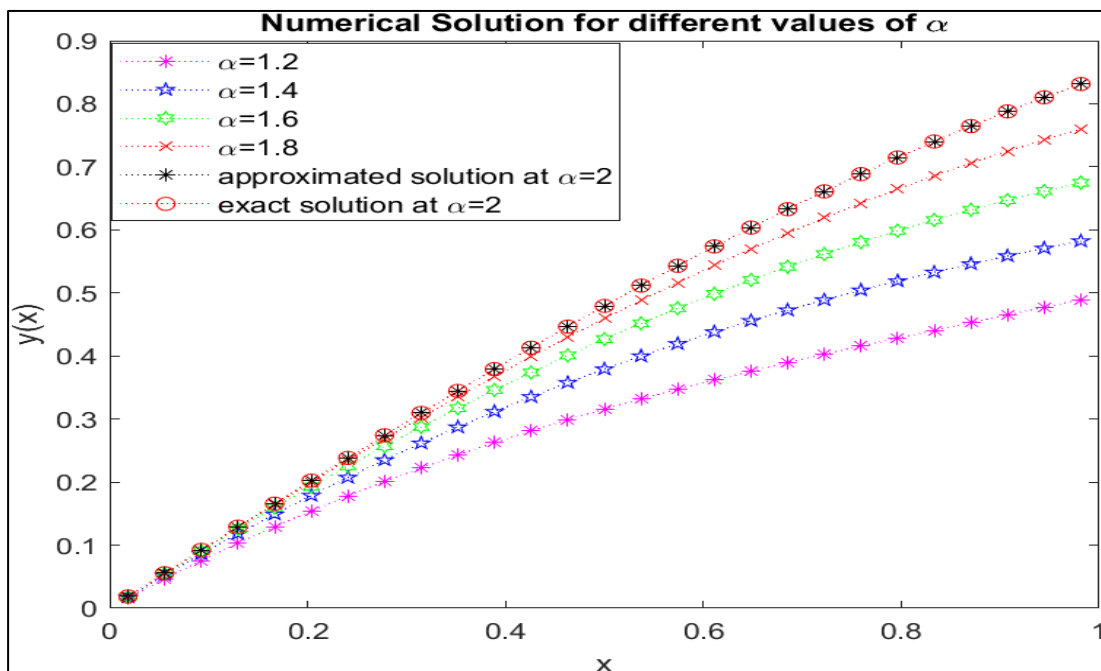


Figure 4.4 Graphical representation of ES and AS at LOR J=2.

4.4.3 Numerical Experiment: Non-linear Oscillator Ordinary Differential Equation

$$D^\alpha y(x) + (y')^2(x) - y(x) + y^2(x) - 1 = 0, \quad 1 < \alpha \leq 2 \quad (4.30)$$

With IC,

$$y(0) = 2, y'(0) = 0 \quad (4.31)$$

The value of ES at $\alpha = 2$ given as,

$$y(x) = 1 + \cos(x) \quad (4.32)$$

Solution: On Applying QT to equation (4.30) and the equation becomes

$$D^\alpha y_{s+1}(x) + 2y'_s(x)y'_{s+1}(x) - (1 - 2y_s(x))y_{s+1}(x) = y_s^2(x) + (y'_s)^2(x) + 1 \quad (4.33)$$

With ICs,

$$y_{s+1}(0) = 2, y'_s(0) = 0 \quad (4.34)$$

we apply HS3WM to (4.30), we approximate the term which contains highest derivatives by HWS as:

$$D^\alpha y_{s+1}(x) = \sum_{l=1}^{3M} c_l h_l(x) \quad (4.35)$$

On integrating the above equation (4.35) we obtained the lower derivatives and by using the IC we have,

$$y_{s+1}(x) = \sum_{l=1}^{3M} c_l P_{\alpha,l}(x) + y_{s+1}(0) \quad (4.36)$$

$$y_{s+1}(x) = \sum_{l=1}^{3M} c_l P_{\alpha,l}(x) + 2 \quad (4.37)$$

$$y'_{s+1}(x) = \sum_{l=1}^{3M} c_l P_{\alpha-1,l}(x) \quad (4.38)$$

Now substituting equations (4.36), (4.37) and (4.38) in equation (4.33) we get

$$\begin{aligned} \sum_{l=1}^{3M} c_l [h_l(x) + 2y'_s(x) P_{\alpha-1,l}(x) - (1 - 2y'_s(x)) P_{\alpha,l}(x)] \\ = y_s^2(x) + y_s'^2(x) + 2(1 - 2y_s(x)) + 1 \end{aligned} \quad (4.39)$$

With ICs

$$y_0(x) = 2, y'_0(x) = 0 \quad (4.40)$$

For $\alpha = 2$, we assign the differential order to Eq. (4.33) and at J=2 LOR. Table 4.5 and 4.6 shows the comparative study of the ES and AS as well as value of errors respectively derived using the HS3WM and graphical results are shown in Figure 4.5. The absolute inaccuracy decreases as the number of iterations increases. At a constant LOR, the ES at $\alpha = 1$ and the HWS at various α 's are shown in figure 4.6. The HW resolution is investigated for various parameter values ranging from 1.2 to 1.8. The results are depicted graphically. As the parameter values approach 2, AS converges towards the ES. This convergence demonstrates the effectiveness of the proposed method.

Table 4.5 Comparison of ES and AS at different values of x . Discussion of Absolute Error by HS3WM with HSW.

At $\alpha=2$, for different value of x	ES	AS	Value by HS2WM[63].	Absolute Error by HS3WM
0.1	1.995004165	1.995004166	1.995004166	3.734e-06
0.2	1.980066578	1.980066579	1.980066581	1.568e-05
0.3	1.955336489	1.955336492	1.955336496	3.958e-05
0.4	1.921060994	1.921060999	1.921061007	7.543e-05
0.5	1.877582562	1.877582576	1.877582583	1.232e-04
0.6	1.825335615	1.825335628	1.825335647	1.830e-04
0.7	1.764842187	1.764842204	1.764842233	2.547e-04
0.8	1.696706709	1.696706740	1.696706772	3.384e-04
0.9	1.621609968	1.621609998	1.621601051	4.341e-04
1.0	1.540302306	1.540302356	1.540302414	5.417e-04

Table 4.6 Comparison of value of Error HS3WM at different LOR

LOR	J=2	J=3	J=4
HSWM3 L_2 error	8.69048147e-06	9.66118381e-07	1.07352784e-07
HSWM3 L_∞ error	3.71196461e-05	4.25861607e-06	4.78242174e-07

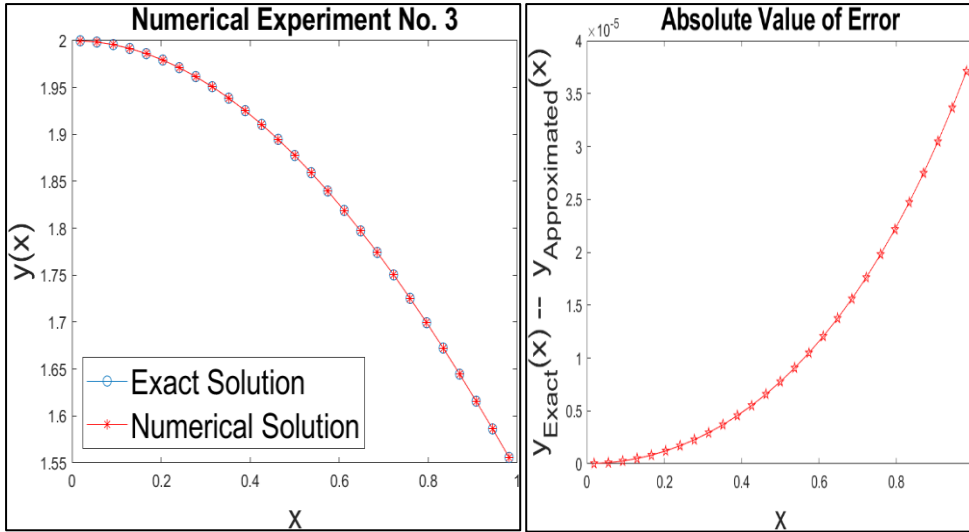


Figure 4.5 Graphical representation of ES and AS

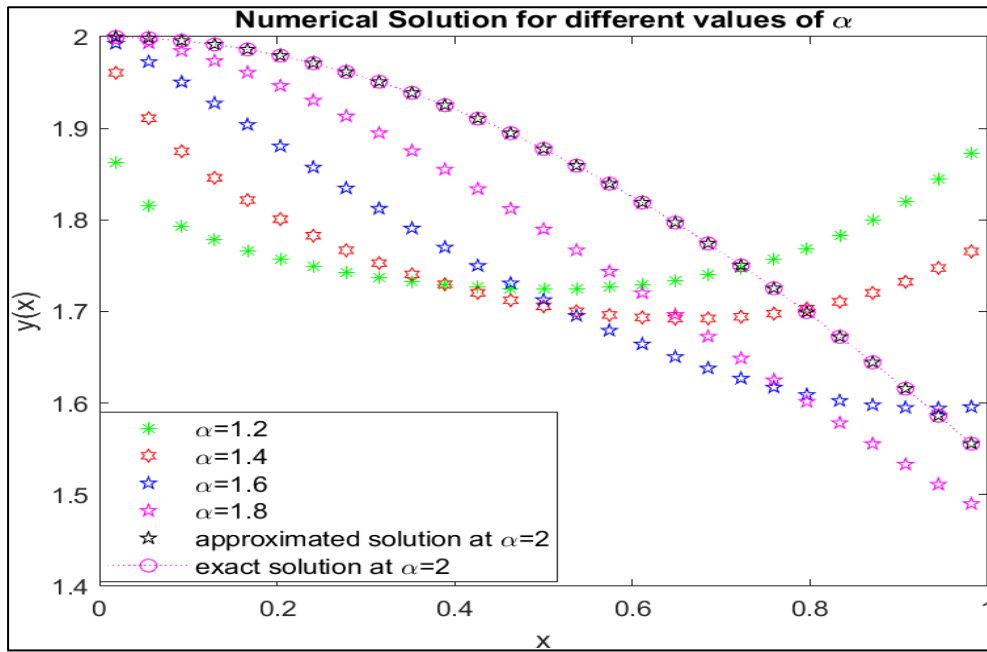


Figure 4.6 Graphical representation ES and AS for different values of α lies between 0 and 1. At J=2 resolution level.

4.4.4 Numerical Experiment: Composite Fractional Oscillation Equation.

$$D^\alpha y(x) + y(x) = f(x), 0 < \alpha < 1 \tag{4.41}$$

With IC,

$$y(0) = 0, \text{ where } f(x) = x^2 + \frac{2x^{2-\alpha}}{\Gamma(3-\alpha)} \quad (4.42)$$

For $\alpha = 1$, the ES of the equation is

$$y(x)=x^2 \quad (4.43)$$

Solution:

We apply HS3WM to (4.41), we estimated the advanced derivatives term by HWS as:

$$D^\alpha y(x) = \sum_{l=1}^{3M} c_l h_l(x) \quad (4.44)$$

On integrating the above equation (4.44) we obtained the lower derivatives and by using the IC we have,

$$y(x) = \sum_{l=1}^{3M} c_l P_{\alpha,l}(x) \quad (4.45)$$

now using equation (4.44) and (4.45) in equation (4.41).

$$\sum_{l=1}^{3M} c_l [h_l(x) + P_{\alpha,l}(x)] = x^2 + \frac{2x^{2-\alpha}}{\Gamma(3-\alpha)} \quad (4.46)$$

We assign the differential order to Eq. (4.41) for $\alpha = 1$, and the LOR to J2. Figure 4.7 depicts the ES and AS obtained using the HS3W approach. With more iterations, the absolute error reduces. The precise solution at $\alpha = 1$ and the HWS at distinct α 's are represented in figure 4.8 via QT at a fixed resolution level. The HW resolution is investigated for various parameter values ranging from 0.2 to 0.8. The results are depicted graphically. As the parameter values approach 1, AS converges towards the ES. This convergence demonstrates the effectiveness of the proposed method.

Table 4.7 Comparison of ES and AS at different values of x . Discussion of Absolute Error by HS3WM with HSW at different values of α .

For different value of x	ES	AS	Absolute Error by HS3WM. ($\alpha = 0.25$)	Absolute Error by HS2WM ($\alpha = 0.25$) [57]	Absolute Error by HS3WM ($\alpha = 0.50$)	Absolute Error by HS2WM ($\alpha = 0.50$) [57]
0.1	0.01	0.01016911	4.225e-06	9.000e-03	4.1904e-06	4.000e-03

0.2	0.04	0.04149865	4.105e-06	8.000e-03	4.3903e-06	5.000e-03
0.3	0.09	0.09149070	4.004e-06	4.000e-03	4.0882e-06	1.000e-03
0.4	0.16	0.16099201	3.939e-06	2.800e-03	3.9885e-06	8.000e-03
0.5	0.25	0.25000256	3.875e-06	6.300e-03	3.9234e-06	2.300e-03
0.6	0.36	0.36346740	3.843e-06	3.200e-03	3.8435e-06	6.000e-03
0.7	0.49	0.49230933	3.812e-06	2.000e-03	1.6807e-06	7.000e-03
0.8	0.64	0.64066050	4.088e-06	9.000e-03	1.5997e-06	0.000
0.9	0.81	0.81593848	3.796e-06	5.200e-03	1.7160e-06	1.400e-03
1.0	1	0.99589056	3.369e-06	4.400e-03	1.6397e-06	2.300e-03

Table 4.8 Comparison of value of Error of HS2WM and HS3WM at different LOR

LOR	J=2	J=3	J=4
HSWM3 L_2 error	5.0450146e-04	5.602634e-05	6.2247865e-06
HSWM3 L_∞ error	3.3670033e-04	3.787018e-05	4.2250783e-06

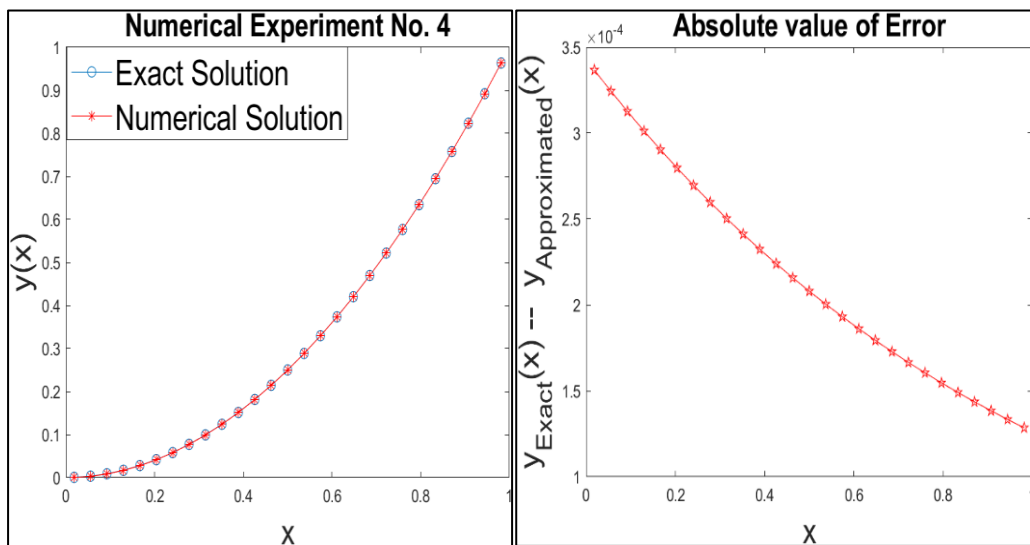


Figure 4.7 Graphical representation of ES and AS.

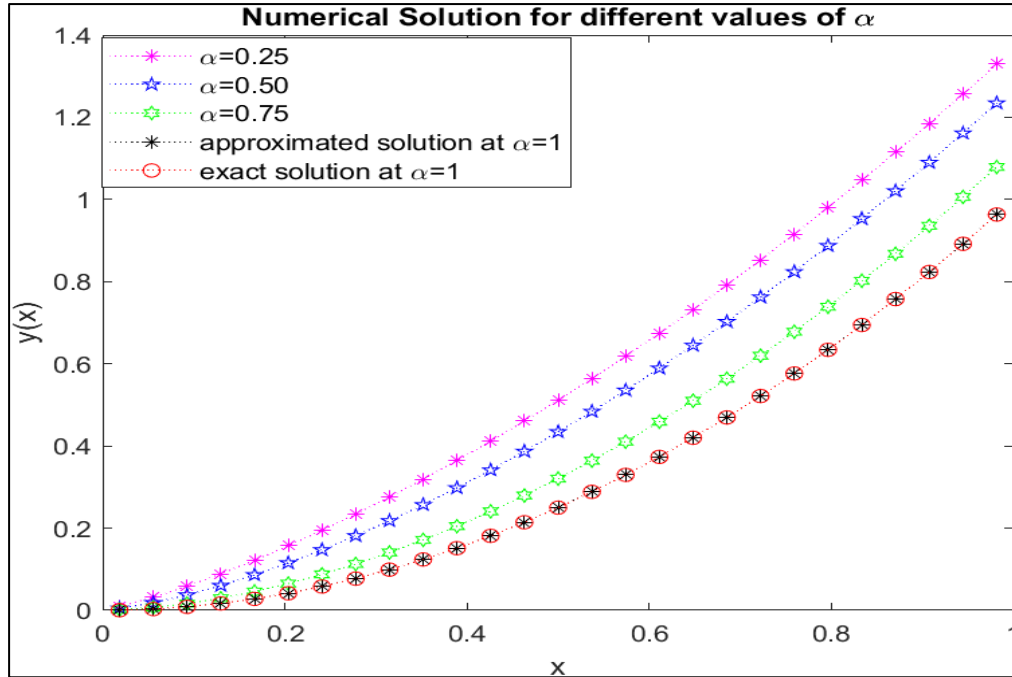


Figure 4.8 Graphical representation ES and AS for different values of α lies between 0 and 1. At J=2 resolution level.

4.4.5 Numerical Experiment: Fractional Relaxation-Oscillation Equation.

$$D^\alpha y(x) + y(x) = f(x), 0 < \alpha < 1 \quad (4.47)$$

With IC,

$$y(0) = 0 \quad (4.48)$$

here,

$$f(x) = 1 - 4x + 5x^2 - \frac{4}{\Gamma(2-\alpha)} x^{1-2\alpha} + \frac{10}{\Gamma(3-\alpha)} x^{2-\alpha} \quad (4.49)$$

for $\alpha = 1$, the ES of the given equation is

$$y(x) = 1 - 4x + 5x^2 \quad (4.50)$$

Solution:

we apply HS3WM to (4.47), we approximate the term which has derivatives by HW series as:

$$D^\alpha y(x) = \sum_{l=1}^{3M} c_l h_l(x) \quad (4.51)$$

On integrating the above equation (4.51) we obtained the lower derivatives and by using the IC we have,

$$y(x) = \sum_{l=1}^{3M} c_l P_{\alpha,l}(x) \quad (4.52)$$

now using equation (4.51) and (4.52) in equation (4.47).

$$\begin{aligned} \sum_{l=1}^{3M} c_l [h_l(x) + P_{\alpha,l}(x)] & \quad (4.53) \\ & = 1 - 4x + 5x^2 - \frac{4}{\Gamma(2-\alpha)} x^{1-2\alpha} \\ & \quad + \frac{10}{\Gamma(3-\alpha)} x^{2-\alpha} \end{aligned}$$

We assign the differential order to Equation (4.47) for $\alpha = 1$, and the LOR to $J=2$. Figure 4.9 depicts the ES and AS obtained using the HS3W approach. With more iterations, the absolute error reduces. The precise solution at $\alpha = 1$ and the HW solution at distinct α 's are represented in Figure 4.10 at a fixed LOR. The HW resolution is investigated for various parameter values ranging like 0.25 and 0.50. The results are depicted graphically. As the parameter values approach 0.75, the AS converges towards the ES. This convergence demonstrates the effectiveness of the proposed method.

Table 4.9 Comparison of ES and AS at different values of x . Discussion of Absolute Error by HS3WM with HSW at different values of α .

For different value of x	ES	AS	Absolute Error by HS3WM ($\alpha = 0.25$)	Absolute Error by HS2WM ($\alpha = 0.25$) [57]	Absolute Error by HS3WM ($\alpha = 0.50$)	Absolute Error by HS2WM ($\alpha = 0.50$) [57]
0.1	0.6500	0.6475563	2.1038e-05	8.000e-03	2.0525e-05	2.300e-03
0.2	0.4000	0.4058143	2.0441e-05	1.700e-03	1.4646e-05	3.000e-03
0.3	0.2500	0.2500128	1.9942e-05	2.000e-03	1.3941e-05	1.000e-03
0.4	0.2000	0.2006316	1.9536e-05	3.100e-03	1.3601e-05	2.200e-03
0.5	0.2500	0.2542126	1.5579e-05	1.210e-03	1.1873e-05	6.800e-03

0.6	0.4000	0.4142480	1.5199e-05	8.400e-03	1.0238e-05	2.200e-03
0.7	0.6500	0.6599499	9.1999e-04	6.000e-03	1.0017e-05	2.600e-03
0.8	1.0000	1.0016564	8.9387e-04	2.700e-03	9.5078e-05	0.0000
0.9	1.4500	1.4665236	7.8681e-04	1.720e-03	1.9536e-05	5.300e-03
1.0	2.0000	1.9976832	2.8766e-05	3.300e-03	1.2543e-05	4.320e-03

Table 4.10 Comparison of value of Error of HSW2M and HSW3M at different LOR

LOR	J=2	J=3	J=4
HSWM3 L_2 error	1.382717e-03	1.53448107e-04	1.704744e-05
HSWM3 L_∞ error	1.683501e-03	1.89350905e-04	2.112539e-05

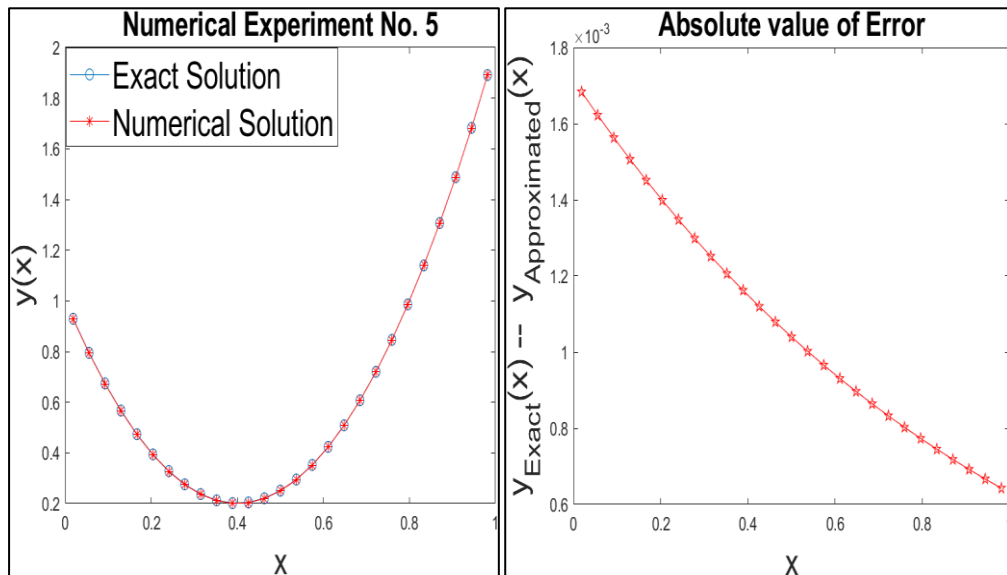


Figure 4.9 Graphical representation of ES and AS

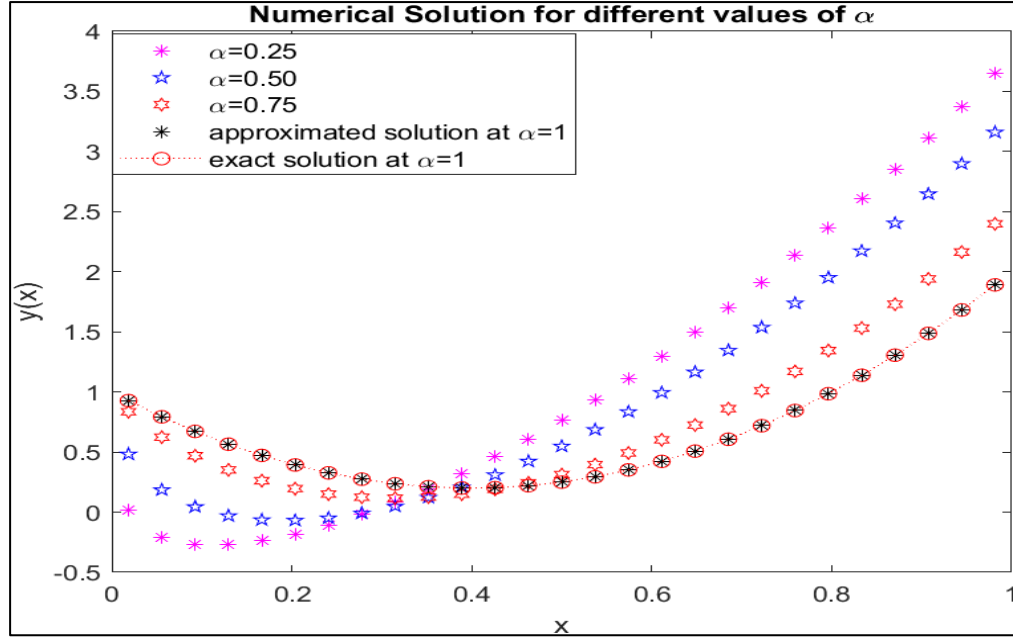


Figure 4.10 Graphical representation ES and AS for different values of α lies between 0 and 1. At Resolution-level J=2

4.4.6 Numerical Experiment: Fractional Kawahara Equation

The KE, which plays a crucial role in describing the behavior of non-linear water waves in the region having long wavelength, since it has weaker dispersion but large non-linearity which makes this equation interesting. The Kawahara have been the focus of in-depth study for many years. In order to depict solitary-wave propagation in media, Kawahara first proposed the KE in 1972. Both the theory of shallow water waves with surface tension and plasma magneto-acoustic waves. The modified KE is also widely applicable to capillary-gravity water waves, plasma waves, and other phenomena.

$$D_t^\mu \varphi(z, t) + \varphi \varphi_z + \varphi_{zzz} - \varphi_{zzzzz} = F(z, t) \quad (4.54)$$

$$\varphi(z, 0) = 0 \quad (4.55)$$

With forcing term,

$$F(z, t) = \frac{2t^{2-\mu}}{\Gamma(3-\mu)} \sin z + \frac{1}{2} t^4 \sin 2z - 2t^2 \cos z \quad (4.56)$$

Exact solution:

$$\varphi(z, t) = t^2 \sin z \quad (4.57)$$

the solution computed by the proposed method for $z, t \in [0, 2\pi] \times [0, 1]$.

$$\varphi_t(z, t) + \varphi\varphi_z + \varphi_{zzz} - \varphi_{zzzzz} = F(z, t) \quad (4.58)$$

$$F(z, t) = 2t\sin z + \frac{1}{2}t^4\sin 2z - 2t^2\cos z \quad (4.59)$$

For $\mu = 1$,

$$\begin{aligned} \varphi_t(z, t) + \varphi\varphi_z + \varphi_{zzz} - \varphi_{zzzzz} \\ = 2t\sin z + \frac{1}{2}t^4\sin 2z - 2t^2\cos z \end{aligned} \quad (4.60)$$

By using QT for non-linear term,

$$\varphi_t(z, t) + \varphi\varphi_z + \varphi_{zzz} - \varphi_{zzzzz} = 2t\sin z + \frac{1}{2}t^4\sin 2z - 2t^2\cos z \quad (4.61)$$

$$\begin{aligned} \varphi_t(z, t) + \varphi_{r+1}\varphi_z - \varphi_r\varphi_z + (\varphi_z)_{r+1}\varphi + \varphi_{zzz} - \varphi_{zzzzz} \\ = 2t\sin z + \frac{1}{2}t^4\sin 2z - 2t^2\cos z \end{aligned} \quad (4.62)$$

Approximate the HOD:

$$\varphi_{tzzzzz}(z, t) = \sum_{i=1}^{3p} \sum_{l=1}^{3p} a_{iz} H_i(z) H_l(t) \quad (4.63)$$

Integrating the equation with respect to t between 0 to t,

$$\varphi_{zzzzz}(z, t) - \varphi_{zzzzz}(z, 0) = \sum_{i=1}^{3p} \sum_{l=1}^{3p} a_{iz} H_i(z) P_{1,l}(t) \quad (4.64)$$

$$\varphi_{zzzzz}(z, t) = \sum_{i=1}^{3p} \sum_{l=1}^{3p} a_{iz} H_i(z) P_{1,l}(t) + \varphi_{zzzzz}(z, 0) \quad (4.65)$$

Integrating w.r.t z between 0 to z,

$$\begin{aligned} \varphi_{zzzz}(z, t) - \varphi_{zzzz}(0, t) \\ = \sum_{i=1}^{3p} \sum_{l=1}^{3p} a_{iz} P_{1,i}(z) P_{1,l}(t) + [\varphi_{zzzz}(z, 0) - \varphi_{zzzz}(0, 0)] \end{aligned} \quad (4.66)$$

$$\begin{aligned} \varphi_{zzzz}(z, t) - \varphi_{zzzz}(0, t) \\ = \sum_{i=1}^{3p} \sum_{l=1}^{3p} a_{iz} P_{1,i}(z) P_{1,l}(t) + [\varphi_{zzzz}(z, 0) - \varphi_{zzzz}(0, 0)] \end{aligned} \quad (4.67)$$

Again, integrating w.r.t z,

$$\varphi_{zzz}(z, t) - \varphi_{zzz}(0, t) \quad (4.68)$$

$$\begin{aligned} &= \sum_{i=1}^{3p} \sum_{l=1}^{3p} a_{iz} P_{2,i}(z) P_{1,l}(t) + [\varphi_{zzz}(z, 0) - \varphi_{zzz}(0, 0)] \\ &\quad + z[\varphi_{zzzz}(0, t) - \varphi_{zzzz}(0, 0)] \\ \varphi_{zzz}(z, t) &= \sum_{i=1}^{3p} \sum_{l=1}^{3p} a_{iz} P_{2,i}(z) P_{1,l}(t) + [\varphi_{zzz}(z, 0) - \varphi_{zzz}(0, 0)] \\ &\quad + z[\varphi_{zzzz}(0, t) - \varphi_{zzzz}(0, 0)] + \varphi_{zzz}(0, t) \end{aligned} \quad (4.69)$$

$$\begin{aligned} \varphi_{zzz}(z, t) &= \sum_{i=1}^{3p} \sum_{l=1}^{3p} a_{iz} P_{2,i}(z) P_{1,l}(t) + [\varphi_{zzz}(z, 0) - \varphi_{zzz}(0, 0)] \\ &\quad + z[\varphi_{zzzz}(0, t) - \varphi_{zzzz}(0, 0)] + \varphi_{zzz}(0, t) \end{aligned} \quad (4.70)$$

Again, integrating w.r.t z,

$$\begin{aligned} \varphi_{zz}(z, t) - \varphi_{zz}(0, t) &\quad (4.71) \\ &= \sum_{i=1}^{3p} \sum_{l=1}^{3p} a_{iz} P_{3,i}(z) P_{1,l}(t) + [\varphi_{zz}(z, 0) - \varphi_{zz}(0, 0)] \\ &\quad + \frac{z^2}{2} [\varphi_{zzzz}(0, t) - \varphi_{zzzz}(0, 0)] + z[\varphi_{zzz}(0, t) \\ &\quad - \varphi_{zzz}(0, 0)] \end{aligned}$$

$$\begin{aligned} \varphi_{zz}(z, t) &= \sum_{i=1}^{3p} \sum_{l=1}^{3p} a_{iz} P_{3,i}(z) P_{1,l}(t) + [\varphi_{zz}(z, 0) - \varphi_{zz}(0, 0)] \\ &\quad + \frac{z^2}{2} [\varphi_{zzzz}(0, t) - \varphi_{zzzz}(0, 0)] + z[\varphi_{zzz}(0, t) \\ &\quad - \varphi_{zzz}(0, 0)] + \varphi_{zz}(0, t) \end{aligned} \quad (4.72)$$

Again, integrating w.r.t z,

$$\varphi_z(z, t) - \varphi_z(0, t) \quad (4.73)$$

$$\begin{aligned} &= \sum_{i=1}^{3p} \sum_{l=1}^{3p} a_{iz} P_{4,i}(z) P_{1,l}(t) + [\varphi_z(z, 0) - \varphi_z(0, 0)] \\ &+ \frac{z^3}{6} [\varphi_{zzzz}(0, t) - \varphi_{zzzz}(0, 0)] + \frac{z^2}{2} [\varphi_{zzz}(0, t) \\ &- \varphi_{zzz}(0, 0)] + z[\varphi_{zz}(0, t) - \varphi_{zz}(0, 0)] \end{aligned}$$

$$\begin{aligned} \varphi_z(z, t) &= \sum_{i=1}^{3p} \sum_{l=1}^{3p} a_{iz} P_{4,i}(z) P_{1,l}(t) + [\varphi_z(z, 0) - \varphi_z(0, 0)] \quad (4.74) \\ &+ \frac{z^3}{6} [\varphi_{zzzz}(0, t) - \varphi_{zzzz}(0, 0)] + \frac{z^2}{2} [\varphi_{zzz}(0, t) \\ &- \varphi_{zzz}(0, 0)] + z[\varphi_{zz}(0, t) - \varphi_{zz}(0, 0)] + \varphi_z(0, t) \end{aligned}$$

$$\varphi(z, t) - \varphi(0, t) \quad (4.75)$$

$$\begin{aligned} &= \sum_{i=1}^{3p} \sum_{l=1}^{3p} a_{iz} P_{5,i}(z) P_{1,l}(t) + [\varphi(z, 0) - \varphi(0, 0)] \\ &+ \frac{z^4}{24} [\varphi_{zzzz}(0, t) - \varphi_{zzzz}(0, 0)] + \frac{z^3}{6} [\varphi_{zzz}(0, t) \\ &- \varphi_{zzz}(0, 0)] + \frac{z^2}{2} [\varphi_{zz}(0, t) - \varphi_{zz}(0, 0)] \\ &+ z[\varphi_z(0, t) - \varphi_z(0, 0)] \end{aligned}$$

$$\begin{aligned} \varphi(z, t) &= \sum_{i=1}^{3p} \sum_{l=1}^{3p} a_{iz} P_{5,i}(z) P_{1,l}(t) + [\varphi(z, 0) - \varphi(0, 0)] \quad (4.76) \\ &+ \frac{z^4}{24} [\varphi_{zzzz}(0, t) - \varphi_{zzzz}(0, 0)] + \frac{z^3}{6} [\varphi_{zzz}(0, t) \\ &- \varphi_{zzz}(0, 0)] + \frac{z^2}{2} [\varphi_{zz}(0, t) - \varphi_{zz}(0, 0)] \\ &+ z[\varphi_z(0, t) - \varphi_z(0, 0)] + \varphi(0, t) \end{aligned}$$

$$\begin{aligned}
\varphi_t(z, t) = & \sum_{i=1}^{3p} \sum_{l=1}^{3p} a_{iz} P_{5,i}(z) H_l(t) + [\varphi(z, 0) - \varphi(0, 0)]_t & (4.77) \\
& + \frac{z^4}{24} [\varphi_{zzzz}(0, t) - \varphi_{zzzz}(0, 0)]_t \\
& + \frac{z^3}{6} [\varphi_{zzz}(0, t) - \varphi_{zzz}(0, 0)]_t \\
& + \frac{z^2}{2} [\varphi_{zz}(0, t) - \varphi_{zz}(0, 0)]_t + z[\varphi_z(0, t) - \varphi_z(0, 0)]_t \\
& + [\varphi(0, t)]_t
\end{aligned}$$

$$\varphi_t(z, t) + m\varphi_z + \varphi_{zzz} - \varphi_{zzzzz} = F(z, t) \quad (4.78)$$

$$\begin{aligned}
& \sum_{i=1}^{3p} \sum_{l=1}^{3p} a_{iz} P_{5,i}(z) H_l(t) + [\varphi(z, 0) - \varphi(0, 0)]_t + \frac{z^4}{24} [\varphi_{zzzz}(0, t) - \varphi_{zzzz}(0, 0)]_t \\
& + \frac{z^3}{6} [\varphi_{zzz}(0, t) - \varphi_{zzz}(0, 0)]_t + \frac{z^2}{2} [\varphi_{zz}(0, t) - \varphi_{zz}(0, 0)]_t \\
& + z[\varphi_z(0, t) - \varphi_z(0, 0)]_t + [\varphi(0, t)]_t \\
& + m \left\{ \sum_{i=1}^{3p} \sum_{l=1}^{3p} a_{iz} P_{4,i}(z) P_{1,l}(t) + [\varphi_z(z, 0) - \varphi_z(0, 0)] \right. \\
& + \frac{z^3}{6} [\varphi_{zzzz}(0, t) - \varphi_{zzzz}(0, 0)] + \frac{z^2}{2} [\varphi_{zzz}(0, t) - \varphi_{zzz}(0, 0)] \\
& \left. + z[\varphi_{zz}(0, t) - \varphi_{zz}(0, 0)] + \varphi_z(0, t) \right\} \sum_{i=1}^{3p} \sum_{l=1}^{3p} a_{iz} P_{2,i}(z) P_{1,l}(t) \\
& + [\varphi_{zzz}(z, 0) - \varphi_{zzz}(0, 0)] + z[\varphi_{zzzz}(0, t) - \varphi_{zzzz}(0, 0)] \\
& + \varphi_{zzz}(0, t) \\
& - \sum_{i=1}^{3p} \sum_{l=1}^{3p} a_{iz} H_i(z) P_{1,l}(t) + \varphi_{zzzzz}(z, 0) - F(z, t) = 0
\end{aligned}$$

$$\begin{aligned}
& \sum_{i=1}^{3p} \sum_{l=1}^{3p} a_{iz} P_{5,i}(z) H_l(t) + [\varphi(z, 0) - \varphi(0, 0)]_t \tag{4.79} \\
& \quad + \frac{z^4}{24} [\varphi_{zzzz}(0, t) - \varphi_{zzzz}(0, 0)]_t \\
& \quad + \frac{z^3}{6} [\varphi_{zzz}(0, t) - \varphi_{zzz}(0, 0)]_t \\
& \quad + \frac{z^2}{2} [\varphi_{zz}(0, t) - \varphi_{zz}(0, 0)]_t \\
& \quad + z[\varphi_z(0, t) - \varphi_z(0, 0)]_t + [\varphi(0, t)]_t + \\
& + m \left\{ \sum_{i=1}^{3p} \sum_{l=1}^{3p} a_{iz} P_{4,i}(z) P_{1,l}(t) + [\varphi_z(z, 0) - \varphi_z(0, 0)] \right. \\
& \quad + \frac{z^3}{6} [\varphi_{zzzz}(0, t) - \varphi_{zzzz}(0, 0)] + \frac{z^2}{2} [\varphi_{zzz}(0, t) \\
& \quad \left. - \varphi_{zzz}(0, 0)] + z[\varphi_{zz}(0, t) - \varphi_{zz}(0, 0)] + \varphi_z(0, t) \right\} \\
& + \sum_{i=1}^{3p} \sum_{l=1}^{3p} a_{iz} P_{2,i}(z) P_{1,l}(t) + [\varphi_{zzz}(z, 0) - \varphi_{zzz}(0, 0)] \\
& \quad + z[\varphi_{zzzz}(0, t) - \varphi_{zzzz}(0, 0)] + \varphi_{zzz}(0, t) \\
& \quad - \sum_{i=1}^{3p} \sum_{l=1}^{3p} a_{iz} H_i(z) P_{1,l}(t) + \varphi_{zzzzz}(z, 0) = F(z, t)
\end{aligned}$$

$$\begin{aligned}
& \sum_{i=1}^{3p} \sum_{l=1}^{3p} a_{iz} P_{5,i}(z) H_l(t) + m \sum_{i=1}^{3p} \sum_{l=1}^{3p} a_{iz} P_{4,i}(z) P_{1,l}(t) \tag{4.80} \\
& \quad + \sum_{i=1}^{3p} \sum_{l=1}^{3p} a_{iz} P_{2,i}(z) P_{1,l}(t) \\
& \quad - \sum_{i=1}^{3p} \sum_{l=1}^{3p} a_{iz} H_i(z) P_{1,l}(t)
\end{aligned}$$

$$\begin{aligned}
&= F(z, t) - [\varphi(z, 0) - \varphi(0, 0)]_t - \frac{z^4}{24} [\varphi_{zzzz}(0, t) - \varphi_{zzzz}(0, 0)]_t \\
&\quad - \frac{z^3}{6} [\varphi_{zzz}(0, t) - \varphi_{zzz}(0, 0)]_t \\
&\quad - \frac{z^2}{2} [\varphi_{zz}(0, t) - \varphi_{zz}(0, 0)]_t - z[\varphi_z(0, t) - \varphi_z(0, 0)]_t \\
&\quad - [\varphi(0, t)]_t - m[\varphi_z(z, 0) - \varphi_z(0, 0)] \\
&\quad - m \frac{z^3}{6} [\varphi_{zzzz}(0, t) - \varphi_{zzzz}(0, 0)] - m \frac{z^2}{2} [\varphi_{zzz}(0, t) \\
&\quad - \varphi_{zzz}(0, 0)] - mz[\varphi_{zz}(0, t) - \varphi_{zz}(0, 0)] - m\varphi_z(0, t) \\
&\quad - [\varphi_{zzz}(z, 0) - \varphi_{zzz}(0, 0)] \\
&\quad - z[\varphi_{zzzz}(0, t) - \varphi_{zzzz}(0, 0)] - \varphi_{zzz}(0, t) \\
&\quad - \varphi_{zzzzz}(z, 0)
\end{aligned}$$

$$\begin{aligned}
&\sum_{i=1}^{3p} \sum_{l=1}^{3p} a_{iz} P_{5,i}(z) H_l(t) + m \sum_{i=1}^{3p} \sum_{l=1}^{3p} a_{iz} P_{4,i}(z) P_{1,l}(t) \tag{4.81} \\
&\quad + \sum_{i=1}^{3p} \sum_{l=1}^{3p} a_{iz} P_{2,i}(z) P_{1,l}(t) \\
&\quad - \sum_{i=1}^{3p} \sum_{l=1}^{3p} a_{iz} H_i(z) P_{1,l}(t) \\
&= F(z, t) - [\varphi(z, 0) - \varphi(0, 0)]_t \\
&\quad - \frac{z^4}{24} [\varphi_{zzzz}(0, t) - \varphi_{zzzz}(0, 0)]_t \\
&\quad - \frac{z^3}{6} [\varphi_{zzz}(0, t) - \varphi_{zzz}(0, 0)]_t \\
&\quad - \frac{z^2}{2} [\varphi_{zz}(0, t) - \varphi_{zz}(0, 0)]_t \\
&\quad - z[\varphi_z(0, t) - \varphi_z(0, 0)]_t
\end{aligned}$$

$$\begin{aligned}
& -[\varphi(0, t)]_t - m[\varphi_z(z, 0) - \varphi_z(0, 0)] \\
& - m \frac{z^3}{6} [\varphi_{zzzz}(0, t) - \varphi_{zzzz}(0, 0)] - m \frac{z^2}{2} [\varphi_{zzz}(0, t) \\
& - \varphi_{zzz}(0, 0)] - mz[\varphi_{zz}(0, t) - \varphi_{zz}(0, 0)] - m\varphi_z(0, t) \\
& - [\varphi_{zzz}(z, 0) - \varphi_{zzz}(0, 0)] \\
& - z[\varphi_{zzzz}(0, t) - \varphi_{zzzz}(0, 0)] - \varphi_{zzz}(0, t) \\
& - \varphi_{zzzzz}(z, 0)
\end{aligned}$$

Table 4.11 At different values of z and t , comparison of AS and ES with the value of Absolute error.

z	t	AS	ES	Value of Absolute error
0.055555555555555	0.055555555555555	0.000057152654610	0.000057152654610	9.15e-18
0.166666666666666	0.166666666666666	0.000006350294957	0.000006350294957	1.06e-18
0.277777777777777	0.277777777777777	0.001428816365253	0.001428816365253	2.28e-16
0.388888888888888	0.388888888888888	0.002800480075895	0.002800480075896	4.48e-16
0.500000000000000	0.500000000000000	0.004629365023419	0.004629365023420	7.40e-16
0.611111111111111	0.611111111111111	0.006915471207824	0.006915471207825	1.10e-15
0.722222222222222	0.722222222222222	0.009658798629109	0.009658798629110	1.54e-15
0.833333333333333	0.833333333333333	0.012859347287275	0.012859347287277	9.76e-15
0.944444444444444	0.944444444444444	0.016517117182322	0.016517117182325	2.64e-15

Table 4.12 At different values of μ , value of L_2 -error and L_∞ -error.

For different values of μ	$\mu = 0.25$	$\mu = 0.50$	$\mu = 0.75$	$\mu = 1$
L_2 -error	2.3274996e-03	1.454231e-03	6.7407088e-04	2.4911575e-06
L_∞ -error	2.9885388e-03	1.867226e-03	9.4193127e-04	2.9707930e-06

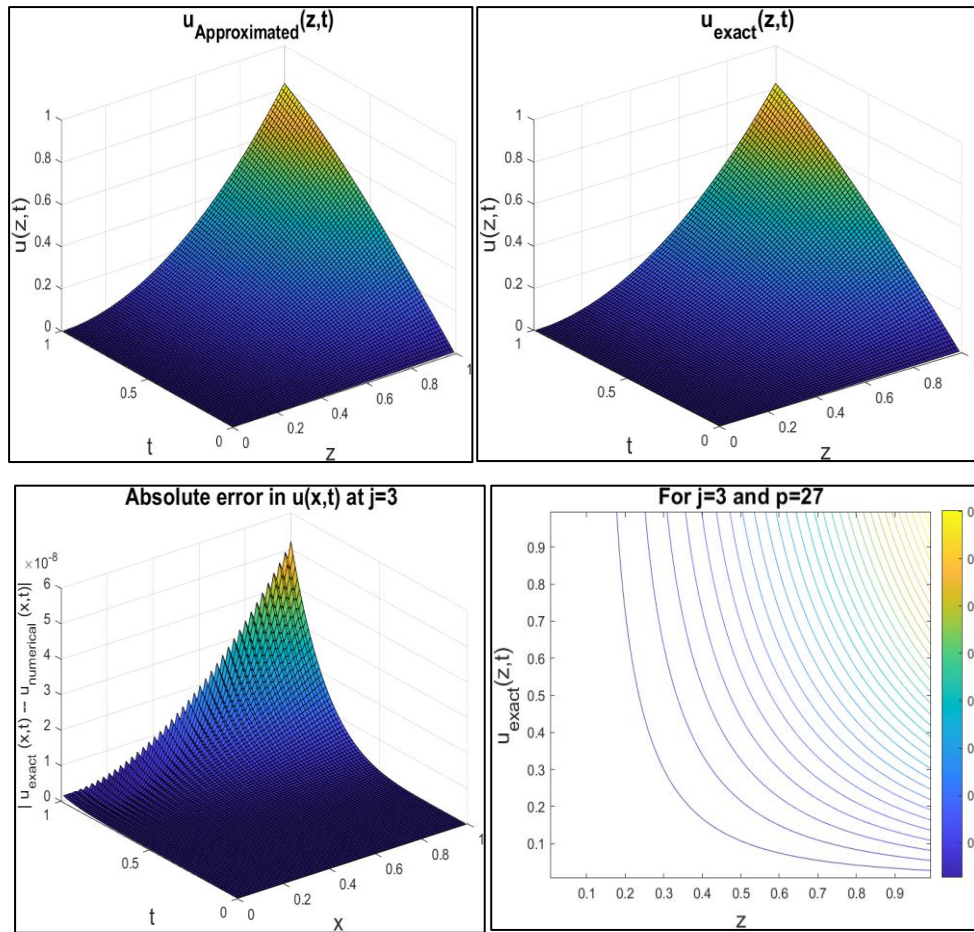
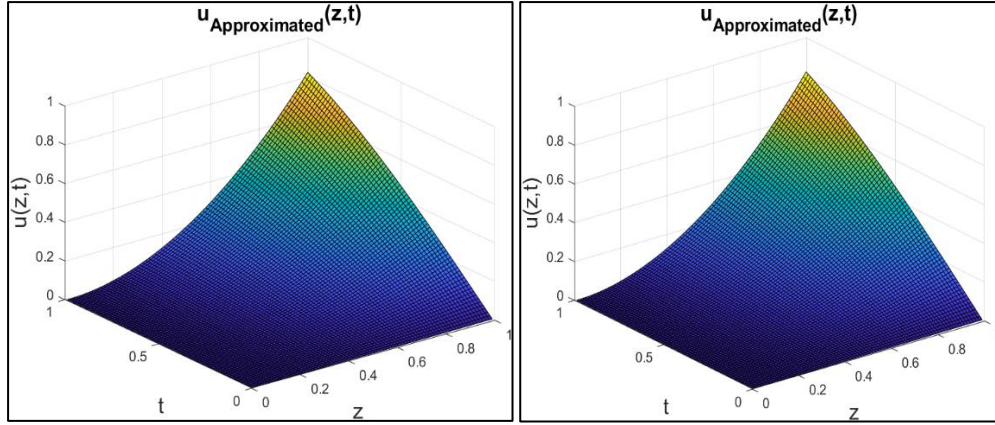


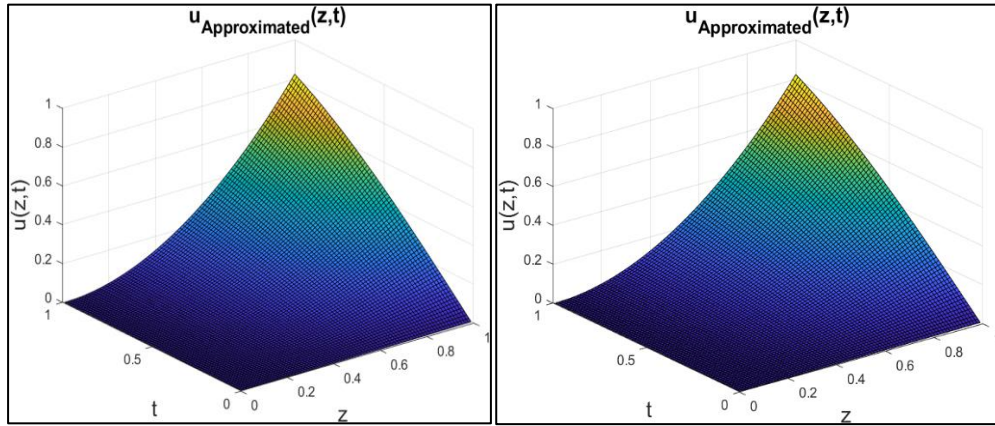
Figure 4.11 Graphical Representation of AS, ES and absolute error with contour view of ES.

By Discontinuous Galerkin method for the different value of μ , norm representation attains third order level of accuracy [165]. But the proposed method at similar values of μ , 3D graphical representation attains third as well as fourth level of accuracy. The HW resolution is investigated for various parameter values ranging from 0.25, 0.50 and 0.75. The results are depicted graphically. As the parameter values approach 1, the AS converges towards the ES. This convergence demonstrates the effectiveness of the proposed method.



$\mu = 1$

$\mu = 0.25$



$\mu = 0.50$

$\mu = 0.75$

Figure 4.12 Graphical representation for $\mu=0.25, 0.50$ and 0.75 with AS at $\mu=1$.

4.4.7 Numerical experiment 4.5.7: Fractional Kawahara Equation

$$D_t^\mu \varphi(z, t) + \left(\frac{\varphi^2}{2} + \frac{\varphi^3}{3}\right)_z + \varphi_{zzz} - \varphi_{zzzz} = F(z, t) \quad (4.82)$$

$$\varphi(z, 0) = 0 \quad (4.83)$$

With source term,

$$F(z, t) = \frac{2t^{2-\mu}}{\Gamma(3-\mu)} \cos(2\pi z) - t^4 \pi \sin(4\pi z) - t^6 \pi \cos(2\pi z) \sin(4\pi z) \quad (4.84)$$

$$+ 8\pi^3 t^2 \sin(2\pi z) + 32\pi^5 t^2 \sin(2\pi z)$$

ES,

$$\varphi(z, t) = t^2 \cos(2\pi z) \quad (4.85)$$

calculation of accuracy of proposed technique for $z, t \in [0,1] \times [0,1]$.

For $\mu = 1$,

$$\varphi_t(z, t) + \left(\frac{\varphi^2}{2} + \frac{\varphi^3}{3}\right)_z + \varphi_{zzz} - \varphi_{zzzzz} = F(z, t) \quad (4.86)$$

After solving the above equation, it becomes,

$$\begin{aligned} \varphi_t + \varphi\varphi_z + \varphi^2\varphi_z + \varphi_{zzz} - \varphi_{zzzzz} \\ = 2t\cos(2\pi z) - t^4\pi\sin(4\pi z) - t^6\pi\cos(2\pi z)\sin(4\pi z) \\ + 8\pi^3t^2\sin(2\pi z) + 32\pi^5t^2\sin(2\pi z) \end{aligned} \quad (4.87)$$

After applying QT on non-linear terms,

$$\begin{aligned} \varphi_t + \varphi_{r+1}\varphi_z - \varphi_z\varphi + (\varphi_z)_{r+1}\varphi + 2(\varphi_z)_{r+1}\varphi\varphi_z - 2\varphi^2\varphi_z \\ + \varphi^2(\varphi_z)_{r+1} + \varphi_{zzz} - \varphi_{zzzzz} \\ = 2t\cos(2\pi z) - t^4\pi\sin(4\pi z) - t^6\pi\cos(2\pi z)\sin(4\pi z) \\ + 8\pi^3t^2\sin(2\pi z) + 32\pi^5t^2\sin(2\pi z) \end{aligned} \quad (4.88)$$

Table 4.13 At different values of z and t , comparison of AS and ES with the value of Absolute error at $\mu=1$.

z	t	AS	ES	Value of Absolute error
0.0555555555555556	0.0555555555555556	0.00460711028235	0.00460711028246	1.09e-13
0.1666666666666667	0.1666666666666667	0.03202132022695	0.03202132022771	7.57e-13
0.2777777777777778	0.2777777777777778	0.08410831912169	0.08410831912367	2.61e-12
0.3888888888888889	0.3888888888888889	0.16086810696656	0.16086810697036	3.08e-12
0.5000000000000000	0.5000000000000000	0.26230068376157	0.26230068376778	6.20e-12
0.6111111111111111	0.6111111111111111	0.38840604950672	0.38840604951591	9.81e-11
0.7222222222222222	0.7222222222222222	0.53918420420202	0.53918420421476	1.27e-11
0.8333333333333333	0.8333333333333333	0.71463514784745	0.71463514786434	1.68e-11
0.9444444444444444	0.9444444444444444	0.91475888044302	0.91475888046464	2.16e-11

Table 4.14 Value L_2 and L_∞ errors for Test problem 4.47 at $\mu=0.2, 0.4$ and 0.6

For different values of μ	L_2 error (HSW3)	L_2 error [165]	L_∞ errors (HSW3M)	L_∞ errors [165]
0.2	7.7e-003	1.013271e-002	9.9e-003	4.082594e-002
0.4	7.5e-003	1.013270e-002	9.7e-003	4.082593e-002
0.6	7.4e-003	1.013270e-002	9.3e-003	4.082592e-002

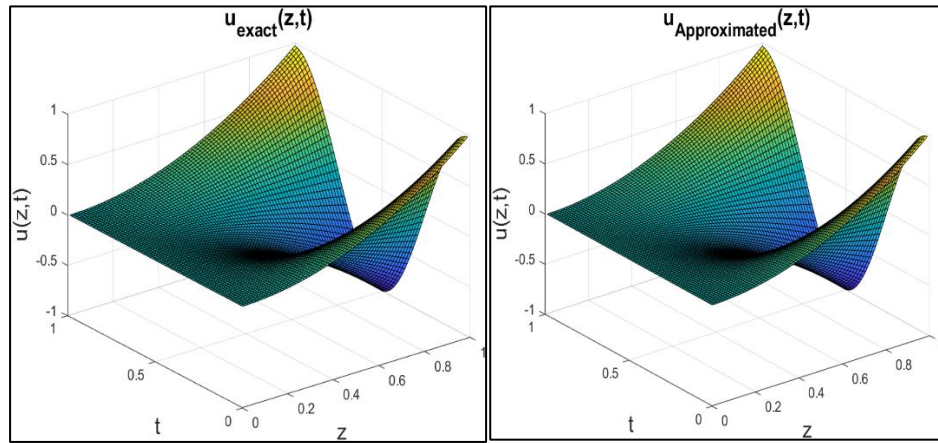
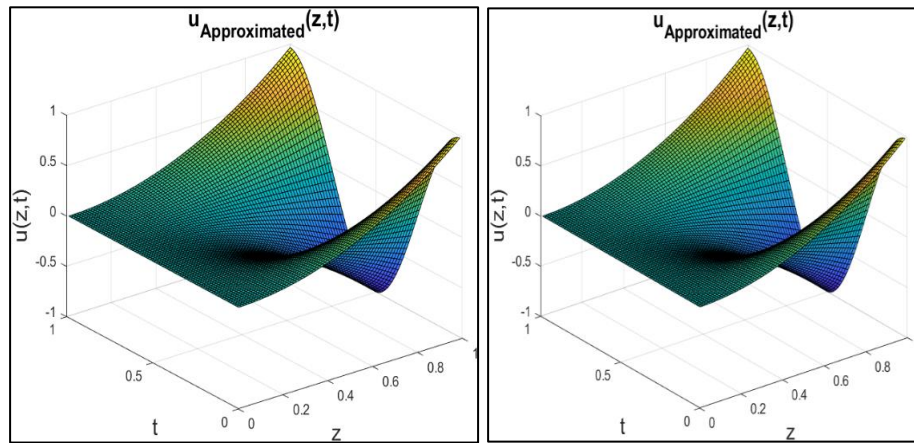


Figure 4.13 Graphical Representation of AS, ES at $\mu = 1$.



$\mu = 0.20$

$\mu = 0.40$

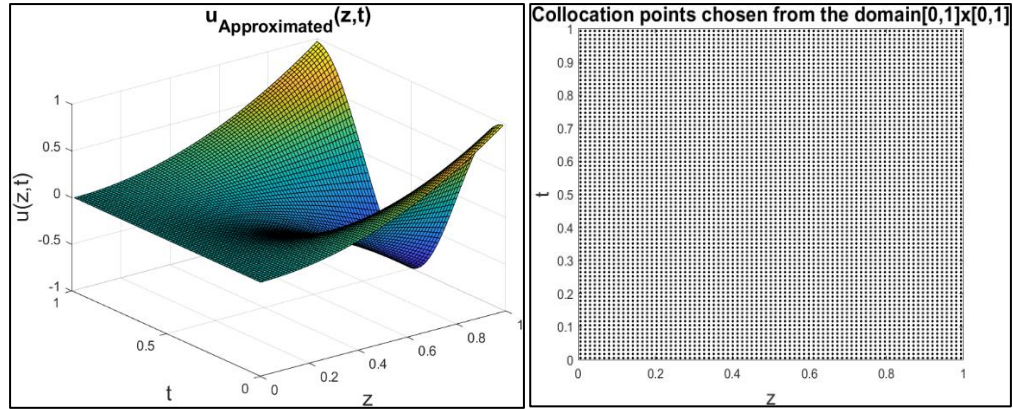


Figure 4.14 Graphical representation for $\mu=0.20, 0.40$ and 0.60 with graph of collocation points.

It is explored HW resolution for parameter values between 0.20, 0.40 and 0.60. The results are shown graphically. As the parameter values get closer to 1, AS converges towards the ES. This convergence confirms the effectiveness of the proposed method.

4.4.8 Conclusion:

In this chapter, FEs like Riccati, Vander-Pol and the time-fractional KEs are solved using the HSWM, and the stability and error analysis for the linear case is carried out. The numerical experiments are provided to show the method's accuracy and capacity. Higher-dimensional issues and other types of time-FEs can be easily solved using the same approach and analytical technique. With the support of graphics, the results are examined and discussed while taking various parameter values into account. Results show that the AS converges to the ES as the value of FOD. Researchers may find our method attractive for solving fractional-order problems that are emerging in the science of technology because it can be made more precise by assuming high approximations.

Chapter 5

Conclusion and Future Work

The majority of physical phenomena can be effectively represented through DEs, facilitating in-depth exploration and analysis. However, obtaining analytical solutions for these DEs becomes an exceptionally challenging endeavour when the mathematical model incorporates elements such as variable coefficients, nonlinearities, or a higher number of variables (resulting in higher dimensionality). Consequently, there is a necessity for advanced numerical techniques that can be considered robust solvers, allowing us to obtain precise numerical solutions for these types of complex DEs. Researchers are persistently dedicating their efforts to enhancing current methodologies and innovating new hybrid approaches, all with the goal of creating potent solvers tailored to address these types of equations. Within the existing body of literature, dyadic wavelets are prevalent, characterized by dilation factors following powers of 2. The primary objective of this thesis is to create and investigate the utilization of numerical methods based on HS3W, which are non-dyadic and employ a dilation factor of 3. This innovative approach is employed to compute numerical solutions for a variety of significant problems, including higher-order linear and nonlinear BVP, time-dependent PDEs, and FDEs. Within this thesis, we have employed HS3W and HS2W as the primary framework, complemented by established numerical approaches like the collocation method, Quasilinearization process, and the Gauss elimination method, to derive solutions for a wide spectrum of linear and nonlinear higher-order, ODEs, PDEs, and FDEs. We have also established the conditions for the convergence of these numerical techniques. Ultimately, we introduce a novel HS3W (non-dyadic) based technique, showcasing its superior efficiency when compared to the traditional HS2W dyadic wavelet-based approach. The proposed wavelet techniques, specifically the HS3W (non-dyadic) collocation method and the HS3W (non-dyadic) Quasilinearization method, have demonstrated their remarkable utility across a wide spectrum of real-world problems. Leveraging the inherent advantages of HS3W (non-dyadic), such as computational efficiency, conceptual simplicity, memory efficiency, and orthonormality with compact support, these methods emerge as enhanced alternatives to traditional numerical approaches. Indeed, their simplicity, the sparsity of HS3W matrices, and the representation of solutions with a significantly reduced number of wavelet coefficients contribute to accelerated convergence rates for this method. The HS3W (non-

dyadic) based approach yields improved results even with a lower LOR. This method requires only a small number of collocation points, effectively reducing computational expenses.

While the main discoveries of the proposed techniques have been previously elucidated in the preceding chapters, we will now provide a condensed overview of their advantages as follows:

- I. The introduced approach represents a relatively novel concept employed for calculating numerical solutions to significant problems encompassing higher-order linear and nonlinear DEs, including those with BCs, as well as time-dependent PDEs, FDEs, and nonlinear systems of fractional FPDEs.
- II. The operational matrices and integral matrices associated with HS3W (non-dyadic) exhibit sparsity, which significantly enhances computational efficiency and leads to a considerable reduction in computational costs.
- III. Regarding the convergence analysis of the equations under consideration, the utilization of HS3W bases leads to a faster rate of convergence when compared to the HS2W basis functions.
- IV. During the implementation of HS3W basis functions in conjunction with the collocation method, it becomes evident that the collocation method is notably more straightforward to apply when paired with HS3W, particularly when contrasted with other numerical techniques like finite element methods.
- V. The HS3W (non-dyadic) method offers a high degree of convenience in addressing BOP within ODE, PDE, and FDE. This convenience arises from the automatic incorporation of BCs into the method's inherent processes.
- VI. The primary constraint associated with the HS3W family lies in the discontinuity of its members at partition points. Consequently, the application of a derivative-based approach at the initial stage is not feasible. Instead, one must employ an integration procedure to ascertain the coefficients governing the weights of the wavelets.
- VII. In conclusion, the utilization of HS3W has demonstrated elegance, effectiveness, and substantial potential in addressing a diverse range of mathematical models. Their performance surpasses that of the results found in existing literature.

FUTURE SCOPE

In the context of the physical problems investigated within this thesis, the utilization of the HS3W (non-dyadic) approach has demonstrated elegance, effectiveness, and significant potential for addressing a wide array of mathematical models. The research conducted in this thesis has generated several noteworthy findings that could serve as valuable directions for future research. A selection of these potential research avenues is outlined below:

- I. The proposed method has the potential to be expanded for use with two-dimensional integral equations, integro-differential equations, and fractional integro-differential equations, making use of the latest developments in fractional calculus, such as the Atangana-Baleanu fractional operator and the Caputo-Fabrizio definitions. Furthermore, the HS3W (non-dyadic) techniques presented here can be customized to seek solutions for novel forms of linear and nonlinear ODEs, PDEs, and FDEs.
- II. In this thesis, HS3W has been employed as the primary tool in conjunction with established numerical methods such as the Quasilinearization process, Gauss elimination, and collocation method. Nevertheless, the literature contains an extensive array of wavelets with diverse structures and characteristics, including Shannon, Daubechies, Gabor, Bernoulli, Legendre, Hermite, Spline, ultraspherical, Chebyshev, Gegenbauer, Bessel, Laguerre among others. To assess the efficiency and accuracy of a numerical technique based on a specific wavelet, conducting a comparative study holds significant promise, offering motivation and interest for further exploration.
- III. In the application of the HS3W (non-dyadic) collocation method, nonlinear problems are addressed through a linearization process employing the Quasilinearization formula, as elaborated in this thesis. Additionally, there is the possibility of further exploring the applicability of this technique in conjunction with other established methods for handling nonlinearities within equations. Examples of such methods include the method of lines and the generalized Newton-Raphson method, among others.
- IV. The majority of the PDEs and FDEs governing the various real-world phenomena addressed in this research pertain to second-order equations in one or two dimensions. However, it is worth noting that the proposed method has the potential to be extended for the resolution of HODEs frequently encountered in the fields of engineering and the sciences.

- V. In this research study, the collocation method has been employed in conjunction with non-dyadic HW basis functions. These wavelet basis functions can also be integrated into other established numerical methods and subsequently compared with various numerical and semi-analytical techniques, such as the FEM and alternative wavelet-based approaches, among others.
- VI. In the current research, the convergence of the proposed methods has been rigorously demonstrated in the individual chapters. However, it's important to note that there are additional avenues for validation, including stability analysis and statistical assessments such as paired t-tests and ANOVA, which can further substantiate the obtained results.

References

- [1] S.Das, *Functional Fractional Calculus*, Second. Berlin Heidelberg: Springer- Verlag., 2011.
- [2] Y. Z. Povstenko, “Thermoelasticity that uses fractional heat conduction equation,” *J. Math. Sci.*, vol. 162, no. 2, 2009, doi: 10.1007/s10958-009-9636-3.
- [3] D. Tripathi, S. K. Pandey, and S. Das, “Peristaltic flow of viscoelastic fluid with fractional Maxwell model through a channel,” *Appl. Math. Comput.*, vol. 215, no. 10, 2010, doi: 10.1016/j.amc.2009.11.002.
- [4] A. M. Lopes, J. A. Tenreiro Machado, C. M. A. Pinto, and A. M. S. F. Galhano, “Fractional dynamics and MDS visualization of earthquake phenomena,” *Comput. Math. with Appl.*, vol. 66, no. 5, 2013, doi: 10.1016/j.camwa.2013.02.003.
- [5] Zalmanzon LA., *Fourier, Walsh, and Haar transforms and their applications in control, communication and other fields*. Moscow: Nauka, 1989.
- [6] S. G. Mallat, “Multiresolution approximations and wavelet orthonormal bases of $L_2(\mathbb{R})$,” in *Fundamental Papers in Wavelet Theory*, 2009, pp. 524–542.
- [7] U. Saeed and M. U. Rehman, “Haar wavelet-quasilinearization technique for fractional nonlinear differential equations,” *Appl. Math. Comput.*, vol. 220, 2013, doi: 10.1016/j.amc.2013.07.018.
- [8] V. Mishra and Sabina, “Wavelet Galerkin solutions of ordinary differential equations,” *Int. J. Math. Anal.*, vol. 5, no. 9–12, 2011.
- [9] N. Truong and S. Gilbert, *Wavelets and Filter Banks*. Wellesley Cambridge Press, USA, 1996.
- [10] Ü. Lepik, “Application of wavelet transform techniques to vibration studies,” *Proc. Est. Acad. Sci. Physics. Math.*, vol. 50, no. 3, 2001, doi: 10.3176/phys.math.2001.3.05.
- [11] A. Haar, “Zur theorie der orthogonalen funktionen systeme,” *Math. Ann.*, vol. 69, no. 3, pp. 331–371, 1910, doi: 10.1007/BF01456326.
- [12] M. P.S, *Pattern recognition transforms*. Newyork: Wiley, 1992.
- [13] Castleman K.R, *Digital image processing*. Englewood Cliffs: Prentice-Hall, 1996.
- [14] Y. L.P, *Digital picture processing: an introduction*. Berlin: Springer, 1979.
- [15] G. H. Burrus CS, Gophinat RA, *Introduction to wavelets and wavelet transforms*. Englewood Cliffs, Prentice Hall, 1988.
- [16] K. cevi c J. Vetterli M, *Wavelets and subband coding*. Upper Sadle River: Prentice-

- Hall, 1995.
- [17] S. JE, “Shore JE. On the applications of Haar functions. 22:206–16.,” *IEEE Trans Commun*, vol. 22, pp. 206–216, 1973.
- [18] W. C, “Generalization of Haar functions,” *Tohoku Math J*, vol. 8, pp. 286–290, 1956.
- [19] Z. Y. Zhang QS, *Theory and applications of bridge functions*. Beijing: Defense Industry Publisher, 1992.
- [20] K. W, *Systems of spectral analysis of digital data*. Warsaw: WKL, 1984.
- [21] Z. QS, *New methods of signal information transfer*. Beijing: Aeronautics and Astronautics Publishers, 1989.
- [22] O. M, “Approximation of analytic functions by Haar functions. 105(5):101–8.,” *IEICE Trans*, vol. 105, no. 5, pp. 101–108, 1985.
- [23] Y. Meyer, *Orthonormal wavelets*. In *Wavelets: Time-Frequency Methods and Phase Space*. Berlin, Heidelberg: Springer Berlin Heidelberg., 1989.
- [24] I. Daubechies, “Orthonormal bases of compactly supported wavelets.,” *Commun. pure Appl. Math.*, vol. 41, no. 7, pp. 909-996., 1988.
- [25] A. Cohen, “Ten Lectures on Wavelets, CBMS-NSF Regional Conference Series in Applied Mathematics, Vol. 61, I. Daubechies, SIAM, 1992, xix + 357 pp.,” *J. Approx. Theory*, vol. 78, no. 3, 1994, doi: 10.1006/jath.1994.1093.
- [26] C. F. Chen and C. H. Hsiao, “Haar wavelet method for solving lumped and distributed-parameter systems,” *IEE Proc. Control Theory Appl.*, vol. 144, no. 1, 1997, doi: 10.1049/ip-cta:19970702.
- [27] Ü. Lepik and E. Tamme, “Application of the Haar Wavelets for Solution of Linear Integral Equations,” *Dyn. Syst. Appl.*, no. July, 2004.
- [28] Ü. Lepik, “Numerical solution of differential equations using Haar wavelets,” *Math. Comput. Simul.*, vol. 68, no. 2, 2005, doi: 10.1016/j.matcom.2004.10.005.
- [29] Ü. Lepik, “Numerical solution of evolution equations by the Haar wavelet method,” *Appl. Math. Comput.*, vol. 185, no. 1, 2007, doi: 10.1016/j.amc.2006.07.077.
- [30] P. Chang and P. Piau, “Haar Wavelet Matrices Designation in Numerical Solution of Ordinary Differential Equations,” *Int. J. Appl. Math.*, vol. 38, no. 3, 2008.
- [31] Ü. Lepik, “Solving fractional integral equations by the Haar wavelet method,” *Appl. Math. Comput.*, vol. 214, no. 2, 2009, doi: 10.1016/j.amc.2009.04.015.
- [32] E. Babolian and A. Shamsavaran, “Numerical solution of nonlinear Fredholm integral equations of the second kind using Haar wavelets,” *J. Comput. Appl. Math.*, vol. 225,

- no. 1, 2009, doi: 10.1016/j.cam.2008.07.003.
- [33] G. Hariharan and K. Kannan, "Haar wavelet method for solving some nonlinear Parabolic equations," *J. Math. Chem.*, vol. 48, no. 4, 2010, doi: 10.1007/s10910-010-9724-0.
- [34] D. G. Hariharan, "Solving Finite Length Beam Equation by the Haar Wavelet Method," *Int. J. Comput. Appl.*, vol. 9, no. 1, 2010, doi: 10.5120/1349-1819.
- [35] G. Hariharan, "Haar Wavelet Method for Solving the Klein-Gordon and the Sine-Gordon Equations," *ISSN Int. J. Nonlinear Sci.*, vol. 11, no. 2, 2011.
- [36] Ü. Lepik, "Exploring vibrations of cracked beams by the Haar wavelet method," *Est. J. Eng.*, vol. 18, no. 1, 2012, doi: 10.3176/eng.2012.1.05.
- [37] V. Mishra, H. Kaur, and R. C. Mittal, "Haar wavelet algorithm for solving certain Differential, Integral and Integro-differential equations," *Int. J. Appl. Math Mech*, vol. 8, no. 6, 2012.
- [38] Ü. Lepik, "Solving PDEs with the aid of two-dimensional Haar wavelets," *Comput. Math. with Appl.*, vol. 61, no. 7, 2011, doi: 10.1016/j.camwa.2011.02.016.
- [39] H. Wavelet, "SOLUTION OF WAVE-LIKE EQUATION BASED ON HAAR WAVELET NARESH BERWAL - DINESH PANCHAL - C . L . PARIHAR," *Le Mat.*, vol. LXVII, 2012.
- [40] G. Hariharan, "Wavelet method for a class of fractional Klein-Gordon equations," *J. Comput. Nonlinear Dyn.*, vol. 8, no. 2, 2013, doi: 10.1115/1.4006837.
- [41] S. Sekar and C. Jaisankar, "Numerical strategies for the nonlinear integro-differential equations using single-term Haar wavelet series," *Appl. Math. Sci.*, no. 49–52, 2014, doi: 10.12988/ams.2014.43167.
- [42] N. Berwal, D. Panchal, and C. L. Parihar, "Numerical solution of series l-c-r equation based on haar wavelet," *Ital. J. Pure Appl. Math.*, no. 30, 2013.
- [43] R. C. Kaur, H., Mishra, V., & Mittal, "Numerical solution of a laminar viscous flow boundary layer equation using uniform Haar wavelet quasi-linearization method.," *Proc. World Acad. Sci. Eng. Technol.*, vol. 79, p. 1682, 2013.
- [44] U. Saeed and M. ur Rehman, "Assessment of Haar Wavelet-Quasilinearization Technique in Heat Convection-Radiation Equations," *Appl. Comput. Intell. Soft Comput.*, vol. 2014, 2014, doi: 10.1155/2014/454231.
- [45] R. C. Mittal, H. Kaur, and V. Mishra, "Haar wavelet-based numerical investigation of coupled viscous Burgers' equation," *Int. J. Comput. Math.*, vol. 92, no. 8, 2015, doi:

10.1080/00207160.2014.957688.

- [46] V. H. Patel, A. C., & Pradhan, “Wavelet galerkin scheme for nonlinear partial differential equations,” . *Int. J. Res. Applied, Nat. Soc. Sci.*, vol. 2, no. 8, pp. 69–78, 2014.
- [47] S. Arora, Y. Singh Brar, and S. Kumar, “Haar Wavelet Matrices for the Numerical Solutions of Differential Equations,” *Int. J. Comput. Appl.*, vol. 97, no. 18, 2014, doi: 10.5120/17108-7759.
- [48] A. M. Osama, H. M., Fadhel, S. F., & Zaid, “Numerical solution of fractional variational problems using direct Haar wavelet method.,” *Int. J. Innov. Res. Sci. Eng. Technol*, vol. 3, no. 5, pp. 1–9, 2014.
- [49] S. S. Ray, “Two reliable approaches involving Haar wavelet method and Optimal Homotopy Asymptotic method for the solution of fractional Fisher type equation,” in *Journal of Physics: Conference Series*, 2014, vol. 574, no. 1, doi: 10.1088/1742-6596/574/1/012131.
- [50] Oruç, F. Bulut, and A. Esen, “A Haar wavelet-finite difference hybrid method for the numerical solution of the modified burgers’ equation,” *J. Math. Chem.*, vol. 53, no. 7, 2015, doi: 10.1007/s10910-015-0507-5.
- [51] M. Kumar and S. Pandit, “An efficient algorithm based on Haar wavelets for numerical simulation of Fokker-Planck equations with constants and variable coefficients,” *Int. J. Numer. Methods Heat Fluid Flow*, vol. 25, no. 1, 2015, doi: 10.1108/HFF-03-2014-0084.
- [52] A. B. Shiralashetti, S. C., & Deshi, “An efficient Haar wavelet collocation method for the numerical solution of multi-term fractional differential equations.,” *Nonlinear Dyn.*, vol. 83, pp. 293-303., 2016.
- [53] K. Fallahpour, M., Khodabin, M., & Maleknejad, “Approximation solution of two-dimensional linear stochastic Volterra integral equation by applying the Haar wavelet.,” *arXiv preprint arXiv:1505.04855.*, 2015. .
- [54] S. C. Shiralashetti, A. B. Deshi, and P. B. Mutalik Desai, “Haar wavelet collocation method for the numerical solution of singular initial value problems,” *Ain Shams Eng. J.*, vol. 7, no. 2, 2016, doi: 10.1016/j.asej.2015.06.006.
- [55] I. Singh, S. Arora, and S. Kumar, “Numerical solution of wave equation using Haar wavelet,” *Int. J. Pure Appl. Math.*, vol. 98, no. 4, 2015, doi: 10.12732/ijpam.v98i4.4.
- [56] S. C. Shiralashetti, L. M. Angadi, A. B. Deshi, and M. H. Kantli, “Haar wavelet method

- for the numerical solution of Klein-Gordan equations,” *Asian-European J. Math.*, vol. 9, no. 1, 2016, doi: 10.1142/S1793557116500121.
- [57] F. A. Shah, R. Abass, and L. Debnath, “Numerical Solution of Fractional Differential Equations Using Haar Wavelet Operational Matrix Method,” *Int. J. Appl. Comput. Math.*, vol. 3, no. 3, 2017, doi: 10.1007/s40819-016-0246-8.
- [58] A. C. Patel and V. H. Pradhan, “Numerical solution of one dimensional contaminant transport equation with variable coefficient (temporal) by using Haar wavelet,” *Glob. J. Pure Appl. Math.*, vol. 12, no. 2, 2016.
- [59] Oruç, F. Bulut, and A. Esen, “Numerical Solutions of Regularized Long Wave Equation By Haar Wavelet Method,” *Mediterr. J. Math.*, vol. 13, no. 5, 2016, doi: 10.1007/s00009-016-0682-z.
- [60] H. Kaur and S. M. Kang, “Haar wavelets based time discretization technique for solving nonlinear partial differential equations,” *Int. J. Pure Appl. Math.*, vol. 108, no. 1, 2016, doi: 10.12732/ijpam.v108i1.8.
- [61] S. C. Shiralashetti, L. M. Angadi, M. H. Kantli, and A. B. Deshi, “Numerical solution of parabolic partial differential equations using adaptive grid Haar wavelet collocation method,” *Asian-European J. Math.*, vol. 10, no. 2, 2017, doi: 10.1142/S1793557117500267.
- [62] S. Arbabi, A. Nazari, and M. T. Darvishi, “A two-dimensional Haar wavelets method for solving systems of PDEs,” *Appl. Math. Comput.*, vol. 292, 2017, doi: 10.1016/j.amc.2016.07.032.
- [63] U. Saeed, “Haar wavelet operational matrix method for system of fractional nonlinear differential equations,” *Int. J. Wavelets, Multiresolution Inf. Process.*, vol. 15, no. 5, 2017, doi: 10.1142/S0219691317500436.
- [64] R. A. Shiralashetti, S. C., & Mundewadi, “Numerical solution of nonlinear volterra-fredholm integral equations using haar wavelet collocation method,” *Bull. Math. Sci. Appl*, vol. 18, no. 51, 2017.
- [65] J. Majak, M. Pohlak, K. Karjust, M. Eerme, J. Kurnitski, and B. S. Shvartsman, “New higher order Haar wavelet method: Application to FGM structures,” *Compos. Struct.*, vol. 201, 2018, doi: 10.1016/j.compstruct.2018.06.013.
- [66] R. C. Mittal and S. Pandit, “Quasilinearized Scale-3 Haar wavelets-based algorithm for numerical simulation of fractional dynamical systems,” *Eng. Comput. (Swansea, Wales)*, vol. 35, no. 5, 2018, doi: 10.1108/EC-09-2017-0347.

- [67] I. H. Muhammad A., Imtiaz A., Masood A., “A numerical Haar wavelet-finite difference hybrid method for linear and non-linear Schrödinger equation,” *Math. Comput. Simul.*, vol. 165, pp. 13–25, 2019.
- [68] S. Mittal, R. C., & Pandit, “New scale-3 haar wavelets algorithm for numerical simulation of second order ordinary differential equations,” *Proc. Natl. Acad. Sci. India Sect. Phys. Sci.*, vol. 89, pp. 799-808., 2019.
- [69] A. Ratas, M., & Salupere, “Application of higher order Haar wavelet method for solving nonlinear evolution equations,” *Math. Model. Anal.*, vol. 25, no. 2, pp. 271–288, 2020.
- [70] I. (2020) Pervaiz, N., & Aziz, “Haar wavelet approximation for the solution of cubic nonlinear Schrodinger equations.,” *Phys. A Stat. Mech. its Appl.*, vol. 545, 2020.
- [71] B. Lin, “A new numerical scheme for third-order singularly Emden–Fowler equations using quintic B-spline function,” *Int. J. Comput. Math.*, vol. 98, no. 12, 2021, doi: 10.1080/00207160.2021.1900566.
- [72] S. Chandrasekhar, *An Introduction to the Study of Stellar Structure*. New York.: Dover, 1967.
- [73] E. Momoniat and C. Harley, “Approximate implicit solution of a Lane-Emden equation,” *New Astron.*, vol. 11, no. 7, 2006, doi: 10.1016/j.newast.2006.02.004.
- [74] A. M. Wazwaz, “The Variational Iteration Method for Solving New Fourth-Order Emden–Fowler Type Equations,” *Chemical Engineering Communications*, vol. 202, no. 11. 2015, doi: 10.1080/00986445.2014.952814.
- [75] K. Parand, M. Dehghan, A. R. Rezaei, and S. M. Ghaderi, “An approximation algorithm for the solution of the nonlinear Lane-Emden type equations arising in astrophysics using Hermite functions collocation method,” *Comput. Phys. Commun.*, vol. 181, no. 6, 2010, doi: 10.1016/j.cpc.2010.02.018.
- [76] Y. Öztürk and M. Gülsu, “An approximation algorithm for the solution of the Lane-Emden type equations arising in astrophysics and engineering using Hermite polynomials,” *Comput. Appl. Math.*, vol. 33, no. 1, 2014, doi: 10.1007/s40314-013-0051-5.
- [77] H. Aminikhah and S. Moradian, “Numerical Solution of Singular Lane-Emden Equation,” *ISRN Math. Phys.*, vol. 2013, 2013.
- [78] H. Singh, “An efficient computational method for the approximate solution of nonlinear Lane-Emden type equations arising in astrophysics,” *Astrophys. Space Sci.*, vol. 363,

- no. 4, 2018, doi: 10.1007/s10509-018-3286-1.
- [79] D. T. Amit K. Verma, “Higher resolution methods based on Quasilinearization and Haar Wavelets on Lane-Emden Equations,” *Int. J. Wavelets, Multiresolution Inf. Process.*, vol. 17, no. 3, 2019.
- [80] R. C. M. and V. M. H. Kaur, “Haar wavelet approximate solutions for the generalized Lane-Emden equations arising in astrophysics,” *Comput. Phys. Commun.*, vol. 184, pp. 2169–2177, 2013.
- [81] H. G. and V. G. R. Singh, “Haar wavelet collocation method for Lane-Emden equations with Dirichlet, Neumann and Neumann-Robin boundary conditions,” *J. Comput. Appl. Math.*, vol. 346, pp. 150–161, 2019.
- [82] M. Singh and A. K. Verma, “An effective computational technique for a class of Lane-Emden equations,” *J. Math. Chem.*, vol. 54, no. 1, 2016, doi: 10.1007/s10910-015-0557-8.
- [83] S. Gümğüm, “Taylor wavelet solution of linear and nonlinear Lane-Emden equations,” *Appl. Numer. Math.*, vol. 158, pp. 44–53, 2020.
- [84] K. A. A.S.V. Ravi Kanth, “He’s variational iteration method for treating nonlinear singular boundary value problems,” *Comput. Math. Appl.*, vol. 60, pp. 821–829, 2010.
- [85] R. Singh and J. Kumar, “An efficient numerical technique for the solution of nonlinear singular boundary value problems,” *Comput. Phys. Commun.*, vol. 185, no. 4, 2014, doi: 10.1016/j.cpc.2014.01.002.
- [86] B. Gürbüz and M. Sezer, “Laguerre polynomial approach for solving Lane-Emden type functional differential equations,” *Appl. Math. Comput.*, vol. 242, 2014, doi: 10.1016/j.amc.2014.05.058.
- [87] S. Iqbal and A. Javed, “Application of optimal homotopy asymptotic method for the analytic solution of singular Lane-Emden type equation,” *Appl. Math. Comput.*, vol. 217, no. 19, 2011, doi: 10.1016/j.amc.2011.02.083.
- [88] R. Singh, “Analytical approach for computation of exact and analytic approximate solutions to the system of Lane-Emden-Fowler type equations arising in astrophysics,” *Eur. Phys. J. Plus*, vol. 133, no. 8, 2018, doi: 10.1140/epjp/i2018-12140-9.
- [89] A. Isah and C. Phang, “A collocation method based on Genocchi operational matrix for solving Emden-Fowler equations,” in *Journal of Physics: Conference Series*, 2020, vol. 1489, no. 1, doi: 10.1088/1742-6596/1489/1/012022.
- [90] G. Akram, “Quartic spline solution of a third order singularly perturbed boundary value

- problem,” *ANZIAM J.*, vol. 52, 2012, doi: 10.21914/anziamj.v53i0.4526.
- [91] H. N. Caglar, S. H. Caglar, and E. H. Twizell, “Numerical solution of third-order boundary-value problems with fourth-degree B-spline functions,” *Int. J. Comput. Math.*, vol. 71, no. 3, 1999, doi: 10.1080/00207169908804816.
- [92] K. Aruna and A. S. V. Ravi Kanth, “A novel approach for a class of higher order nonlinear singular boundary value problems,” *Int. J. Pure Appl. Math.*, vol. 84, no. 4, 2013, doi: 10.12732/ijpam.v84i4.2.
- [93] S. A. Khuri, “An Alternative Solution Algorithm for the Nonlinear Generalized Emden-Fowler Equation,” *Int. J. Nonlinear Sci. Numer. Simul.*, vol. 2, no. 3, 2001, doi: 10.1515/IJNSNS.2001.2.3.299.
- [94] A. M. Wazwaz and S. A. Khuri, “The variational iteration method for solving the Volterra integro-differential forms of the Lane-Emden and the Emden-Fowler problems with initial and boundary value conditions,” *Open Eng.*, vol. 5, no. 1, 2015, doi: 10.1515/eng-2015-0006.
- [95] Y. Q. Hasan and L. M. Zhu, “Solving singular boundary value problems of higher-order ordinary differential equations by modified Adomian decomposition method,” *Commun. Nonlinear Sci. Numer. Simul.*, vol. 14, no. 6, 2009, doi: 10.1016/j.cnsns.2008.09.027.
- [96] S. ALKAN, “Haar wavelet collocation method for the approximate solutions of Emden-Fowler type equations,” *Nat. Eng. Sci.*, vol. 2, no. 3, 2017, doi: 10.28978/nesciences.349267.
- [97] N. Verma, A. K., & Kumar, “Haar wavelets collocation on a class of Emden-Fowler equation via Newton’s quasi-linearization and Newton-Raphson techniques.,” *arXiv preprint arXiv:1911.05819.*, 2019. .
- [98] N. A. Khan, A. Shaikh, and M. Ayaz, “Accurate numerical approximation of nonlinear fourth order Emden-Fowler type equations: A Haar based wavelet-collocation approach,” *Waves, Wavelets and Fractals*, vol. 3, no. 1, 2017, doi: 10.1515/wwfaa-2017-0007.
- [99] I. Singh and M. Kaur, “WAVELET METHODS FOR SOLVING THIRD ORDER ODEs,” *Int. J. Appl. Math.*, vol. 34, no. 6, 2021, doi: 10.12732/ijam.v34i6.9.
- [100] M. Heydari, Z. Avazzadeh, and N. Hosseinzadeh, “Haar Wavelet Method for Solving High-Order Differential Equations with Multi-Point Boundary Conditions,” *J. Appl. Comput. Mech.*, vol. 8, no. 2, 2022, doi: 10.22055/jacm.2020.31860.1935.

- [101] K. K. Ali, M. S. Mehanna, M. Ismail Abdelrahman, and M. A. Shaalan, “Analytical and Numerical solutions for fourth order Lane–Emden–Fowler equation,” *Partial Differ. Equations Appl. Math.*, vol. 6, 2022, doi: 10.1016/j.padiff.2022.100430.
- [102] S. Mittal, R. C., & Pandit, “Quasilinearized Scale-3 Haar wavelets-based algorithm for numerical simulation of fractional dynamical systems,” *Eng. Comput. (Swansea, Wales)*, vol. 35, no. 5, pp. 1907–1931., 2018.
- [103] R. C. Mittal and S. Pandit, “Sensitivity analysis of shock wave Burgers’ equation via a novel algorithm based on scale-3 Haar wavelets,” *Int. J. Comput. Math.*, vol. 95, no. 3, 2018, doi: 10.1080/00207160.2017.1293820.
- [104] R. Kumar, “Historical Development in Haar Wavelets and Their Application - An Overview”,” *J Emerg Technol Innov Res.*, vol. 5, no. 11, pp. 1287–96, 2018.
- [105] A. Haar, “Zur theorie der orthogonalen funktionen systeme,” *Math. Ann.*, vol. 69, no. 3, pp. 331–371, 1910.
- [106] C. K. Chui and J. A. Lian, “Construction of compactly supported symmetric and antisymmetric orthonormal wavelets with scale = 3,” *Appl. Comput. Harmon. Anal.*, vol. 2, no. 1, 1995, doi: 10.1006/acha.1995.1003.
- [107] G. Arora, R. Kumar, and H. Kaur, “A novel wavelet based hybrid method for finding the solutions of higher order boundary value problems,” *Ain Shams Eng. J.*, vol. 9, no. 4, 2018, doi: 10.1016/j.asej.2017.12.006.
- [108] R. Kumar and J. Gupta, “Numerical analysis of linear and non-linear dispersive equation using Haar scale-3 wavelet,” *Math. Eng. Sci. Aerosp.*, vol. 13, no. 4, 2022.
- [109] Swati, K. Singh, A. K. Verma, and M. Singh, “Higher order Emden–Fowler type equations via uniform Haar Wavelet resolution technique,” *J. Comput. Appl. Math.*, vol. 376, 2020, doi: 10.1016/j.cam.2020.112836.
- [110] H. Singh, “An efficient computational method for the approximate solution of nonlinear Lane-Emden type equations arising in astrophysics,” *Astrophys. Sp. Sci*, vol. 363, no. 71, 2018.
- [111] O. Koch, P. Kofler, and E. B. Weinmüller, “Implicit Euler method for the numerical solution of singular initial value problems,” *Appl. Numer. Math.*, vol. 34, no. 2, 2000, doi: 10.1016/S0168-9274(99)00130-0.
- [112] A. Kilbas, H. Srivastava, and J. Trujillo, “Theory and applications of fractional differential equations,” *J. Electrochem. Soc.*, vol. 129, no. 204, 2006.
- [113] I. Petráš, *Fractional-Order Nonlinear Systems. Modeling, Analysis and Simulation.*

2011.

- [114] S. Guo, L. Mei, Y. He, and Y. Li, “Time-fractional Schamel-KdV equation for dust-ion-acoustic waves in pair-ion plasma with trapped electrons and opposite polarity dust grains,” *Phys. Lett. Sect. A Gen. At. Solid State Phys.*, vol. 380, no. 9–10, 2016, doi: 10.1016/j.physleta.2016.01.002.
- [115] J. H. Choi, H. Kim, and R. Sakthivel, “Exact solution of the Wick-type stochastic fractional coupled KdV equations,” *J. Math. Chem.*, vol. 52, no. 10, 2014, doi: 10.1007/s10910-014-0406-1.
- [116] M. T. Gencoglu, H. M. Baskonus, and H. Bulut, “Numerical simulations to the nonlinear model of interpersonal relationships with time fractional derivative,” in *AIP Conference Proceedings*, 2017, vol. 1798, doi: 10.1063/1.4972695.
- [117] Z. Pinar and H. Kocak, “Exact solutions for the third-order dispersive-Fisher equations,” *Nonlinear Dyn.*, vol. 91, no. 1, 2018, doi: 10.1007/s11071-017-3878-2.
- [118] N. A. Larkin and J. Luchesi, “Initial-Boundary Value Problems for Generalized Dispersive Equations of Higher Orders Posed on Bounded Intervals,” *Appl. Math. Optim.*, vol. 83, no. 2, 2021, doi: 10.1007/s00245-019-09579-w.
- [119] D. Kaya, “An application for the higher order modified KdV equation by decomposition method,” *Commun. Nonlinear Sci. Numer. Simul.*, vol. 10, no. 6, 2005, doi: 10.1016/j.cnsns.2003.12.009.
- [120] M. Dehghan and A. Shokri, “A numerical method for KdV equation using collocation and radial basis functions,” *Nonlinear Dyn.*, vol. 50, no. 1–2, 2007, doi: 10.1007/s11071-006-9146-5.
- [121] Q. Wang, “Homotopy perturbation method for fractional KdV-Burgers equation,” *Chaos, Solitons and Fractals*, vol. 35, no. 5, 2008, doi: 10.1016/j.chaos.2006.05.074.
- [122] S. Momani and Z. Odibat, “Analytical approach to linear fractional partial differential equations arising in fluid mechanics,” *Phys. Lett. Sect. A Gen. At. Solid State Phys.*, vol. 355, no. 4–5, 2006, doi: 10.1016/j.physleta.2006.02.048.
- [123] A. Yokus and H. Bulut, “Numerical simulation of KdV equation by finite difference method,” *Indian J. Phys.*, vol. 92, no. 12, 2018, doi: 10.1007/s12648-018-1207-3.
- [124] Oruç, F. Bulut, and A. Esen, “Numerical solution of the KdV equation by Haar wavelet method,” *Pramana - J. Phys.*, vol. 87, no. 6, 2016, doi: 10.1007/s12043-016-1286-7.
- [125] S. Saha Ray and A. K. Gupta, “Two-dimensional Legendre wavelet method for travelling wave solutions of time-fractional generalized seventh order KdV equation,”

- Comput. Math. with Appl.*, vol. 73, no. 6, 2017, doi: 10.1016/j.camwa.2016.06.046.
- [126] A. Raza, A. Khan, and K. Ahmad, "A new approach for solving partial differential equations based on finite-difference and haar wavelet methods," *Jordan J. Math. Stat.*, vol. 14, no. 2, 2021.
- [127] L. Zada and I. Aziz, "The numerical solution of fractional Korteweg-de Vries and Burgers' equations via Haar wavelet," *Math. Methods Appl. Sci.*, vol. 44, no. 13, 2021, doi: 10.1002/mma.7430.
- [128] S. Saleem and M. Z. Hussain, "Numerical Solution of Nonlinear Fifth-Order KdV-Type Partial Differential Equations via Haar Wavelet," *Int. J. Appl. Comput. Math.*, vol. 6, no. 6, 2020, doi: 10.1007/s40819-020-00907-1.
- [129] M. Dehghan and A. Shokri, "Numerical solution of the nonlinear Klein-Gordon equation using radial basis functions," *J. Comput. Appl. Math.*, vol. 230, no. 2, 2009, doi: 10.1016/j.cam.2008.12.011.
- [130] A. Sadighi and D. D. Ganji, "Analytic treatment of linear and nonlinear Schrödinger equations: A study with homotopy-perturbation and Adomian decomposition methods," *Phys. Lett. Sect. A Gen. At. Solid State Phys.*, vol. 372, no. 4, 2008, doi: 10.1016/j.physleta.2007.07.065.
- [131] B. Jang, "Two-point boundary value problems by the extended Adomian decomposition method," *J. Comput. Appl. Math.*, vol. 219, no. 1, 2008, doi: 10.1016/j.cam.2007.07.036.
- [132] G. Adomian, *Solving Frontier Problems of Physics: The Decomposition Method*, 60th ed. USA: Boston, Mass, 1994.
- [133] A. M. Wazwaz, "Exact solutions to nonlinear diffusion equations obtained by the decomposition method," *Appl. Math. Comput.*, vol. 123, no. 1, 2001, doi: 10.1016/S0096-3003(00)00064-3.
- [134] E. Yusufoglu, "The variational iteration method for studying the Klein-Gordon equation," *Appl. Math. Lett.*, vol. 21, no. 7, 2008, doi: 10.1016/j.aml.2007.07.023.
- [135] A. Yildirim, "An algorithm for solving the fractional nonlinear Schrödinger equation by means of the homotopy perturbation method," *Int. J. Nonlinear Sci. Numer. Simul.*, vol. 10, no. 4, 2009, doi: 10.1515/IJNSNS.2009.10.4.445.
- [136] A. Ebaid, "Exact solutions for the generalized Klein-Gordon equation via a transformation and Exp-function method and comparison with Adomian's method," *J. Comput. Appl. Math.*, vol. 223, no. 1, 2009, doi: 10.1016/j.cam.2008.01.010.

- [137] J. Rashidinia and M. Jokar, "Numerical solution of nonlinear Klein-Gordon equation using polynomial wavelets," in *Advances in Intelligent Systems and Computing*, 2016, vol. 441, doi: 10.1007/978-3-319-30322-2_14.
- [138] F. Yin, T. Tian, J. Song, and M. Zhu, "Spectral methods using Legendre wavelets for nonlinear Klein\ Sine-Gordon equations," *J. Comput. Appl. Math.*, vol. 275, 2015, doi: 10.1016/j.cam.2014.07.014.
- [139] K. H. Kumar, "Legendre Wavelet Quasilinearization Method for Nonlinear Klein-Gordon Equation with Initial Conditions," in *Communications in Computer and Information Science*, 2019, vol. 1046, doi: 10.1007/978-981-13-9942-8_31.
- [140] S. C. Shiralashetti and S. Kumbinarasaiah, "Hermite wavelets operational matrix of integration for the numerical solution of nonlinear singular initial value problems," *Alexandria Eng. J.*, vol. 57, no. 4, 2018, doi: 10.1016/j.aej.2017.07.014.
- [141] S. C. Shiralashetti and S. Kumbinarasaiah, "Laguerre wavelets collocation method for the numerical solution of the Benjamina–Bona–Mohany equations," *J. Taibah Univ. Sci.*, vol. 13, no. 1, 2019, doi: 10.1080/16583655.2018.1515324.
- [142] K. H. Vijesh, V. A., & Kumar, "Wavelet based numerical simulation of non linear Klein/Sine Gordon equation.," *J. Comb. Inf. Syst. Sci.*, vol. 40, no. 1–4, p. 225, 2015.
- [143] K. A. Pant Sangeeta Chaube Shshank*, "Image denoising based on wavelet transform using visu thresholding technique.," *Int. J. Math. Eng. Manag. Sci.*, vol. 3, no. 4, pp. 444–449, 2018.
- [144] and R. R. N. Nagendra Babu Mahadasu, Venkatesh Ambati, "Seismic lithofacies distribution modeling using the single normal equation simulation (snesim) algorithm of multiple-point geostatistics in upper assam basin, india.," *Int. J. Math. Eng. Manag. Sci.*, vol. 6, no. 3, 2021.
- [145] and L. K. J. Anuj Kumar, Sangeeta Pant, "Wavelet variance, covariance and correlation analysis of bse Series., and nse indexes financial time," *Int. J. Math. Eng. Manag. Sci.*, vol. 1, no. 1, p. 26, 2016.
- [146] H. Kaur, R. Kumar, and G. Arora, "Non-dyadic wavelets based computational technique for the investigation of Bagley-Torvik equations," *Int. J. Emerg. Technol.*, vol. 10, no. 2, 2019.
- [147] R. Kumar, H. Kaur, and G. Arora, "Numerical solution by Haar wavelet collocation method for a class of higher order linear and nonlinear boundary value problems," in *AIP Conference Proceedings*, 2017, vol. 1860, doi: 10.1063/1.4990337.

- [148] R. Kumar, "Historical Development in Haar Wavelets and Their Application-An Overview.," *J Emerg Technol Innov Res.*, vol. 5, no. 11, pp. 1287–96, 2018.
- [149] M. Lakestani and M. Dehghan, "Collocation and finite difference-collocation methods for the solution of nonlinear Klein-Gordon equation," *Comput. Phys. Commun.*, vol. 181, no. 8, 2010, doi: 10.1016/j.cpc.2010.04.006.
- [150] B. Bülbül and M. Sezer, "A new approach to numerical solution of nonlinear Klein-Gordon equation," *Math. Probl. Eng.*, vol. 2013, 2013, doi: 10.1155/2013/869749.
- [151] J. Oldham, K., & Spanier, *The fractional calculus theory and applications of differentiation and integration to arbitrary order*. Elsevier, 1974.
- [152] C. Li and F. Zeng, *Numerical methods for fractional calculus*. Florida, US.: Chapman and Hall/CRC, 2015.
- [153] B. Miller, K. S., & Ross, *An introduction to the fractional calculus and fractional differential equations*. 1993.
- [154] I. Podlubny, *Fractional differential equations*. New York: Academic Press, 1999.
- [155] D. Baleanu and B. Shiri, "Collocation methods for fractional differential equations involving non-singular kernel," *Chaos, Solitons and Fractals*, vol. 116, 2018, doi: 10.1016/j.chaos.2018.09.020.
- [156] R. Almeida and N. R. O. Bastos, "A Numerical Method to Solve Higher-Order Fractional Differential Equations," *Mediterr. J. Math.*, vol. 13, no. 3, 2016, doi: 10.1007/s00009-015-0550-2.
- [157] A. Gowrisankar and R. Uthayakumar, "Fractional Calculus on Fractal Interpolation for a Sequence of Data with Countable Iterated Function System," *Mediterr. J. Math.*, vol. 13, no. 6, 2016, doi: 10.1007/s00009-016-0720-x.
- [158] Y. Chen, M. Yi, and C. Yu, "Error analysis for numerical solution of fractional differential equation by Haar wavelets method," *J. Comput. Sci.*, vol. 3, no. 5, 2012, doi: 10.1016/j.jocs.2012.04.008.
- [159] H. Sun, W. Chen, C. Li, and Y. Chen, "Finite difference schemes for variable-order time fractional diffusion equation," *Int. J. Bifurc. Chaos*, vol. 22, no. 4, 2012, doi: 10.1142/S021812741250085X.
- [160] K. Rabiei and M. Razzaghi, "Fractional-order Boubaker wavelets method for solving fractional Riccati differential equations," *Appl. Numer. Math.*, vol. 168, 2021, doi: 10.1016/j.apnum.2021.05.017.
- [161] K. Shah, Z. A. Khan, A. Ali, R. Amin, H. Khan, and A. Khan, "Haar wavelet collocation

- approach for the solution of fractional order COVID-19 model using Caputo derivative,” *Alexandria Eng. J.*, vol. 59, no. 5, 2020, doi: 10.1016/j.aej.2020.08.028.
- [162] F. Amin, R., Shah, K., Asif, M., Khan, I., & Ullah, “An efficient algorithm for numerical solution of fractional integro-differential equations via Haar wavelet.,” *J. Comput. Appl. Math.*, vol. 381, 2021.
- [163] R. Kumar and S. Bakhtawar, “An improved algorithm based on Haar scale 3 wavelets for the numerical solution of integro-differential equations,” *Math. Eng. Sci. Aerosp.*, vol. 13, no. 3, 2022.
- [164] RC Mittal and Sapna Pandit., “New scale-3 haar wavelets algorithm for numerical simulation of second order ordinary differential equations.,” *Proc. Natl. Acad. Sci. India Sect. A Phys. Sci.*, vol. 89, no. 4, pp. 799–808, 2019.
- [165] L. Wei, Y. He, and B. Tang, “Analysis of the fractional Kawahara equation using an implicit fully discrete local discontinuous Galerkin method,” *Numer. Methods Partial Differ. Equ.*, vol. 29, no. 5, 2013, doi: 10.1002/num.21756.

LIST OF PUBLICATION

- Ratesh Kumar, Jaya Gupta “Numerical analysis of linear and non-linear dispersive equation using Haar scale-3 wavelet” published in Q3 Scopus indexed Journal “MATHEMATICS IN ENGINEERING, SCIENCE AND AEROSPACE (MESA)”, Vol. 13, No. 3, pp. 993-1006, 2022. www.journalmesa.com.
- Ratesh Kumar, Jaya Gupta “A Comparative Study using Scale-2 and Scale-3 Haar Wavelet for the Solution of Higher Order Differential Equation” published in Q2 ESCI Journal “International Journal of Mathematical, Engineering and Management Sciences”, Vol.8, No.5, 966-978, 2023. <https://doi.org/10.33889/IJMEMS.2023.8.5.055>
- Ratesh Kumar, Jaya Gupta, Himanshu Chauhan “A Non-Dyadic Haar wavelet approach to Numerical solution of non-linear Klein-Gordon Equation” published in Q3 Journal “European Chemical Bulletin”, Vol. 12, No. 5, 705-715, 2023. <https://eurchembull.com/issue-content/a-non-dyadic-haar-wavelet-approach-to-numerical-solution-of-non-linear-klein-gordon-equation-3479>.
- Ratesh Kumar, Jaya Gupta, “An Effective Computational Scheme for Solving Various Mathematical Fractional Differential Models Via Non-Dyadic Haar Wavelets” is Published in “Malaysian Journal of Science”. Vol.43, No.1, 44-58, 2024. <https://doi.org/10.22452/mjs.vol43no1.5>
- Ratesh Kumar, Jaya Gupta, “Numerical Investigation of fractional Kawahara Equation via Haar Scale Wavelet method.” is Published in “Contemporary Mathematics”. Vol.5, No.1, 478-491, 2024. <https://doi.org/10.37256/cm.5120242510>
- Ratesh Kumar, Jaya Gupta “A Non-dyadic wavelet-based approximation method for the solution of the linear and non-linear Lane Emden equation that appears in Astrophysics” is in Review in the Journal “Pramana”.

LIST OF CONFERENCES

- An Oral Presentation on “Numerical Analysis of Linear and Non-Linear Dispersive Equation using Haar Scale-3 Wavelet” in the 5th International Conference on Mathematical Technique in Engineering Application (ICMTEA 2021) held on 3-4 December 2021 organised by Graphic Era deemed to be University, Uttarakhand, Dehradun, India.
- An Oral Presentation on “A Comparative Study Using Scale-2 and Scale-3 Haar Wavelet for the Solution of Higher Order Differential Equation” in the 1st International Conference on Mathematical Methods and Techniques in Engineering and Sciences (ICMMTES 2022) held on 9-10 December 2022, organised by Graphic Era deemed to be University, Uttarakhand, Dehradun, India.
- An Oral Presentation on “Numerical investigation of fractional Kawahara equation via Haar scale wavelet method” in International Conference on Fractional Calculus: Theory, Applications and Numerics held on 27–29 January, 2023, organised by Department of Mathematics, National Institute of Technology Puducherry, Karaikal.
- An Oral Presentation on “A Wavelet Computational Scheme for the investigation of Higher order non-linear Differential equations” in the 4th International Conference on “Recent Advances in Fundamental and Applied Sciences” (RAFAS 2023) held on March 24-25, 2023, organized by School of Chemical Engineering and Physical Sciences, Lovely Faculty of Technology and Sciences, Lovely Professional University, Punjab.